11-2017

Investigation of Blend Time for Turbulent Newtonian Fluids in Stirred Tanks

Aaron Strand
ajs9009@rit.edu

Investigation of Blend Time for Turbulent Newtonian Fluids in Stirred Tanks

by

Aaron Strand

A Thesis Submitted in Partial Fulfillment of the Requirements for
the Degree of Master of Science in Mechanical Engineering
Department of Mechanical Engineering
Kate Gleason College of Engineering
Rochester Institute of Technology
Rochester, New York

Advised by

Dr. Edward Hensel, PE
Associate Dean for Research and Graduate Studies
Kate Gleason College of Engineering
Rochester Institute of Technology
Rochester, New York

November 2017

Investigation of Blend Time for Turbulent Newtonian Fluids in Stirred Tanks

by

Aaron Strand

A Thesis Submitted in Partial Fulfillment of the Requirements for
the Degree of Master of Science in Mechanical Engineering
Department of Mechanical Engineering
Kate Gleason College of Engineering
Rochester Institute of Technology
Rochester, New York

Advised by

Dr. Edward Hensel, PE
Associate Dean for Research and Graduate Studies
Kate Gleason College of Engineering
Rochester Institute of Technology
Rochester, New York

Approved by

_____

Dr. Edward Hensel, PE, Associate Dean for Research and Graduate Studies
Thesis Advisor, Kate Gleason College of Engineering

_____

Dr. Risa Robinson, Department Head
Committee Member, Department of Mechanical Engineering

_____

Dr. Steven Day, Department Head
Committee Member, Department of Biomedical Engineering

November 2017

Abstract

A blend time investigation for stirred tanks was conducted to study the effect of impeller type (A310 Hydrofoil, Pitched-Blade Turbine, Rushton Turbine), impeller diameter (*D/T = 1/5*, *1/3*, and *1/2*), and impeller off-bottom distance (*C/T = 1/5*, *1/3*, and *1/2*) while considering tank diameter (*T = 0.80* and *1.22 m*) and mean specific energy dissipation (ε *= 0.005* and *0.010 W/kg*) for turbulent Newtonian fluids with square batch aspect ratios. The response of conductivity probes to the injection of a sodium chloride tracer was monitored to experimentally measure blend time for *108* unique setups. The results of the blend time experiments were recorded, analyzed to determine trends, compared to a well-established correlation, and fit to generate modified correlations. A modified turbulent blend time correlation capable of predicting statistically similar blend time for *99%* of experimental setups is proposed as a function of tank diameter, impeller diameter, impeller off-bottom distance, textbook values of impeller power number, and impeller rotational frequency.

Table of Contents

List of Figures

List of Tables

Nomenclature

a	=	correlation coefficient (-)
A_x	=	impeller independent term (-)
b	=	number of blades (-)
c	=	correlation coefficient (-)
C	=	impeller off-bottom distance (m)
C/T	=	relative impeller off-bottom distance (-)
C/H	=	relative impeller off-bottom distance with respect to liquid level (-)
d	=	correlation coefficient (-)
D	=	impeller diameter (m)
D/T	=	relative impeller diameter (-)
e	=	correlation coefficient (-)
f	=	correlation coefficient (-)
Fo	=	Fourier number (-)
h	=	correlation coefficient (-)
H	=	liquid level (m)
H/T	=	batch aspect ratio (-)
j	=	correlation coefficient (-)
k	=	leading coefficient (-)
L	=	integral scale of turbulence (m)
N	=	rotational frequency (Hz)
m	=	number of circulations (-)
p	=	correlation coefficient (-)
P	=	impeller power (W)
P_o	=	impeller power number, drag coefficient (-)
q	=	correlation coefficient (-)
Q	=	impeller primary pumping capacity (m^3/s)
Q_o	=	impeller flow number (-)
R	=	impeller type (-)
Re	=	Reynolds number (-)
T	=	tank diameter (m)
T_s	=	square tank width (m)
V	=	volume (m^3, L, or mL)
V_f	=	volume fraction ($\%$)
w	=	blade width (m)
ε	=	mean specific energy dissipation, power per unit mass (W/kg)
η_Q	=	flow efficiency (-)
ρ	=	fluid density (kg/m^3)
τ	=	torque (Nm)

θ	=	blend time (s)
θ_c	=	circulation time (s)
θ_x	=	$x\%$ homogeneity blend time (s)
θ_{95}	=	95% homogeneity blend time (s)
μ	=	fluid viscosity (Pas)

1.0 Problem Introduction

1.1 Background

Rotating agitators, process equipment composed of a motor, gearbox, shaft, and impeller(s), are installed on vessels and used throughout industry for numerous unit operations. An example of in-tank components of a rotating agitator mounted on an open vessel is shown in Figure 1.1.1.

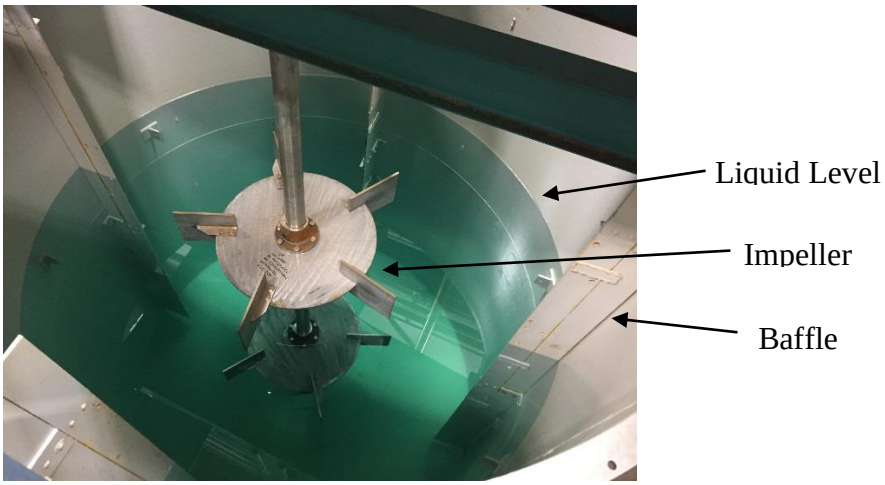

Figure 1.1.1. A *3.05 m* diameter vessel, half-filled with water, with four baffles and in-tank components of an on-center mounted rotating agitator. Photo courtesy of SPX Flow Lightnin.

One common unit operation conducted by rotating agitators is blending; defined as the process of combining miscible components into homogenous solutions [1]. An example of a blending process is displayed in Figure 1.1.2.

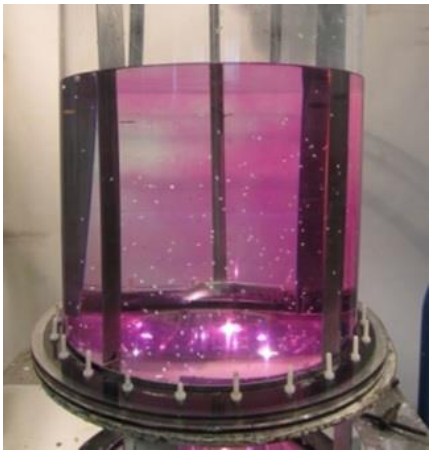

Figure 1.1.2. A neutralization of sodium hydroxide with hydrochloric acid in a mixed tank with phenolphthalein indicator for visualization. Photo courtesy of SPX Flow Lightnin.

Blending, otherwise known as single-phase mixing, is a common unit operation for rotating agitators with devoted chapters in the Industrial Handbook of Mixing and Advances in Industrial

Mixing as well as one of seven presentation categories for the North American Mixing Forum's (NAMF) bi-annual conference [1, 2]. Blending is quantified by the time required for a solution to obtain a certain degree of homogeneity, θ_x. The standard degree of homogeneity is 95%, so the standard nomenclature for 95% homogeneity blend time is θ_{95}.

Blend time is measured by injecting a tracer into a solution, marking the initial time, and monitoring the resultant change in concentration or a related parameter such as resistivity or conductivity as observed in Figure 1.1.3. The monitoring occurs at "last-to-blend" locations, such as behind a baffle, in the vessel and can be found experimentally using *pH* indicators or dyes. Eventually, the solution reaches a new steady-state value and the step change is quantified. Five percent of the step change is added and subtracted from the final steady-state value to create θ_{95} bounds. Then, the time at which the monitored parameter enters the bounded range without exiting is found. θ_{95} is the difference between the final and initial times. Several probes positioned at various locations in the vessel are commonly used at once and the one with the longest time establishes θ_{95}.

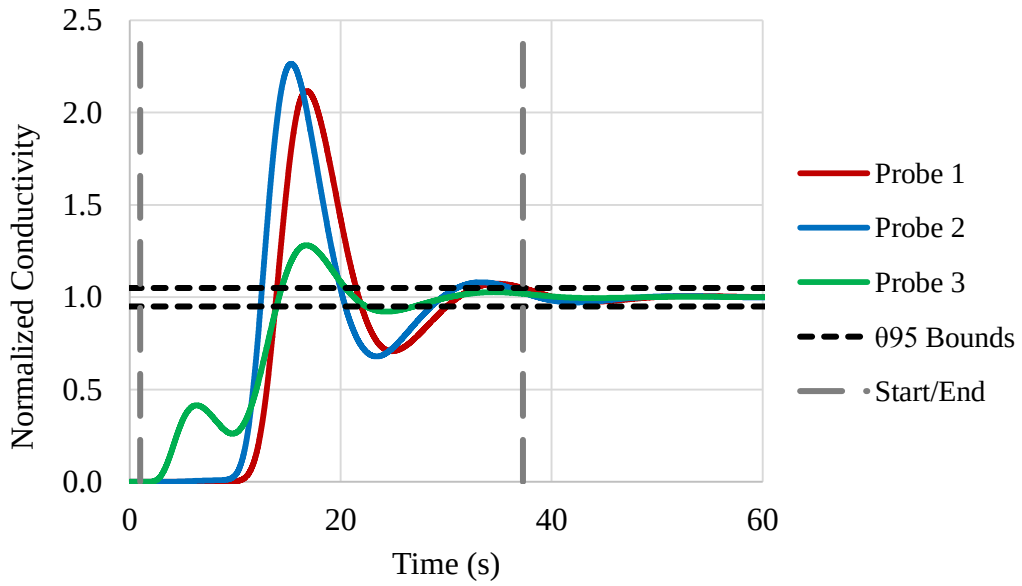

Figure 1.1.3. Example of θ_{95} determination by monitoring conductivity after injection of an aqueous tracer saturated with sodium chloride into a bulk water solution.

For a single impeller agitator, the time required to blend fluids is potentially dependent upon fluid density and rheology (ρ, μ), liquid level (H), impeller diameter (D), impeller off-bottom distance (C), impeller type (R), rotational frequency (N), and tank diameter (T) [3-5]. The geometric parameters, as observed in a cross section of a dish-bottomed tank, are presented in Figure 1.1.4. The type of tank bottom geometry differs across industries, but dished, flat, and cone bottoms are the most common.

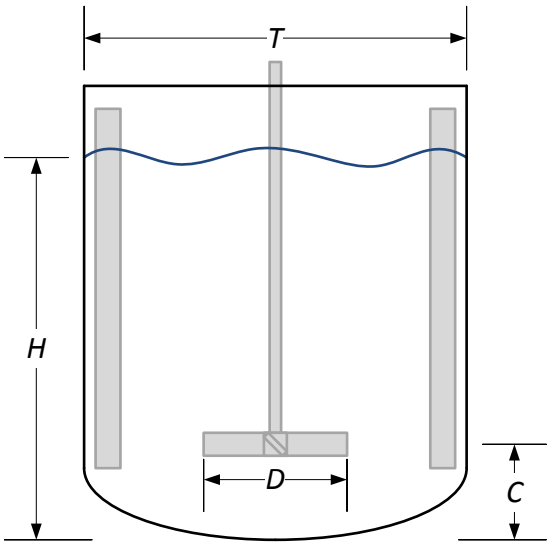

Figure 1.1.4. Geometric parameters for a dish-bottomed vessel with four standard baffles and a single impeller agitator.

Industrialists are interested in minimizing the time required to obtain homogeneity to decrease operating periods (subsequently increasing throughput of bottleneck tanks), and/or minimizing electrical consumption. Therefore, agitator manufacturers are driven to provide efficient solutions for blending applications and accurate prediction of blend times.

The efficient solution for a given blending application is dependent upon fluid rheology and flow regime [1]. Momentum transfer from high shear zones near the impeller to low shear zones near the tank wall differs based on the viscosity of the fluid and necessitates varying agitator designs. A Newtonian fluid often constitutes an impeller selection with an impeller to tank diameter ratio, *D/T*, around *1/3* where as a shear thinning fluid may constitute a higher *D/T* around *1/2* to decrease the relative distance between the impeller and tank wall. To simplify scope, this study focuses on Newtonian fluids.

Agitator design and impeller selection are also highly dependent on flow regime. The flow regime is determined by the Reynolds number, ratio of inertial to viscous forces, which is defined for rotating agitators according to Equation 1.1.1.

$$Re = \frac{\rho N D^2}{\mu} \tag{1.1.1}$$

For mixed tanks, the turbulent flow regime is defined by *Re > 10,000*, transitional flow regime by *Re* between *10* and *10,000*, and laminar flow regime by *Re < 10* [1]. As Reynolds number decreases, the torque required to produce fluid motion increases and the impeller best suited to transmit the torque changes [3]. The torque requirement of an impeller, defined in Equation 1.1.2 where τ is torque and *P* is power, is synonymous with an impeller's power number, P_o, which may be thought of as a drag coefficient and is defined in Equation 1.1.3 [1].

$$\tau = \frac{P}{N} \tag{1.1.2}$$

$$P_o = \frac{P}{\rho N^3 D^5} \tag{1.1.3}$$

Equation 1.1.2 may be substituted into Equation 1.1.3, as shown in Equation 1.1.4, to demonstrate direct proportionality.

$$P_o = \frac{\tau}{\rho N^2 D^5} \tag{1.1.4}$$

Hydrofoil impellers, such as SPX Flow Lightnin's A310 shown in Figure 1.1.5.A, are commonly utilized for blending fluids in the turbulent regime due to their characteristically low torque and P_o (0.30) which leads to decreased agitator capital cost [1].

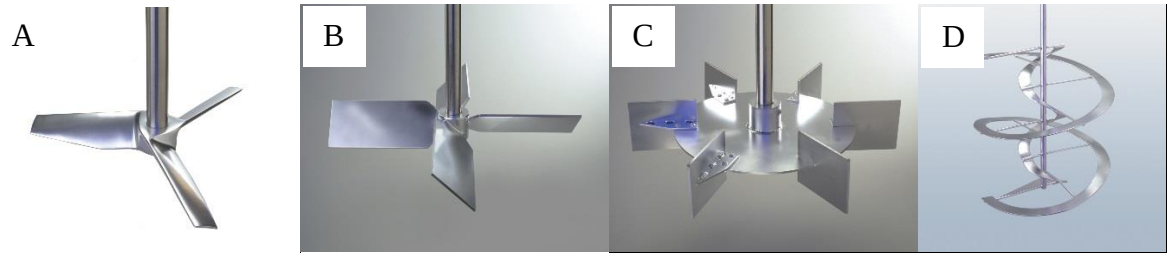

Figure 1.1.5. SPX Flow Lightnin A310 (A), Pitched-Blade Turbine (B), Rushton Turbine (C), and Double Helical Spiral (D) from left to right. Photos courtesy of SPX Flow Lightnin.

For fluids in the transitional regime, impellers with power numbers greater than the A310's are commonly selected as hydrofoils struggle to pump effectively. Two such impellers, also displayed in Figure 1.1.5, are the Pitched-Blade Turbine (PBT, $P_o = 1.27$) and Rushton Turbine (Rushton, $P_o \approx 5.75$) whose origins date back to the dawn of mixing science in the 1940's [1]. Hydrofoil impellers were not invented until the 1980s, so PBTs and RTs can be found blending fluids in the turbulent regime as well. For fluids in the laminar regime, close clearance impellers with *D/T* approaching *1* and P_o exceeding *10* are utilized [1]. An example of an impeller that meets this criteria is a double helical spiral which is also shown in Figure 1.1.5.D. To simplify scope, this study focuses on flows in the turbulent regime.

As mixing science advanced, correlations were developed to predict the blend time for Newtonian and Non-Newtonian fluids in the turbulent, transitional, and laminar flow regimes. The most established and well accepted blend time correlations were developed by Grenville while at the British Hydrodynamic Group's (BHR) Fluid Mixing Processes (FMP) consortium in 1992 [1]. Grenville's blend time correlation for Newtonian fluids in the turbulent flow regime is listed in Equation 1.1.5 [3].

$$P_o^{1/3} N \theta_{95} \frac{D^2}{T^{3/2} H^{1/2}} = 5.2 \tag{1.1.5}$$

By rearranging Equation 1.1.5 and substituting terms, Grenville deduced that blend time for Newtonian fluids in the turbulent regime is independent of fluid properties (ρ,μ), independent of impeller type (*R*) and dependent on impeller diameter (*D*), liquid level (*H*), rotational frequency (*N*), and tank diameter (*T*). All of the trials were performed at an impeller off-bottom distance to tank diameter ratio, *C/T*, of *1/3* so off-bottom distance dependence was not investigated.

Although several subsequent studies supported the Grenville correlation, Liu demonstrated impeller type and relative off-bottom distance dependence, *C/T*, in 2014 which was supported by Myers *et al.* within the context of varying relative liquid level, *H/T* [4, 5]. In 2016, Strand demonstrated a *D/T* and *C/T* interaction that resulted in a measured blend time that exceeded the predicted value from Grenville's correlation [6]. The two studies validated a need to revisit turbulent blending of Newtonian fluids to investigate impeller type (*R*) dependence, impeller off-bottom distance (*C*) dependence, and the interaction between *D/T* and *C/T*. Industrialists seek an improved correlation because they routinely deviate from the existing correlation bounds without considering non-idealities, and the existing correlation does little to intrinsically notify users about optimum impeller diameter and impeller off-bottom distance.

1.2 Societal Context

This investigation is most relevant to the chemical processing industry. The chemical processing industry utilizes cylindrical, dish-bottomed tanks with baffles and vertical on-center agitators with impeller geometry and flow conditions representative of those analyzed. A common requirement faced by the chemical processing industry is blending reactants into the bulk fluid before undesirable side reactions occur and by-products form. Blend time correlations, coupled with knowledge of reaction kinetics, are able to predict whether or not a reactor is capable of incorporating reactants before non-idealities propagate. The results of this thesis are directly applicable to the chemical processing industry.

A second relevant industry is minerals. The minerals industry utilizes cylindrical, flat-bottomed tanks, instead of dish-bottomed, with baffles and vertical on-center agitators with impeller geometry and flow conditions representative of those analyzed in this investigation. The primary unit operation performed by rotating agitators is suspension of mining ore for extraction processes. This is not a blending application, however mining has a number of secondary processes that are blending applications. One example is the production of leaching acids before their addition to solids slurry tanks. The discussed results are applicable to the minerals industry.

A third relevant industry is municipal and industrial waste water and waste water treatment where blending is the most common unit operation performed by rotating agitators. The majority of tanks used by the waste water industry are square or rectangular basins and channels with vertical agitators mounted on-center when possible, but some secondary processes may use cylindrical tanks with baffles and on-center mounted agitators. Kresta *et al.* demonstrated geometric differences between square and cylindrical tanks minutely affect the blend time, suggesting that any derived correlation from this work may only require slight modification for use with square tanks [7]. The secondary operations performed in cylindrical tanks, such as premixing nutrients or chemical substrates for introduction into the basins, will be covered by the discussed results.

A fourth relevant industry is pharmaceutical. For blending applications, blend time correlations become part of the design criteria for rotating agitators in pharmaceuticals as production failures are unacceptable due to compounds costs and product values. The pharmaceutical industry utilizes cylindrical tanks with dish or cone bottoms and typically no baffles due to sanitary standards. The lack of baffling results in swirl which impedes blending. Rotating agitators are often mounted vertical off-center or angular off-center to combat swirl, but it is never fully eliminated. Vickeroy demonstrated the lack of baffling and alternate mounting arrangement affects blend time prediction, suggesting that any derived correlation from this thesis may require modification for use in pharmaceutical applications [8].

2.0 Research Question

Could a correlation predicting 95% tank homogeneity blend time, θ_{95}, for a turbulent, Newtonian fluid as a function of tank diameter, impeller diameter, impeller off-bottom distance, and impeller type be established for a vertical, on-center mounted agitator in a baffled tank that is accurate to within 10% of measured values?

3.0 Literature Review

3.1 Pre-1950

There does not appear to be any literature describing blend time measurement or correlation for Newtonian fluids in the turbulent regime prior to 1950 as noted by Grenville and Nienow [3, 9]. However, three pertinent studies investigating the power required to spin rotating agitators were published between 1850 and 1950 [9].

In 1855, Thomson discovered that the power, *P*, of discs spinning in water was proportional to the rotational frequency, *N*, and impeller diameter, *D*, as described in Equation 3.1.1 [9, 10].

$$P \propto N^3 D^5 \tag{3.1.1}$$

In 1934, White and Brenner stated that the proportionality required an impeller power number, P_o, and fluid density, ρ, to become an equality as previously shown in Equation 1.1.3 which is restated here [9, 11].

$$P_o = \frac{P}{\rho N^3 D^5} \tag{1.1.3}$$

Then in 1950, Rushton *et al.* demonstrated that impeller power number, P_o, was constant in the turbulent regime and defined the Reynolds number for mixed tanks as stated in Equation 1.1.1 which is restated here [9, 12].

$$Re = \frac{\rho N D^2}{\mu} \tag{1.1.1}$$

These three studies are particularly relevant because following studies in the 1990s and 2000s directly related the power of a rotating agitator to blend time through the mean specific energy dissipation rate, ε, which is defined as power per unit mass [3, 7, 13]. Additionally, the proposed work utilized Equations 1.1.1, 1.1.2, and 1.1.3 for pre-determining operating conditions.

3.2 1950 to 2000

The first apparent study of blend time in mixed tanks was performed by Kramers *et al.* in 1953 as noted by Grenville and Nienow [3, 9, 14]. Kramers *et al.* utilized conductivity measurements to determine the blend time for a Marine Propeller, shown in Figure 3.2.1, and Rushton Turbines with flat and curved blades in a *0.64 m* diameter tank.

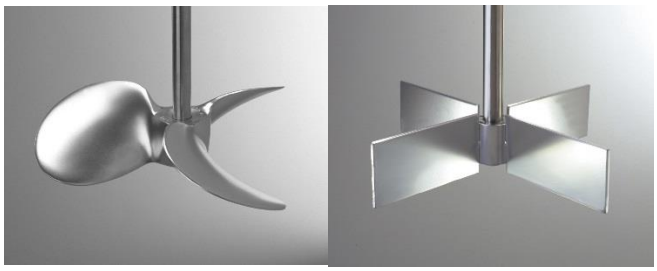

Figure 3.2.1. Additional impeller geometries (Marine Propeller and Flat-Blade Turbine, FBT, from left to right). Photos courtesy of SPX Flow Lightnin.

The impellers had a diameter to tank diameter ratio, *D/T = 1/4*, and the liquid level to tank diameter ratio, *H/T = 1*. The Marine Propeller was also tested in a *0.31 m* diameter tank with equivalent *D/T* and *H/T*. Kramers *et al.* concluded that the product $N\theta$ was constant within *10%* relative standard deviation for Newtonian fluids in the turbulent regime if geometric similarity was maintained. $N\theta$ equaling a constant meant that blend time, θ, scaled inversely with rotational frequency, *N*.

Subsequent studies by Van de Vusse in 1955, Prochazka and Landau in 1961, Hiraoka and Ito in 1977, Havas *et al.* in 1978, Sano and Usui in 1985 and 1987, Mackinnon in 1987, and Raghav Rao and Joshi in 1988 supported that $N\theta$ was constant for turbulent, Newtonian fluids as described by Grenville [3, 15-21]. For these studies, the blend time was measured using refractive index, conductivity, temperature, and color change properties. Most studies were performed with one or two tanks whose diameters were less than *0.5 m*, but Raghav Rao and Joshi as well as Mackinnon performed experiments in three or more tanks whose diameters extended to *1.5 m* and *2.87 m* respectively. Most studies also used dish-bottomed tanks.

Rushton Turbines were predominantly or solely utilized while Marine Propellers, Pitched-Blade Turbines, Flat-Blade Turbines (shown in Figure 3.2.1), and other miscellaneous impellers were tested as well. For cases with multiple impellers, the majority of studies suggested the $N\theta$ constant was dependent on impeller type, *R*. The *D/T* for the studies ranged from *0.1* to *0.7*, and the $N\theta$ constant was dependent on *D/T*. The *H/T* was often held constant at 1, but a couple varied it and found that the $N\theta$ constant was dependent on *H/T*. The values of impeller off-bottom distance to tank diameter ratio, *C/T*, were not widely reported by Grenville, so it's unknown if the ratio was held constant or varied in most studies. Raghav Rao and Joshi reported that the $N\theta$ constant was dependent on *C/T*, but were the only ones to do so. The dependence of the $N\theta$

constant on the various parameters led to the development of several blend time correlations for Newtonian fluids in the turbulent regime.

Prochazka and Landau proposed in 1961 that $N\theta$ was a function of impeller type (R), impeller diameter (D), and tank diameter (T) according to Equation 3.2.1 where k and a were impeller type dependent coefficients [16].

$$N\theta = k\left(\frac{T}{D}\right)^{(2+a)} \tag{3.2.1}$$

The Marine propeller, Pitched-Blade Turbine, and Rushton Turbine had k values of *3.48*, *2.02*, and *0.91* and a values of *0.05*, *0.20*, and *0.57*.

Havas *et al.* proposed in 1978 that $N\theta$ was also a function of R, D, and T as shown in Equation 3.2.2 where k was a constant and P_o was the impeller power number [18].

$$N\theta = \left(\frac{k}{P_o}\right)^{1/3}\left(\frac{T}{D}\right)^{5/3} = \left(\frac{k}{P_o}\right)^{1/3}\left(\frac{D}{T}\right)^{-5/3} \tag{3.2.2}$$

The Havas *et al.* correlation was rearranged to lead with $N\theta$ to maintain continuity with its counterparts. The T/D term was also rearranged to D/T form, and may be rearranged mentally in subsequent equations.

Mackinnon proposed in 1987 a similar correlation to Havas *et al.* as shown in Equation 3.2.3 [20].

$$N\theta = kP_o^{-1/3}\left(\frac{T}{D}\right)^{13/6} \tag{3.2.3}$$

The Mackinnon correlation was also rearranged to lead with $N\theta$. All three correlations presented in Equations 3.2.1, 3.2.2, and 3.2.3 possessed power based impeller type terms and T/D terms with an exponent of approximately *2*. This category of blend time correlations became known as "turbulence based" and focused on the power input of the impeller [3, 13].

The other type of blend time correlations were based on the flow generated by impellers and the subsequent circulation created in the tank. Hiraoka and Ito proposed in 1977 that $N\theta$ was a function of impeller type (R), impeller diameter (D), liquid level (H), and tank diameter (T) according to Equation 3.2.4 where b and w were the number of blades and width of blades, respectively [17].

$$N\theta = 7.2\left(\frac{bw}{D}\right)^{-0.35}\frac{T^{1.4}H^{0.5}}{D^{1.9}} \tag{3.2.4}$$

Sano and Usui proposed in 1985 that $N\theta$ was a constant and proportional to the circulation time, the time required for the fluid volume of the tank to be pumped by the impeller [19]. The blend

time was determined by multiplying the circulation time by *m*, the number of circulations required to achieve homogeneity according to Equation 3.2.5.

$$m = 3.8\left(\frac{D}{T}\right)^{0.5}\left(\frac{bw}{T}\right)^{0.1} \tag{3.2.5}$$

The shortcoming of Equations 3.2.4 and 3.2.5 was that they only applied to radial impellers such as the Rushton Turbine and Flat-Bladed Turbine due to their simple blade geometry. An overarching similarity between Equations 3.2.1-3.2.4 were *T/D* terms with an exponent of approximately *2*, if *T* and *H* were combined in the case of Equation 3.2.4, which promoted the use of larger *D/T*s over smaller ones to reduce blend time. However, Van de Vusse and Havas *et al.* proposed optimum *D/T*s of *0.4* and *0.55* with blend time increasing at larger *D/T*s [15, 18].

The turbulence based blend time correlation was further refined by Grenville in 1992. Grenville reanalyzed Mackinnon's data, obtained an improved fit, and rounded exponents to obtain Equation 3.2.6 in which *k* from Equation 3.2.3 was determined to be a universal constant of *5.2* ± *10%* [3].

$$N\theta = 5.2{P_o}^{-1/3}\left(\frac{T}{D}\right)^2 \tag{3.2.6}$$

Mackinnon's experiment was performed at *H/T = 1* and all impellers were located at *C/T = 1/3*, so neither *H* nor *C* are included in the correlation [3].

Grenville's correlation has a strong theoretical basis that is well explained by Grenville and Nienow and is summarized here with additional analysis [3, 13]. The mean specific energy dissipation rate, *ε*, otherwise known as power per unit mass of a rotating agitator is defined in Equation 3.2.7 where *P* is the power input, *ρ* is fluid density, and *V* is fluid volume [13].

$$\varepsilon = \frac{P}{\rho V} \tag{3.2.7}$$

Equation 1.1.3 provided a substitution for *P* and *V* was proportional to T^3 for the case *H/T = 1*, so Equation 3.2.7 was transformed into Equation 3.2.8 where A_1 was an impeller independent term.

$$\varepsilon = \frac{A_1 P_o N^3 D^5}{T^3} \tag{3.2.8}$$

It was proposed by Corrsin, Evangelista *et al.*, and Brodkey that turbulent blend time was inversely proportional to turbulent diffusion as expressed by Equation 3.2.9 where A_2 was an impeller independent term and *L* was the integral scale of turbulence [22-24].

$$\theta = A_2\left(\frac{\varepsilon}{L^2}\right)^{-1/3} = A_2\left(\frac{\varepsilon}{T^2}\right)^{-1/3} \tag{3.2.9}$$

The integral scale of turbulence was later surmised to be that of the tank diameter and not impeller diameter as the volume away from the impeller determines the blend time [13]. Substitution of Equation 3.2.8 into Equation 3.2.9 and simplification produced Equation 3.2.10.

$$N\theta = A_3 P_o^{-1/3} \left(\frac{T}{D}\right)^{5/3} \tag{3.2.10}$$

Equation 3.2.10 is synonymous with Havas *et al.*'s correlation presented in Equation 3.2.2. This correlation implied that any impeller at any *D/T* ratio would produce equal blend time for equal power. However, this was not observed experimentally. Instead, researchers observed that larger *D/T*s decreased blend time or suggested an optimum *D/T* existed between *0.4* and *0.55* [3, 15-21]. This behavior was thought to occur because larger *D/T* impellers more evenly dissipate energy such that the dissipation rates away from the impeller (controlling the blend time) are on average greater than those away from smaller impellers [13]. Therefore, the existence of an additional *D/T* component was proposed as shown in Equation 3.2.11 with an unknown exponent *a* [3, 13].

$$N\theta = k P_o^{-1/3} \left(\frac{T}{D}\right)^{5/3} \left(\frac{T}{D}\right)^{a} \tag{3.2.11}$$

Mackinnon originally determined the exponent to be *1/2*, but the analysis was skewed since the vast majority of initial impellers had *D/T = 1/3*. Reanalysis with additional impellers of *D/T = 1/2* by Grenville suggested that *a = 1/3*. Additionally, Voncken *et al.*, Cooke *et al.*, and Ruszkowski all reported that blend time was proportional to the square of *T/D*, further verifying that *a = 1/3* [25-27]. If *a = 1/3*, then Equation 3.2.11 may be rearranged, multiplied through by ρ/μ, and substituted with dimensionless groups to form Equation 3.2.12 [3].

$$P_o^{1/3} Re = \frac{k}{Fo} \tag{3.2.12}$$

Where *Re* is defined by Equation 1.1.1 and the Fourier number, *Fo*, is defined by Equation 3.2.13. In this form, the Fourier number describes transient momentum transfer.

$$Fo = \frac{\mu\theta}{\rho T^2} \tag{3.2.13}$$

Once the fundamental proportionality was finalized, Grenville solved the leading coefficient, *k*, by fitting Equation 3.2.12 to experimental data and determined it equaled *5.2 ± 10%* relative standard deviation as shown in Equation 3.2.6 [3]. The correlation was later modified to consider *H/T* dependence resulting in Equation 1.1.5 which is the published standard.

The implication of Grenville's correlation was that all impellers of equal diameter produced equal blend time at equal power regardless of impeller type as shown in a rearranged and substituted form in Equation 3.2.14 [3].

$$\theta \propto \left(\frac{1}{\varepsilon}\right)^{1/3} \left(\frac{T}{D}\right)^{1/3} T^{2/3} \tag{3.2.14}$$

The conclusion was verified by Nienow, who compiled several researchers' results including his own, and Kresta *et al.*, and the concept that turbulent energy dissipation was responsible for blending turbulent Newtonian fluids in agitated vessels was standardized [7, 13]. The turbulent energy dissipation theory and corresponding correlations relied on two core principles. The first was that the ratio of minimum energy dissipation rate away from the impeller to mean specific energy dissipation rate must be equivalent independent of impeller type for equal diameters which was demonstrated by Jaworski et al [13, 28]. The second was that P_o was constant for a given impeller type regardless of geometry (*D/T*, *H/T*, and *C/T*) due to the turbulent flow regime [3, 13].

Nienow also summarized a theoretical basis for blend time correlations based on the flow generated by impellers and subsequent tank circulation. The circulation time, θ_c, was defined according to Equation 3.2.15 where Q was the primary flow rate of an impeller and Q_o was the dimensionless primary flow number of an impeller [13].

$$\theta_c = \frac{V}{Q} = \frac{V}{Q_o N D^3} \tag{3.2.15}$$

Q_o must be determined from experimentation or CFD simulation as with P_o, and is a more difficult term to obtain. The primary flow of an impeller is defined as the high velocity stream discharged by an impeller, and is bounded by the swept circular area of an axial flow impeller or the swept tangential ring of a radial flow impeller as shown in Figure 3.2.2.

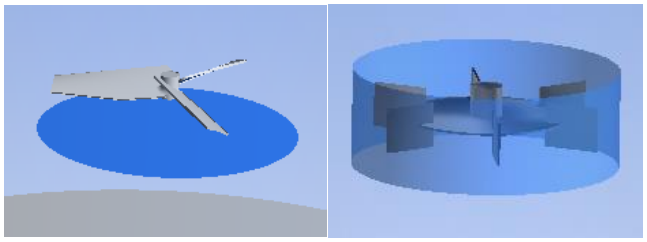

Figure 3.2.2. Depiction of primary flow measurement area for axial flow impellers (left) and radial flow impellers (right). The primary flow area is defined by the swept area for axial impellers (left) and a tangential ring for radial flow impellers (right). Visualization courtesy of SPX Flow Lightnin.

Nienow then proposed that the fluid was blended after a number of circulations such that blend time was defined according to Equation 3.2.16 where m is the number of circulations [13].

$$\theta = m\theta_c = m\left(\frac{V}{Q_o N D^3}\right) = A_4 m Q_o^{-1} N^{-1} \left(\frac{T}{D}\right)^3 \tag{3.2.16}$$

Additionally, the flow efficiency of an impeller, η_Q, was defined as flow rate per unit power as shown in Equation 3.2.17 [13].

$$\eta_Q = \frac{Q}{P} = \frac{Q_o}{P_o} \tag{3.2.17}$$

Since Q_o and P_o are directly proportional to Q and P, it followed that the ratio was also proportional. This implied that flow efficient impellers such as hydrofoils ($Q_o \approx 0.5$, $P_o \approx 0.3$) blended fluids quicker than flow inefficient impellers such as Rushton Turbines ($Q_o \approx 0.75$, $P_o \approx 5.75$) at equal diameter and power according to Equation 3.2.18 [13].

$$\theta \propto \frac{T^3}{Q_o(N^3D^5)^{1/3}D^{4/3}} \propto \frac{T^3}{Q_o\left(\frac{P}{P_o}\right)^{1/3}D^{4/3}} \propto \frac{P_o^{1/3}}{Q_o} \tag{3.2.18}$$

Circulation based blend time theory was demonstrated to be errant on at least two bases. The first was that Equation 3.2.16 predicted *T/D* dependence with an exponent of *3*, however it was experimentally observed to have an exponent of *2* [25-27]. The second was that Equation 3.2.18 predicted hydrofoils to blend fluids nearly twice as fast as Rushton Turbines, but such a vast performance difference was not observed by any researcher [13]. Circulation based blend time theory was deemed flawed, but blend time correlations based on flow have been produced.

3.3 Post-2000

Blend time studies for turbulent stirred tanks with single impeller agitators continued into the 21st century and branched to investigate tank geometries besides cylindrical vessels. In 2006, Kresta *et al*. studied *0.14 m* and *0.24 m* cylindrical tanks as well as *0.18 m* and *0.28 m* square tanks with liquid level, *H*, equal to tank diameter, *T*, or tank width, T_s [7]. Square tanks are often used in the waste water treatment industry so an applicable blend time correlation was desirable. Four impeller geometries (A310, HE3, PBT, and FBT) were studied, *D/T* ranged from *0.14* to *0.60*, and *C/H* equaled *1/2*. The measured values of θ_{95} were fit to the turbulent blend time correlation for the cylindrical tanks and yielded Equation 3.3.1 [7].

$$N\theta = 5.8P_o^{-1/3}\left(\frac{T}{D}\right)^2 \tag{3.3.1}$$

The exponents for P_o and *T/D* matched Grenville's blend time correlation, Equation 3.2.6, and supported turbulence theory, but the leading coefficient was *5.8* instead of *5.2*. The increased constant was likely due to a difference in probe location. Kresta *et al.* positioned probes behind baffles at the liquid surface while FMP, from which Grenville's correlation is derived, positioned the probe furthest from the impeller a distance *T/3* from the surface [3, 7]. Increased distance would result in increased blend time which was accounted for by the increased constant. Kresta *et al*. also utilized a flat-bottom instead of a dish-bottom, used by FMP, which may have also contributed to the increase in leading coefficient.

The measured values of θ_{95} were fit to the turbulent blend time correlation for the square tanks and yielded Equation 3.3.2 [7].

$$N\theta = 6.0{P_o}^{-1/3}\left(\frac{T_s}{D}\right)^2 \tag{3.3.2}$$

The exponents for P_o and *T/D* matched Grenville's blend time correlation, Equation 3.2.6, and supported turbulence theory. The leading coefficient for square tanks was *6.0* which was slightly elevated from the value of *5.8* for cylindrical tanks. Kresta *et al*. concluded that turbulent blend time theory was supported for cylindrical tanks, applicable to square tanks, and that square tank geometries were slightly less efficient than cylindrical tank geometries [7].

Another study focused on blending efficiency in the turbulent regime was presented by Liu in 2014 [4]. Liu utilized Computational Fluid Dynamics (CFD) simulations with a mean age method to compare the effects of impeller type (A310, PBT, and Rushton) and relative impeller off-bottom distance (*C/T = 1/3* and *1/2*) on blend time. Liu determined that power efficiency was impeller type and relative off-bottom distance dependent. Axial flow impellers such as the A310 and PBT were shown to be more energy efficient than radial flow impellers such as the Rushton. Liu also demonstrated that smaller diameter impellers were more energy efficient than larger diameter impellers. Liu's work supported turbulence based blend time theory with circulation based considerations.

Meyers *et al.* also demonstrated impeller type (HE3, PBT, FBT) and relative off-bottom dependence, *C/T*, within the context of varying relative liquid level, *H/T* [5]. Blend time was also shown to be strongly dependent on relative liquid level and impeller pumping direction. All trials were performed in a *0.34 m* dish-bottomed cylindrical vessel with standard baffling and vertical on-center mounted agitator. *H/T* was varied from *0.50* to *1.75*. *C/T* was held at *1/3* for most of the experiment, but was changed so that the impeller was located *T/3* from the liquid surface for a portion.

In 2016, Strand presented work that demonstrated a *D/T* and *C/T* interaction that resulted in a measured blend time that exceeded the predicted value [6]. This initial study by the thesis author is thoroughly described in Section 5 as it strongly informed the following investigation.

Well established blend time correlations for turbulent Newtonian fluids already exist [3, 7, 8]. However, industry users are expected to know the bounds of the correlations as the correlations are not intrinsically informative. The bounds for impeller diameter and off-bottom distance may be ignored by industry users, and lead to inefficient configurations with longer blend times [6]. Therefore, it was desirable to pursue a blend time correlation that guided industry users to an optimal impeller diameter and off-bottom distance. Furthermore, the dependence of blend time on impeller type is contested [4], and the topic benefited from additional research. If blend time was impeller type dependent, it was desirable to produce a blend time correlation that guided industry users to an ideal impeller type.

4.0 Objectives

The following objectives outlined an experimental path towards answering whether a correlation predicting blend time as a function of impeller diameter, off-bottom distance, and impeller type could be established for turbulent, Newtonian fluids with vertical, on-center mounted agitators in baffled vessels.

- Collect and report blend time data while incrementing tank diameter, impeller diameter, impeller off-bottom distance, and impeller type across 3 levels each
- Combine experimental data with published blend time data from previous studies [3, 20]
- Investigate and report on the relationship between blend time, θ_{95}, and off-bottom distance to tank diameter, *C/T*, to further inform the optimal relationship between off-bottom distance and tank diameter
- Investigate and report on the relationship between blend time, θ_{95}, and impeller diameter to tank diameter, *D/T*
- Investigate and report on the relationship between blend time, θ_{95}, and impeller type, *R*
- Propose a universal blend time correlation such that $\theta_{95} = f(C/T, D/T, N, R)$
- Evaluate and report upon the accuracy of the proposed correlation

After completing all objectives, it was known whether a blend time correlation dependent on tank diameter, impeller diameter, off-bottom distance, and impeller type could be established and whether it met acceptance criteria.

5.0 Work Performed Prior to Thesis

5.1 CFD Investigation of P_o and Q_o Variability

In early 2015, the author performed a Computational Fluid Dynamics (CFD) simulation based study investigating the effect of the impeller diameter to tank diameter ratio, *D/T*, and impeller off-bottom distance to impeller diameter ratio, *C/D*, on the impeller power number, P_o, and impeller flow number, Q_o, produced by a Lightnin A310 impeller geometry in a flat-bottomed, *1.22 m* diameter baffled tank filled with water to a liquid level of *1.22 m* as a final project for the Rochester Institute of Technology's CFD class (MECE 731). ANSYS Fluent was utilized for the study and a turbulent RANS realizable kε viscous model was selected. A hybrid swept mesh was implemented with tets discretizing the MRF cylinder and hexs discretizing the bulk fluid. The tank, baffles, and impeller were specified as no-slip walls while the fluid surface was a frozen symmetry plane. An example of the model geometry is shown in Figure 5.1.1.

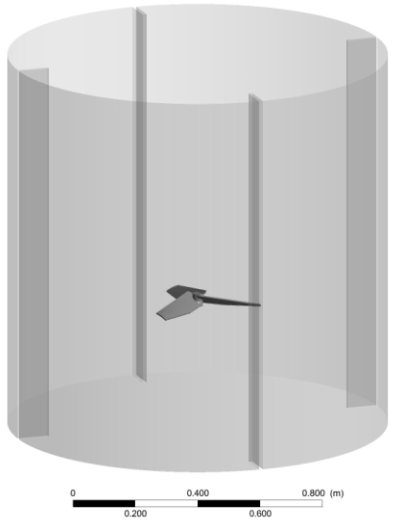

Figure 5.1.1. Example model geometry for CFD simulation based study.

The *D/T* was varied four times and *C/D* was varied three times at each *D/T*; producing *12* total configurations as shown in Table 5.1.1.

Table 5.1.1. Impeller configurations for CFD simulation based study.

		C (m)		
D (m)	*D/T*	*C/D = 1.0*	*C/D = 0.6*	*C/D = 0.3*
0.24	0.20	0.24	0.15	0.07
0.41	0.33	0.41	0.24	0.12
0.49	0.40	0.49	0.29	0.15
0.61	0.5	0.61	0.37	0.18

Every configuration was operated within *15%* of the average power (*0.27 kW*) which was selected to target a power per unit mass, ε, of *0.2 W/kg* as defined in Equation 3.2.7. The P_o was calculated using Equation 1.1.4 with torque measurements extracted from the simulations. A summary of the P_o results are shown in Figure 5.1.2.

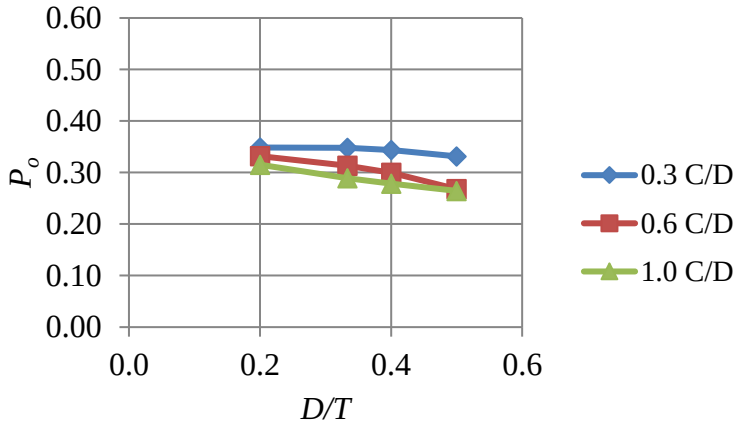

Figure 5.1.2. Effect of impeller diameter to tank diameter ratio, *D/T*, and impeller off-bottom distance to impeller diameter ratio, *C/D*, on the measured power number, P_o, of a Lightnin A310 impeller geometry in a *1.22 m* diameter baffled tank from a CFD simulation based study.

The P_o increased from a minimum value of *0.26* (*D/T = 0.5, C/D = 1*) to a maximum value of *0.35* (*D/T = 0.2, C/D = 0.3*) as both *D/T* and *C/D* decreased. The P_o of the Lightnin A310 varied by as much as *15%* from its stated value of *0.30*. Based on these CFD results, a potential error up to *5%* may occur by using a constant P_o instead of the simulated value in Grenville's turbulence based blend time correlation, Equation 3.2.6.

The Q_o was calculated using Equation 3.2.15 with mass flow rate measurements extracted from the simulations. A summary of the Q_o results are shown in Figure 5.1.3.

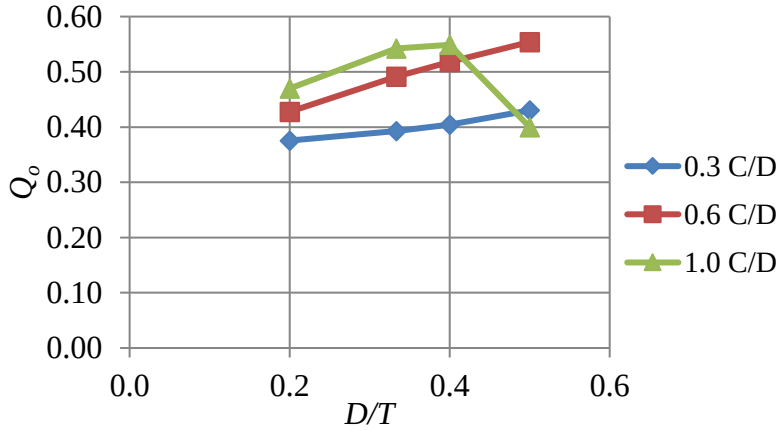

Figure 5.1.3. Effect of impeller diameter to tank diameter ratio, *D/T*, and impeller off-bottom distance to impeller diameter ratio, *C/D*, on the flow number, Q_o, produced by a Lightnin A310 impeller geometry in a *1.22 m* diameter baffled tank from a CFD simulation based study.

The Q_o increased from a minimum value of *0.38* (*D/T = 0.2, C/D = 0.3*) to a maximum value of *0.55* (*D/T = 0.4, C/D = 1* and *D/T = 0.5, C/D = 0.6*) as both *D/T* and *C/D* increased except for the configuration where *D/T = 0.5* and *C/D = 1*. Q_o was heavily dependent on impeller off-bottom distance, *C*, and may have been dependent on *D/T* as well. Regrettably, holding *C/D* constant led to an increase of impeller off-bottom distance as *D/T* increased so *D* was inseparable from *C*. Holding *C/T* constant instead of *C/D* would have alleviated the issue and allowed the effects of *D* and *C* to be considered independently.

The variance of Q_o had significant implications for circulation based blend time theory. As observed in Equation 3.15, Q_o is inversely proportional to blend time, θ, so the predicted blend time would increase by *45%* when moving from an impeller configuration that produced a Q_o = *0.55* to a configuration where Q_o = *0.38*. This would be compounded by the reduction in *D* between the two configurations and somewhat offset by the increase in rotational frequency, *N*.

A notable deviation from increased Q_o as *D/T* and *C/D* increased occurred when the *0.5 D/T* A310 impeller was moved from *0.6 C/D* to *1 C/D*. Q_o decreased sharply from *0.55* to *0.4*, and this was the only instance where the largest *D/T* impeller was outperformed by the smaller three impeller sizes. Comparison of cross-sectional velocity contour plots of an optimum case (*D/T = 0.4, C/D = 1*) and the outlier (*D/T = 0.5* and *C/D = 1*), as observed in Figure 5.1.4, revealed the reason for the sharp drop in Q_o.

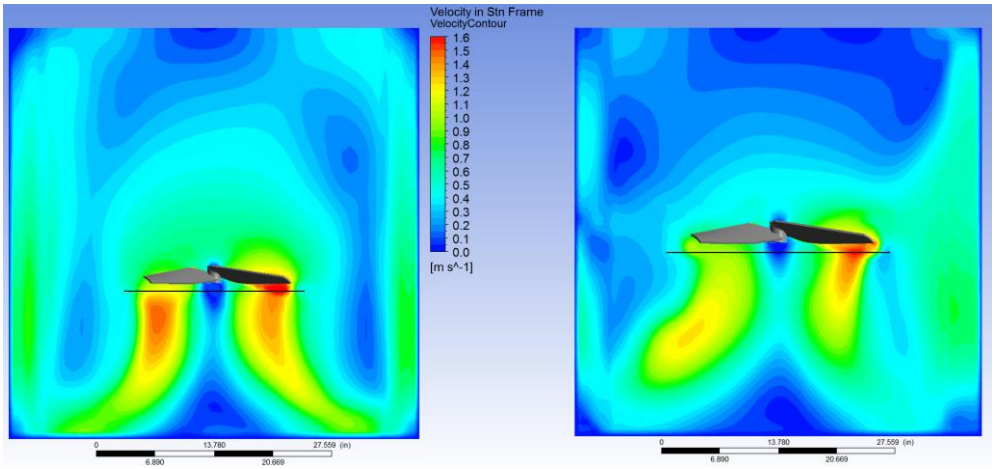

Figure 5.1.4. Velocity contour plots for a cross-section of the vessel for an optimum case (impeller diameter to tank diameter ratio, *D/T = 0.4*, and impeller off-bottom distance to impeller diameter ratio, *C/D = 1*) and outlier case (*D/T = 0.5* and *C/D = 1*) from left to right with the black line under each impeller designating the region of primary flow.

The optimum case exhibited complete tank turnover with a downwards jet reaching the tank floor before rising the entire length of the tank wall. However, the outlier case appeared to interfere with the flow rising along the wall, and the velocities in the upper half of the tank were reduced. The large impeller with *D/T = 0.5* performed well at lower *C/D*, so it was concluded

that an interaction between the two variables may result in lower than expected values of Q_o and potentially cause blend times that exceeded correlation estimates.

5.2 Initial Blend Time Study

An initial blend time study was performed in 2016 to determine if blend time varied with *C/D* and *D/T* (beyond the *D/T* scaling factor shown in Equation 3.2.14) since the CFD study provided evidence that P_o and Q_o, theoretical parameters for blend time, varied with *C/D*, potentially *D/T*, and an interaction between the two. The vessel geometry was identical to the CFD geometry as observed in Figure 5.1.1 and water was used as the bulk fluid. The initial study was small in scope and investigated three specific cases, listed in Table 5.2.1, from the CFD study.

Table 5.2.1. Geometric parameters for initial blend time study cases.

Case	*T (m)*	*D (m)*	*C (m)*	*D/T*	*C/D*	*C/T*
1	1.22	0.25	0.08	0.21	0.30	0.06
2	1.22	0.38	0.38	0.31	1.00	0.31
3	1.22	0.51	0.51	0.42	1.00	0.42

Case 1 was the smallest impeller from the CFD study with $D/T = 0.2$ and was located at the minimum impeller off-bottom ratio of $C/D = 0.3$. It had the maximum power number, $P_o = 0.35$, and minimum flow number, $Q_o = 0.38$. Cases 2 and 3 were the middle-sized impellers with $D/T = 0.3$ and 0.4 and were located at the maximum impeller off-bottom ratio of $C/D = 1$. For Case 2, $P_o = 0.29$ and $Q_o = 0.54$. Similarly for Case 3, $P_o = 0.28$ and $Q_o = 0.55$. Both sets of values were similar to the stated values of $P_o = 0.3$ and $Q_o = 0.56$. Regrettably, the outlier case where $D/T = 0.5$ and $C/D = 1$ was not tested. Cases 2 and 3 were used as experimental checks since their *D/T* and *C/T* were within or near to Grenville's correlation bounds ($0.33 < D/T < 0.5$, $C/T = 0.33$). Case 1 was used to investigate if the measured and predicted values of blend time diverged as the impeller configuration deviated from correlation bounds as suggested by turbulence and circulation based theory due to varying P_o and Q_o.

All three cases were operated at a power per unit volume = 0.00*41 W/kg* which maintained turbulent flow and predicted blend times between *45 s* and *60 s*. Three conductivity probes were used for the experiment. Two probes were attached to the backside of opposing baffles and extended *0.15 m* into the fluid from the surface. The third probe was attached to a dip tube and located a quarter of the tank diameter from center, halfway along the liquid level, and in-line with a baffle between the other two probes. Probe locations are summarized in Figure 5.2.1.

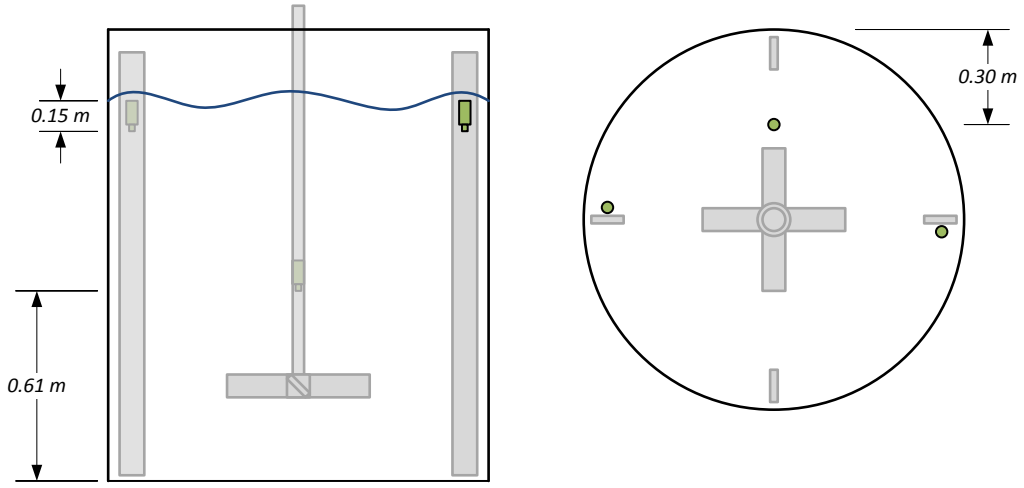

Figure 5.2.1. Cross-sectional and top-down tank illustrations demonstrating conductivity probe locations for the initial blend time study.

Blend time trials were initiated by gently pouring a *0.5 L* saturated sodium chloride solution tracer down the shaft of the agitator from just above the fluid surface at a specified time. The conductivity response of the three probes was monitored with SPX Flow Lightnin's custom LabVIEW blend time application as seen in Figure 5.2.2.

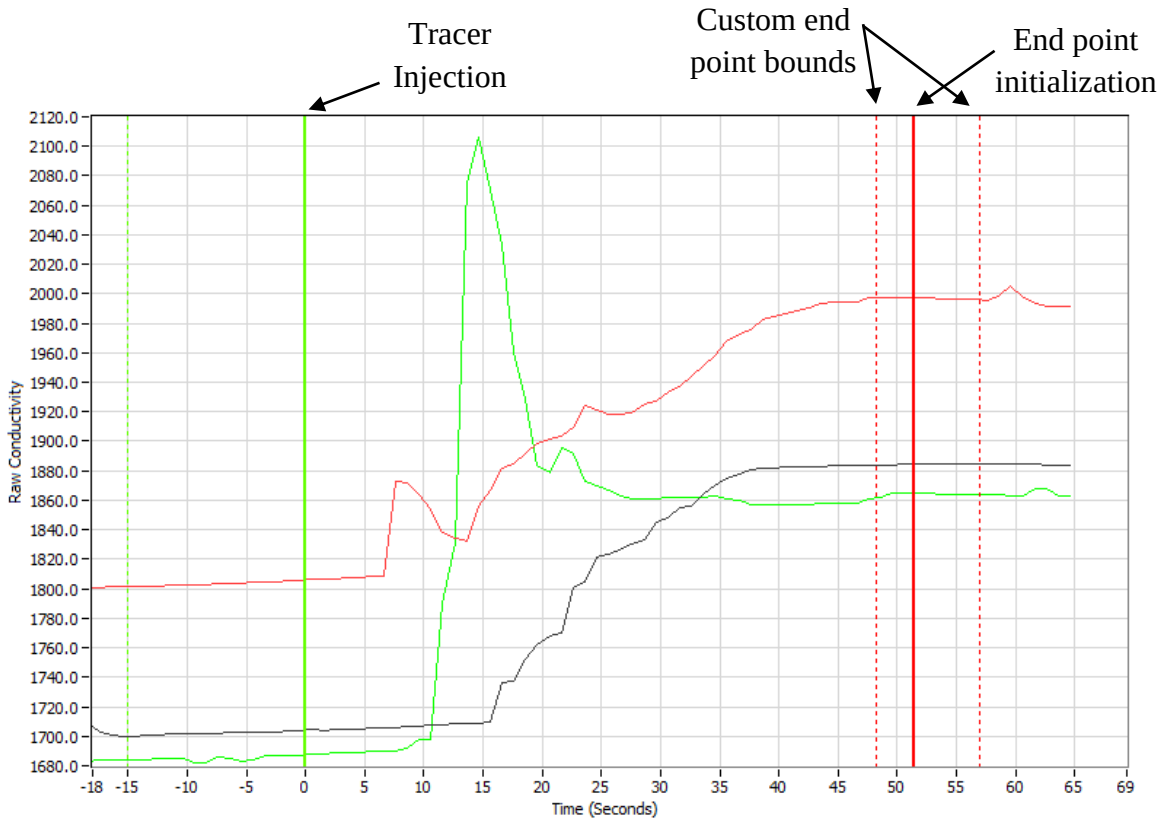

Figure 5.2.2. Example of conductivity response at a sampling rate of *1 s* from SPX Flow Lightnin's custom LabVIEW blend time application for three probes during a blend time test.

The blend time trial was stopped once the conductivity measurement stabilized for all three probes. Stabilization was visually determined by the observer. Signal noise was present in the system, as evidenced by the sharp peaks occurring at *60 s* for the red and green probe responses, and was avoided by setting custom end point bounds for averaging which were specified by dragging the vertical red dotted lines. Notable offsets between the three probe responses was also observed. Future unrelated blend time studies used a larger ratio of tracer to bulk fluid volume to minimize the effect of noise and noticeable difference in probe value offsets.

Once the blend time trial was complete and steady-state bounds were set, the custom LabVIEW application normalized each conductivity response and determined the *95%* homogeneity blend time, θ_{95}, by locating the time at which the last response entered the bounds without exiting as seen in Figure 5.2.3. For this trial, the red response determined that $\theta_{95} = 43\ s$.

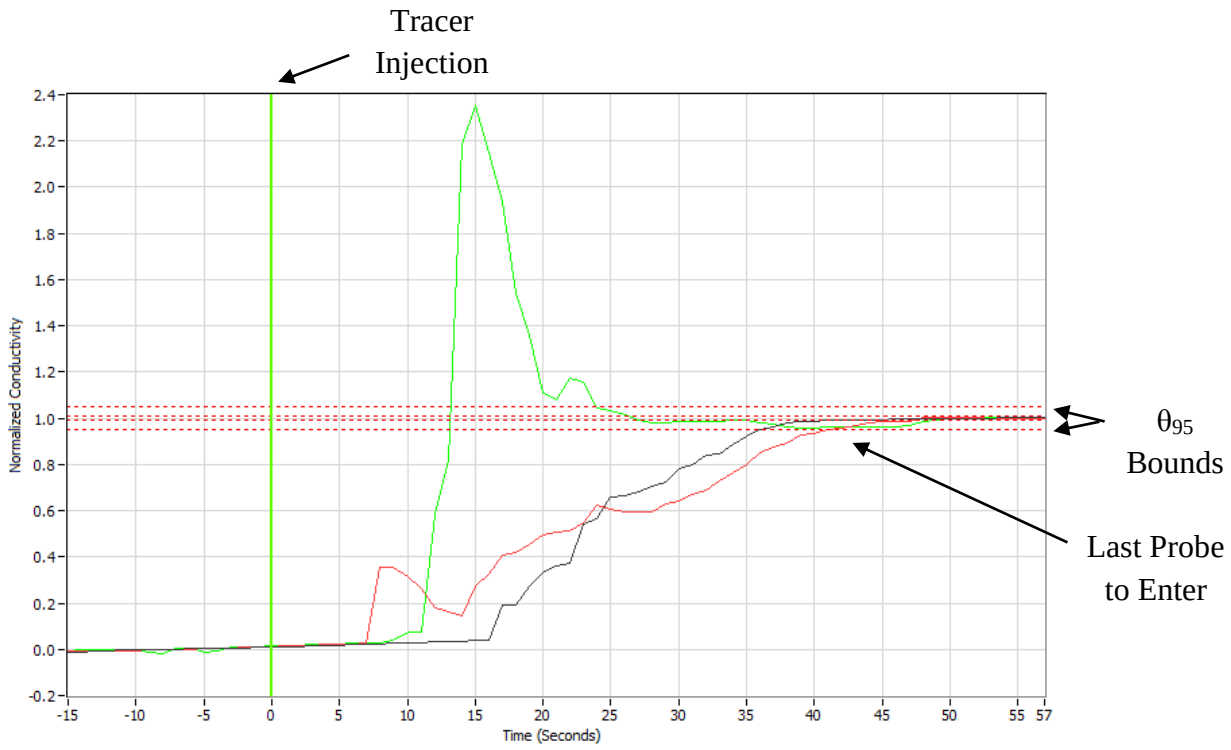

Figure 5.2.3. Example of θ_{95} determination using normalized conductivity responses at a sampling rate of *1 s* from SPX Flow Lightnin's custom LabVIEW blend time application for three probes.

Five blend time trials were performed for each case. The resultant measurements of θ_{95} were averaged and standard deviation calculated. A summary of the cases as well as their predicted blend time based on Grenville's correlation and experimental blend time are presented in Table 5.2.2. Grenville's correlation stated that the standard deviation was predicted to be *10%* of the calculated value.

Table 5.2.2. Predicted and experimental values of mean θ_{95} for the three cases in the initial blend time study.

Configuration			Predicted Values		Experimental Result	
Case	*D/T*	*C/D*	θ_{95} *(s)* [3]	*StDev (s)* [3]	Mean θ_{95} *(s)*	*StDev* (s)
1	0.20	0.33	62	6.2	77	5.4
2	0.33	1.00	55	5.5	54	10.7
3	0.40	1.00	48	4.8	50	4.9

For Cases 2 and 3, the predicted values of θ_{95} were within *5%* of the experimental results and less than half of Grenville's correlation variance of *10%* [3]. However, the predicted value of θ_{95} for Case 1 was *20%* less than the experimental result. The correlation under predicted the measured θ_{95} by double the acceptable variance. For Cases 1 and 3, the predicted and measured standard deviations matched whereas the experimental standard deviation observed for Case 2 was twice the predicted value. When all three cases were combined, the average coefficient of variance was *12%* which was in-line with the predicted value of *10%* [3].

The initial blend time study, though small in scope, demonstrated that Grenville's correlation may not accurately predict blend time when impeller configurations deviated from the correlation bounds. The under prediction of blend time for Case 1 suggested that the variability of Q_o and circulation based blend time theory by extension may be pertinent. The effect of impeller off-bottom distance, *C*, impeller diameter, *D*, and their interaction on the resultant blend time were deemed worthy of further investigation in a study with larger scope as described in the following section.

6.0 Work Plan

6.1 Schematic Diagrams

Experimental work was performed in ASME-like dish-bottomed vessels with standard baffling (four baffles with *T/12* width) where the tank diameter, *T*, impeller diameter, *D*, impeller off-bottom distance, *C*, and liquid level, *H*, were defined as shown in Figure 1.1.4, repeated for convenience.

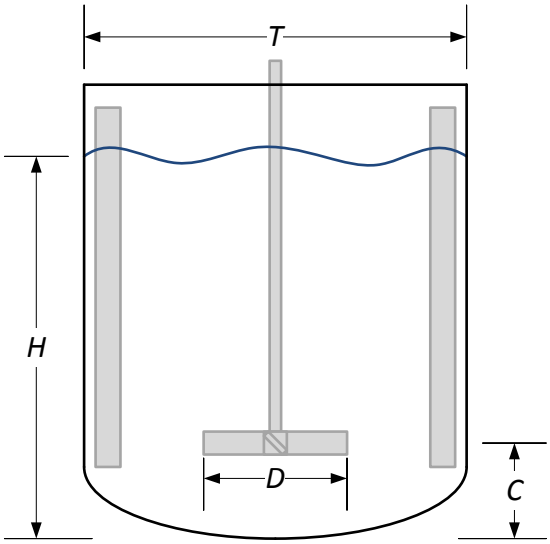

Figure 1.1.4. Geometric parameters for a dish-bottomed vessel with standard baffling and a single impeller agitator.

The tank diameter, impeller diameter, and off-bottom distance were varied while the liquid level was held equal to the tank diameter (*H/T = 1*). The majority of prior studies utilized *H/T = 1*, and the practice was maintained in this study. The impeller diameter and off-bottom distance were related to the tank diameter via dimensionless ratios to maintain geometric similarity as the tank diameter varied. The dimensionless terms were referred to as "*D/T*" and "*C/T*".

Four conductivity probes monitored the response of the system to a saturated sodium chloride tracer injected during blend time trials. Three of the probes shared similarities with the locations from the initial blend time study as observed in Figure 5.2.1. The first two probes were attached to the back side of opposing baffles and extended *0.05 m* into the fluid from the liquid surface. The third probe was attached to a dip tube and located a quarter of the tank diameter from center, elevated three quarters of the liquid level, and in-line with a baffle between the other two probes. The fourth probe was attached to the back side of the remaining baffle and positioned at the tank's lower tangent line where the tank wall and dish met. The positions of the four probes and tracer injection were summarized in Figure 6.1.1.

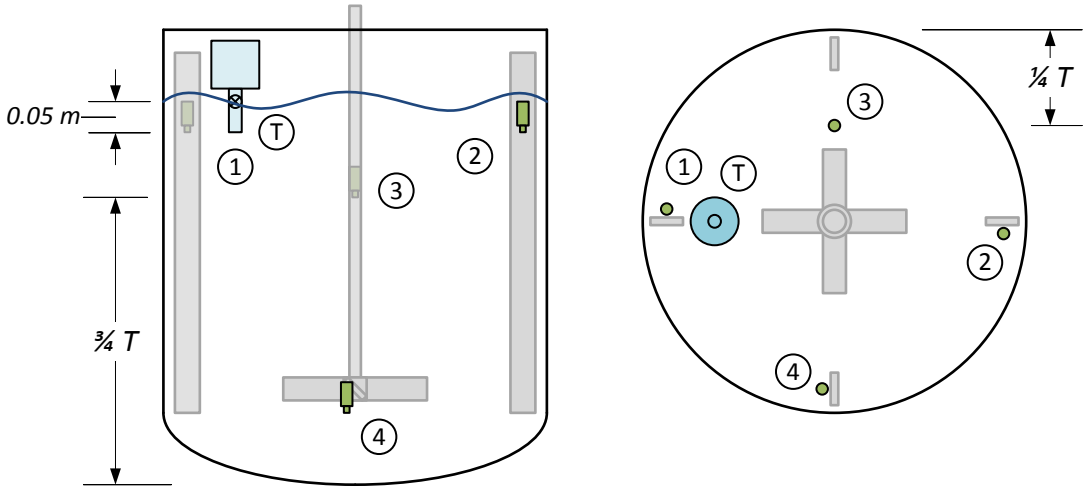

Figure 6.1.1. Cross-sectional and top-down tank illustrations demonstrating conductivity probe and tracer injection locations.

The two near surface probe locations have been proven to be "last-to-blend" locations and result in accurate blend time measurements [4]. The probe located away from the baffles was positioned in a low velocity region as seen in Figure 5.1.4 which occasionally may have been a "last-to-blend" location. The near dish probe location was a precaution in case the "last-to-blend" location flipped from near surface to near dish when the impellers were located further off-bottom.

6.2 Experimental Design

Two ASME-like dish-bottomed vessels with standard baffling and diameters of $T_1 = 0.80\ m$ and $T_2 = 1.22\ m$ were used for the experiment. Three impeller types, *R*, consisting of R_1 = Lightnin A310 hydrofoil (*A310*), R_2 = Pitched-blade turbine (*PBT*), and R_3 = Rushton turbine (*Rushton*) were selected. For each tank diameter, the *D/T* was varied across three levels (*1/5*, *1/3*, and *1/2*) by using different diameter impellers. Each impeller also went through a progression of three *C/T* levels (*1/5*, *1/3*, and *1/2*) by varying the impeller off-bottom distance.

Every geometric configuration was operated at two power per unit mass, ε, levels to maintain power input at two constant ratios across scales. Relatively low power per unit mass, ε, values of *0.005 W/kg* and *0.010 W/kg* were selected so that the vast majority of *95%* homogeneity blend times, θ_{95}, predicted using Grenville's correlation were between *30 s* and *60 s* at all scales while producing fully turbulent Reynolds numbers with the vast majority in the range of *35,000* to *350,000*. Input power, *P*, was calculated from shaft torque, τ, and rotational frequency, *N*,

measurements obtained with a calibrated Lebow strain-gauge torque cell according to Equation 1.1.2. Rotational frequency, *N*, was adjusted to achieve the desired power per unit mass.

An example of progressions through the five variables is shown in Figure 6.2.1.

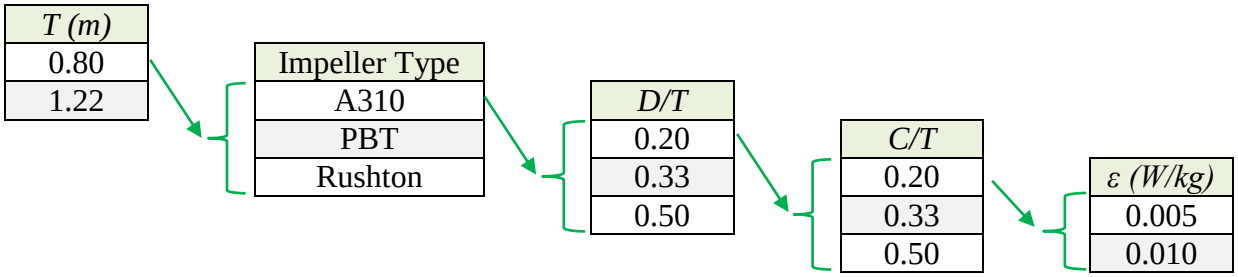

Figure 6.2.1. An example of progressions through the five variables (Tank diameter, *T*, impeller type, *R*, impeller to tank diameter ratio, *D/T*, impeller off-bottom distance to tank diameter ratio, *C/T*, and the mean energy dissipation rate, *ε*) and their respective levels.

Cycling through all five variables (*T*, *R*, *D/T*, *C/T*, and *ε*) and their respective levels (*2*, *3*, *3*, *3*, and *2*) created 108 experimental setups as shown in Tables A.1 and A.2 from Appendix A.

The variables and corresponding levels were selected to investigate specific items without producing an overwhelming scope. Two tank diameters, *T*, and two mean energy dissipations rates, *ε*, were selected to account for varying scale and energy input. The combination of three *D/T* ratios and three *C/T* ratios produced nine different geometric configurations for each impeller type which enabled an investigation into the influence of impeller diameter, *D*, impeller off-bottom distance, *C*, and their interaction on blend time. Since this was done for three impeller types, it also investigated if certain geometric configurations were better suited for certain impeller types or if all impeller types performed the same at a given geometric configuration.

6.3 Experimental Procedure

Experimental blend time measurements were performed as described in Section 5.2 with two main refinements. The first refinement was an increase in the volume fraction, V_f, of the injected sodium chloride tracer as shown in Table 6.3.1.

Table 6.3.1. Comparison of tracer volume fraction between previous blend time study and conducted work.

Study	*T (m)*	*Z (m)*	*V (L)*	V_{tracer} *(mL)*	V_f *(%)*
Previous	1.22	1.22	1425	500	0.035
Conducted	0.80	0.80	380	450	0.118
Conducted	1.22	1.22	1330	1600	0.120

The increased tracer volume fraction minimized the impact of signal noise and conductivity measurement offsets between probes in a separate confidential study, so the technique was adopted for future work.

After the tracer was injected, the response of the conductivity probes was monitored and the researcher determined when the system stabilized as seen in Figure 5.2.2. SPX Flow Lightnin's custom LabVIEW blend time application then calculated the *95%* homogeneity blend time, θ_{95}, as previously illustrated in Figure 5.2.3.

The second modification was an increase in the number of blend time trials per experimental configuration from *5* to *6*. The additional trial per experimental configuration was expected to reduce the standard deviation to within *10%* of the average value for a given set of trials. However, the number of trials per configuration used by Mackinnon and Grenville was *8* [3, 20].

Although the experimental blend times were predicted to be between *30 s* and *60 s* by Grenville's correlation, every trial consumed significantly more time on average. Measuring the tracer injection before a trial, determining the blend time after a trial, changing geometric configurations, and exchanging the bulk fluid in a tank to prevent ion concentrations rising above measurable limits will all increased the average time per trial. An adequate, experience-based estimate of the average time per trial was *10 min*. Investigating *108* experimental configurations and conducting *6* trials per configuration amounted to *648* total trials. If each trial required *10 min* on average due to the additional tasks besides measuring blend time, completing all trials would have required *6,480 min* or *108 hr*. This was an ambitious, yet manageable workload as shown in Section 6.5. If another parameter such as liquid level to tank diameter, *H/T*, had been varied at two levels, the required experimental time would have doubled to *216 hr* and become unmanageable. The proposed experimental design and procedure maximized the investigation of selected parameters with a full factorial design while providing an achievable workload.

6.4 Experimental Equipment

ASME-like dish-bottomed tanks with baffling in *0.80* and *1.22 m* diameters and straight sides exceeding their diameter housed the experiment. The baffling consisted of four standard baffles as described by the *Industrial Handbook of Mixing* [1]. Tank stands and a leveled hydraulic scissor lift provided a platform for the tanks and allowed for easy adjustment of the impeller off-bottom distance. The tanks were filled with Rochester city water such that the liquid height equaled the tank diameter.

Three types of impellers (Lightnin A310, Pitched-Blade Turbine, and Rushton Turbine) of four diameters were required and are listed in Table 6.4.1. The impeller diameters for the *1/3* and *1/2*

D/T cases in the *0.80 m* tank overlapped the impeller diameters for the *1/5* and *1/3 D/T* cases in the *1.22 m* tank: reducing the overall number of required impellers from *18* to *12*. While the actual *D/T* values were utilized in result analysis, the ideal *D/T* values are referenced due to the similarity between actual and ideal.

Table 6.4.1. Utilized impellers by type, diameter, and actual *D/T*.

T (m)	Impeller	*D (m)*	*D/T*
0.80	A310	0.16	0.20
0.80	PBT	0.15	0.19
0.80	Rushton	0.15	0.19
0.80	A310	0.25	0.32
0.80	PBT	0.25	0.32
0.80	Rushton	0.25	0.32
0.80	A310	0.41	0.51
0.80	PBT	0.41	0.51
0.80	Rushton	0.41	0.51
1.22	A310	0.25	0.21
1.22	PBT	0.25	0.21
1.22	Rushton	0.25	0.21
1.22	A310	0.41	0.33
1.22	PBT	0.41	0.33
1.22	Rushton	0.41	0.33
1.22	A310	0.61	0.50
1.22	PBT	0.61	0.50
1.22	Rushton	0.58	0.48

The impellers were set-screwed to shafts with fixed upper couplings. The couplings attached to a *2.25 kW*, *15 Hz* direct drive agitator equipped with an in-line *22.6 Nm* strain-gauge torque cell and tachometer. The agitator was powered with a variable frequency drive (VFD) enabling a rotational frequency operating range between *0.25* and *15 Hz*. Torque and rotational frequency signals from the strain-gauge torque cell and tachometer fed a National Instruments *4-20 mA* 9203 input module slotted into a 9174 cDAQ. The cDAQ communicated the signals to SPX Flow Lightnin's custom LabVIEW application which allowed real-time measurement of rotating agitator parameters such as power input and power number, P_o.

The custom LabVIEW application also had a blend time sub-module for performing blend time trials using conductivity measurements. The blend time sub-module enabled semi-automatic determination of blend time for a given trial. The user determined initial and final steady-state conditions while the sub-module prompted the user to commence tracer injection and analyzed the results by normalizing the step change, setting *95%* homogeneity bounds, and determining the blend time from the last conductivity measurement to enter the bounds and remain there.

Examples of the semi-automatic blend time sub-module outputs were previously presented in Figures 5.2.2 and 5.2.3.

Conductivity measurements were obtained with four GF Signet 2841 conductivity probes positioned at the "last-to-blend" locations, as described in Section 6.1. They were secured to baffles or dip tubes with zip ties. The conductivity measurements were converted to a digital output by GF Signet 2850 transmitters. The signals passed through a GF Signet 8900 controller followed by a National Instruments *4-20 mA* 9203 input module slotted into a 9174 cDAQ. The cDAQ communicated the signals to SPX Flow Lightnin's custom LabVIEW application. A schematic of the conductivity measurement system was shown in Figure 6.4.1.

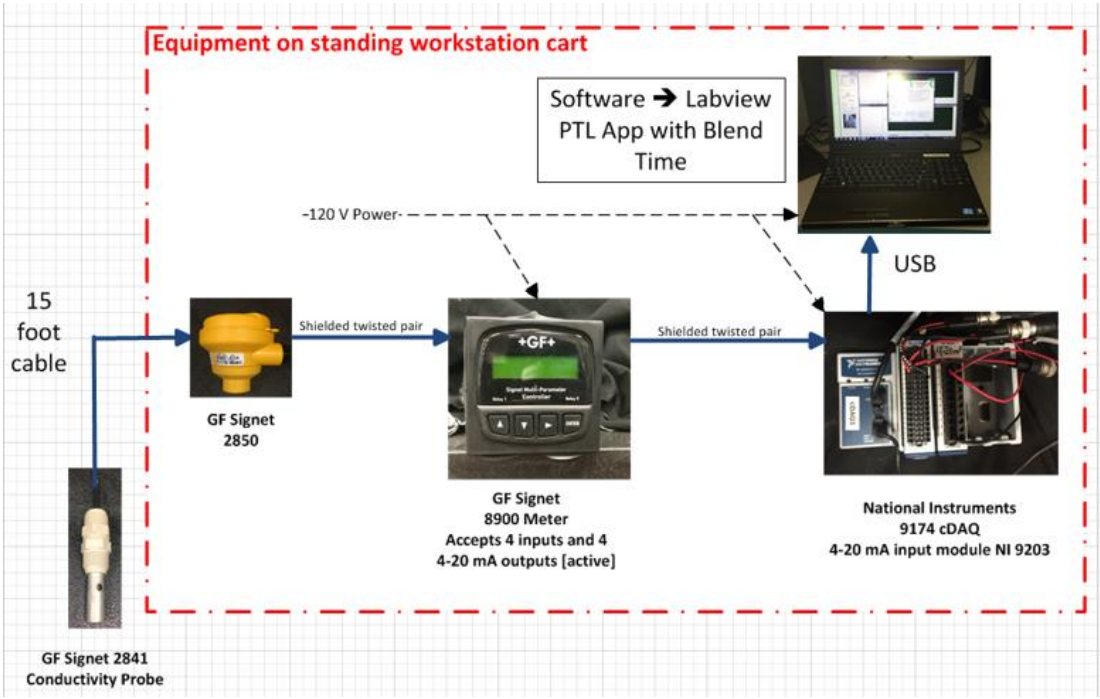

Figure 6.4.1. Schematic of conductivity measurement system. Schematic created by Kevin Logsdon and provided courtesy of SPX Flow Lightnin.

The conductivity tracer was an aqueous solution saturated with sodium chloride. The tracer was prepared in a *208 L* barrel with removable lid using a clamp-mounted SPX Flow Lightnin Labmaster rotating a *0.13 m* A200 impeller at *8.3 Hz*. Approximately *135 kg* of Rochester city water and *45 kg* of Morton Solar Salt were required per batch. The tracer make down apparatus was shown in Figure 6.4.2. The tracer was introduced via hopper with ball valve to improve injection consistency and was located as described in Section 6.1.

Figure 6.4.2. Tracer make down apparatus composed of a 208 L barrel and clamp-mounted SPX Flow Lightnin Labmaster agitator. Photo courtesy of SPX Flow Lightnin.

Photographs of the *0.80 m* diameter tank shown in Figure 6.4.3 illustrate a complete in-tank experimental setup. The vessel was left empty for the photograph to prevent light refraction and image distortion.

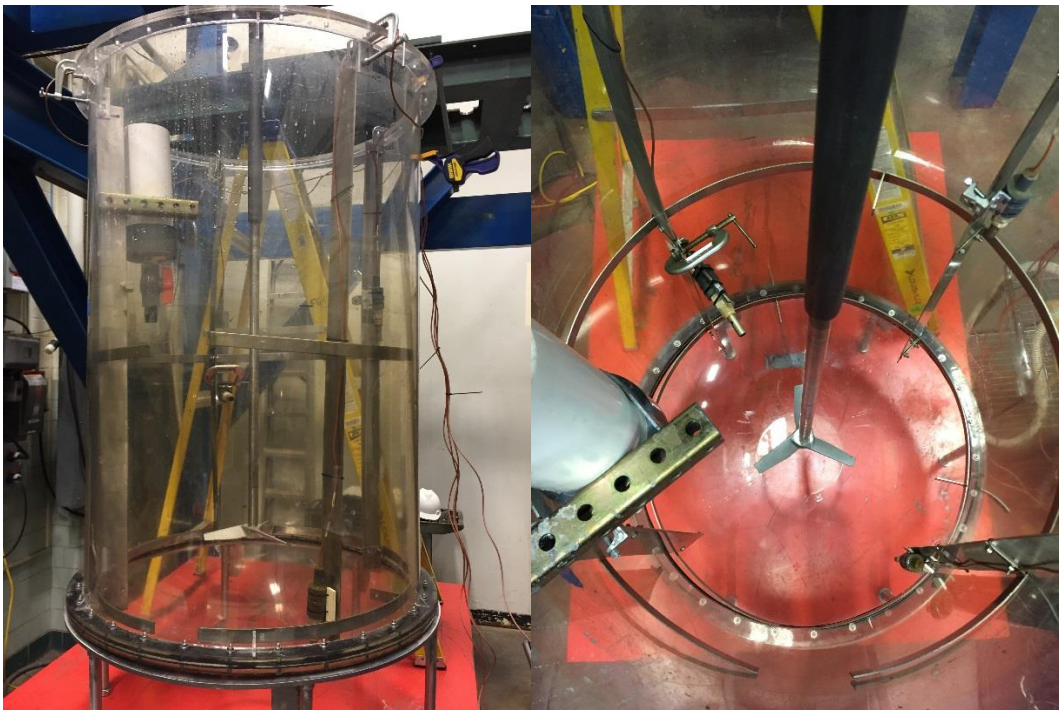

Figure 6.4.3. Example of in-tank experimental setup for *0.80 m* vessel. Photo courtesy of SPX Flow Lightnin.

The photograph shown in Figure 6.4.4 encapsulates the entire test apparatus.

Figure 6.4.4. Example of complete test setup. Photo courtesy of SPX Flow Lightnin.

Experimental data and blend time results were obtained with LabVIEW and exported to Microsoft Excel for compilation and basic analysis. Sets of data were then exported from Excel to Matlab for more rigorous analysis and curve fitting of correlations.

6.5 Project Timeline – Gantt Chart

The thesis investigation of a blend time correlation for fully turbulent, Newtonian fluids in stirred tanks was planned to occur in the six months between February and July, 2017. A Gantt chart outlining specific tasks and their timelines to guide the investigation is displayed in Table 6.5.1. In actuality, the thesis investigation stretched from February to November, 2017. Experimentation finished in May within two weeks of plan. However, data analysis and document generation occurred after experimentation instead of concurrently and led to the delay.

Table 6.5.1. Gantt chart summarizing tasks and timelines required to complete thesis between February and July of 2017.

		Month	February				March					April				May				June					July			
		End Date	3rd	10th	17th	24th	3rd	10th	17th	24th	31st	7th	14th	21st	28th	5th	12th	19th	26th	2nd	9th	16th	23rd	30th	7th	14th	21st	28th
Task	Start Week	End Week	1	2	3	4	5	6	7	8	9	10	11	12	13	14	15	16	17	18	19	20	21	22	23	24	25	26
Finish 21st century literature review	1	4																										
Prepare experimental setup for *0.61 m* tank	1	4																										
Trial runs and trouble shoot *0.61 m* system	3	4																										
Perform trials for *0.61 m* tank (14 *hr/wk*)	4	7																										
Collect information for and write societal context	5	9																										
Compilation and analysis of *0.61 m* tank data	6	9																										
Prepare experimental setup for 1.22 m tank	8	11																										
Trial runs and trouble shoot *1.22 m* system	10	11																										
Write-up experimental setup and procedure	11	14																										
Perform trials for 1.22 *m* tank (14 *hr/wk*)	11	14																										
Compilation and analysis of 1.22 *m* tank data	13	16																										
Compilation and analysis of all data	15	18																										
Correlation investigation	17	18																										
Write results	17	20																										
Write discussion	21	22																										
Deliver final thesis draft to Dr. Hensel	22	22																										
Finalize thesis	23	24																										
Prepare oral presentation of theis	24	25																										
Distribute final thesis to committee	25	25																										
Post thesis announcement	25	25																										
Oral presentation of thesis	26	26																										
Provide thesis copies to library	26	26																										

Key	
Experiment	
Data Analysis	
Document Generation	

7.0 Results

7.1 Probe Location and Blend Time Determination

In total, *648* blend time trials were performed during the study. The four probes monitored local conductivity response and the last probe to enter the *95%* homogeneity range during a trial determined the blend time. The blend time determining probe was recorded and each probe's final count is displayed in Figure 7.1.1. In the case of a tie, all probes determining blend time were recorded.

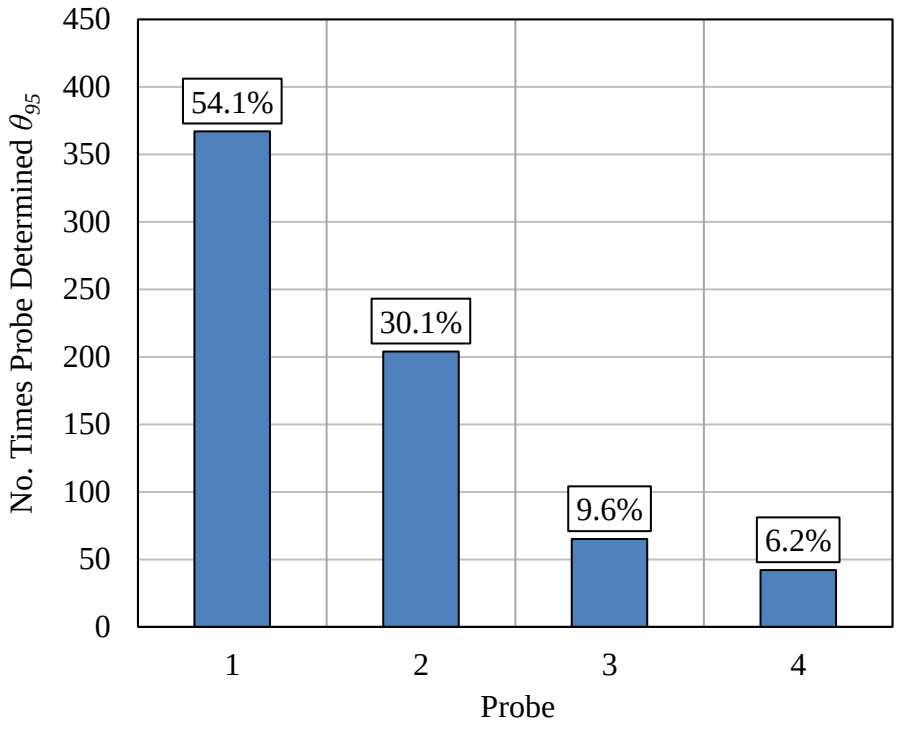

Figure 7.1.1. Total number of times that each probe determined θ_{95} during the course of the study.

7.2 Mean specific energy dissipation, ε, and impeller power number, P_o

The mean specific energy dissipation, ε, was calculated from the measured torque, operating speed, and volume during each trial. The average was taken for the six trials that comprised a setup, and the average values for all 108 setups are reported in Figure 7.2.1.

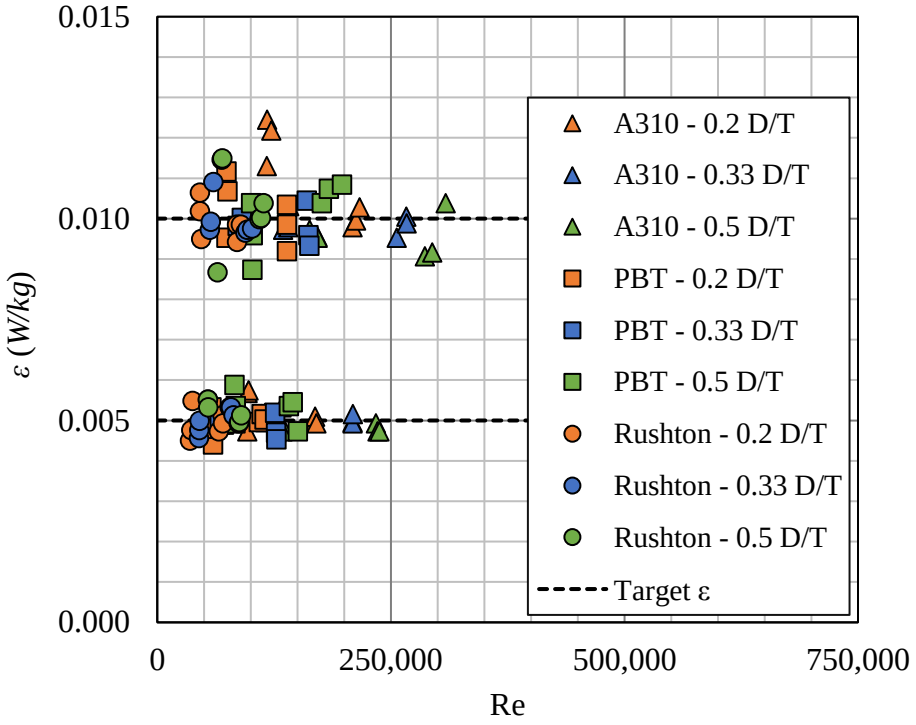

Figure 7.2.1. Average values, obtained from six measurements during corresponding trials, of the mean specific energy dissipation, ε, for all 108 experimental setups.

The impeller power number, P_o, was calculated from the measured torque, operating speed, and impeller diameter during each trial. Measured power numbers for each trial are listed in Table B.1 in Appendix B. The *6* trials for a given experimental setup were averaged, and the mean power numbers for the *108* experimental setups are reported in Table B.2 in Appendix B. The mean P_o for a geometric configuration (comprised of an impeller type, *D/T*, and *C/T*) and its *95%* confidence interval were determined by averaging the *24* applicable trials. Mean power numbers with *95%* confidence intervals for the *9* A310, PBT, and Rushton geometric configurations are presented in Figures 7.2.2-4.

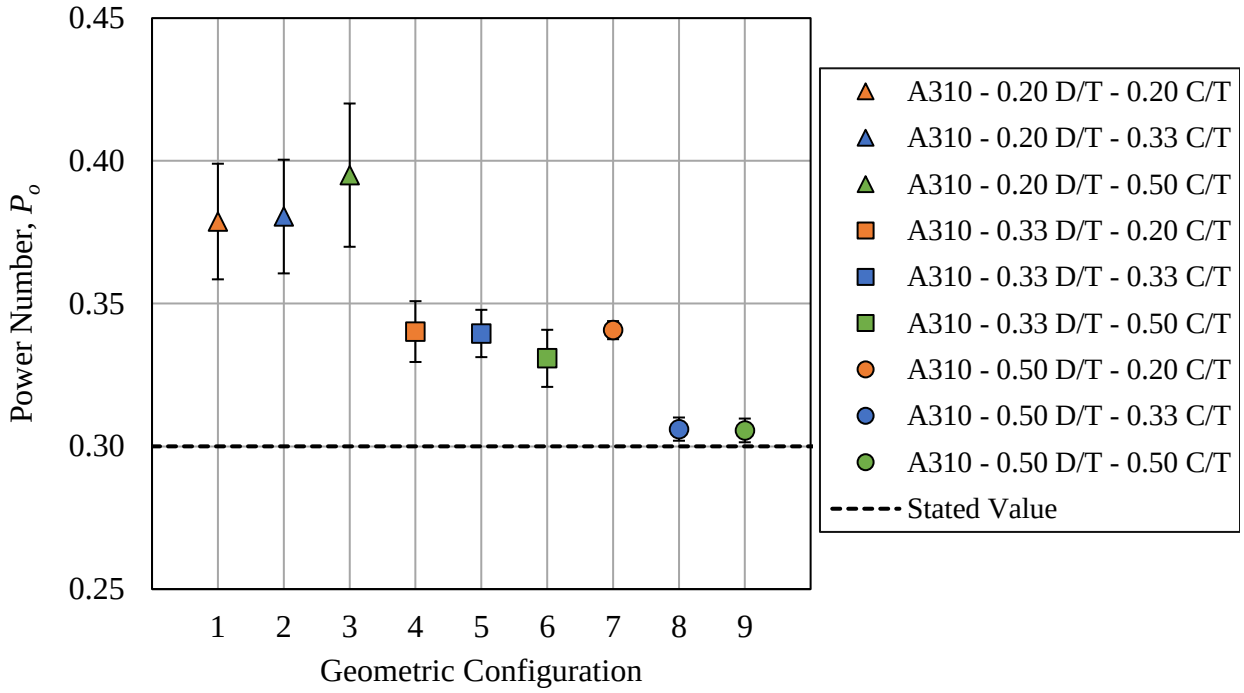

Figure 7.2.2. Average power numbers with *95%* confidence intervals, obtained from *24* measurements, for *9* A310 geometric configurations.

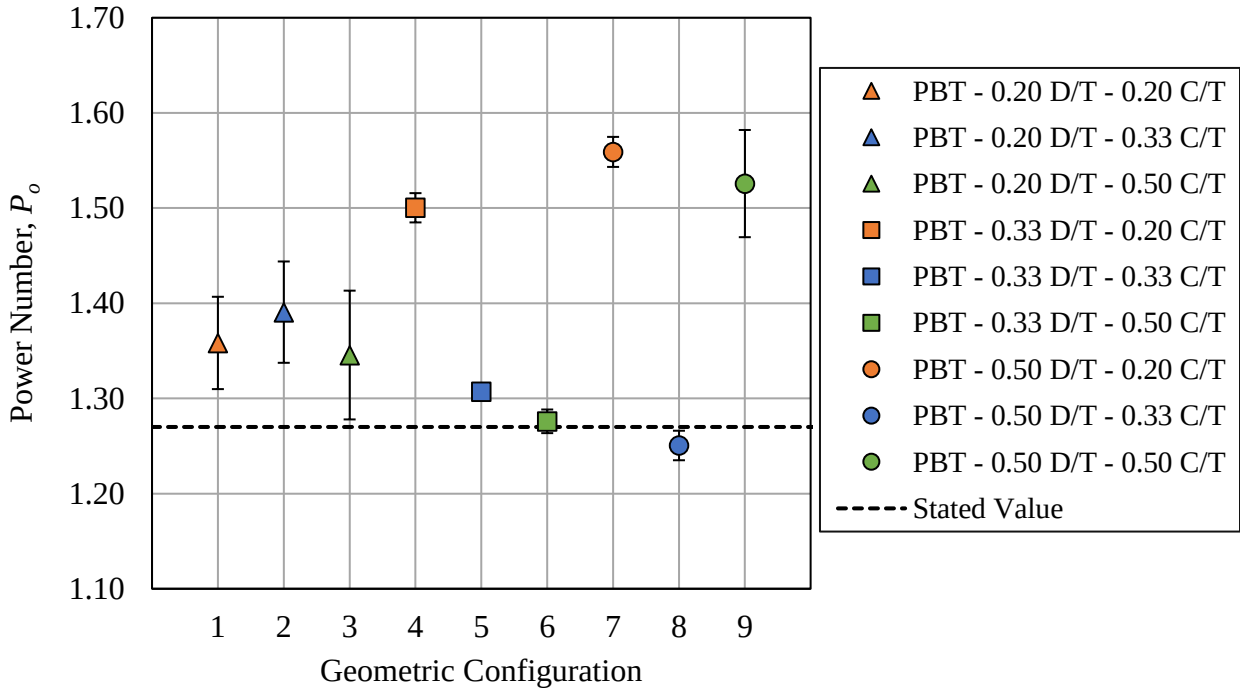

Figure 7.2.3. Average power numbers with *95%* confidence intervals, obtained from *24* measurements, for *9* PBT geometric configurations.

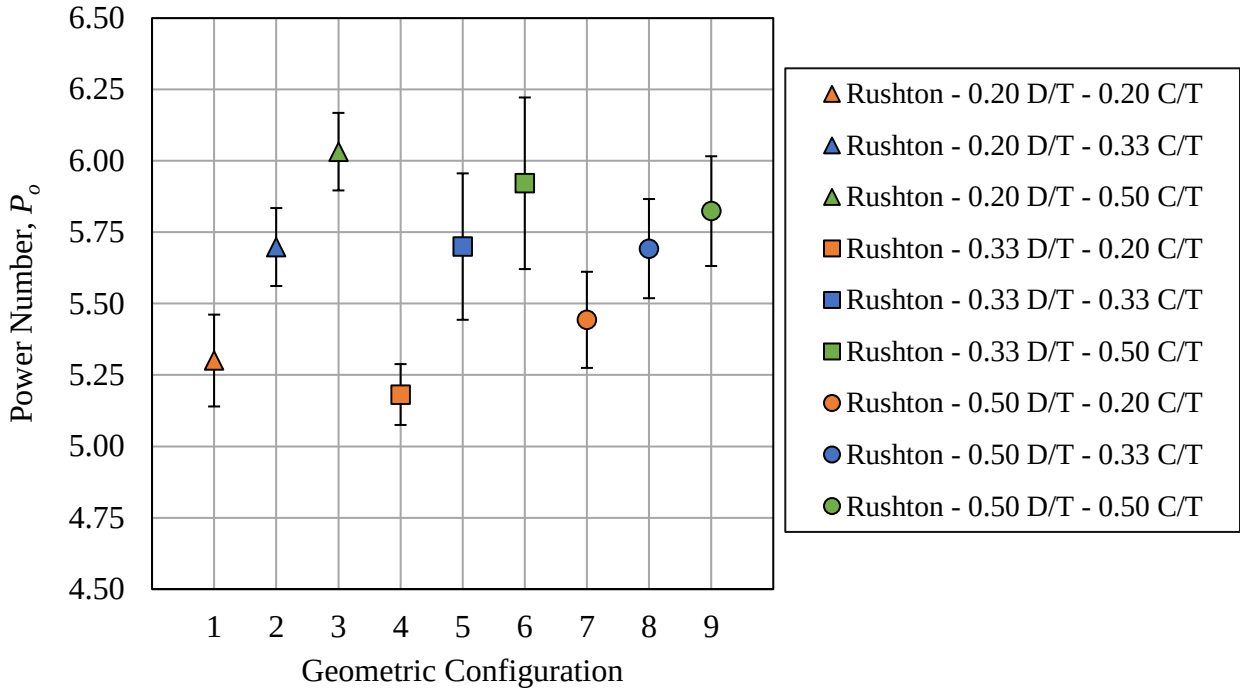

Figure 7.2.4. Average power numbers with *95%* confidence intervals, obtained from *24* measurements, for *9* Rushton geometric configurations.

Single power number values for the A310, PBT, and Rushton impellers were calculated by averaging all *216* power number measurements for each impeller. The standard deviation, coefficient of variance, and *95%* confidence interval were also calculated from each set of *216* measurements. The single P_o values for the A310, PBT, and Rushton impellers and corresponding statistical analysis is presented in Table 7.2.1.

Table 7.2.1. Nominal measured impeller power numbers with statistical analysis and comparison to stated values.

Impeller	A310	PBT	Rushton
P_o	0.35	1.39	5.64
StDev	0.04	0.14	0.52
CoeffVar	12.8%	10.1%	9.2%
95% CI	0.01	0.02	0.07
Adjusted P_o (*-10%*)	0.31	1.25	5.08
Adjusted *95% CI* (*-10%*)	0.01	0.02	0.06
Stated P_o	0.30	1.27	(5.10)

7.3 *Nθ*

Nθ was calculated from the rotational frequency and measured blend time for each trial. Measured θ_{95} and calculated values of *Nθ* for each trial are listed in Table B.1 in Appendix B. The *6* trials for a given experimental setup were averaged, and the mean θ_{95} and *Nθ* for the *108* experimental setups are reported in Table B.2 in Appendix B. The mean *Nθ* for a geometric configuration (comprised of an impeller type, *D/T*, and *C/T*) and its *95%* confidence interval were determined by averaging the *24* applicable trials. Mean *Nθ* with *95%* confidence intervals for the *9* A310, PBT, and Rushton geometric configurations are presented in Figures 8.3.1-3

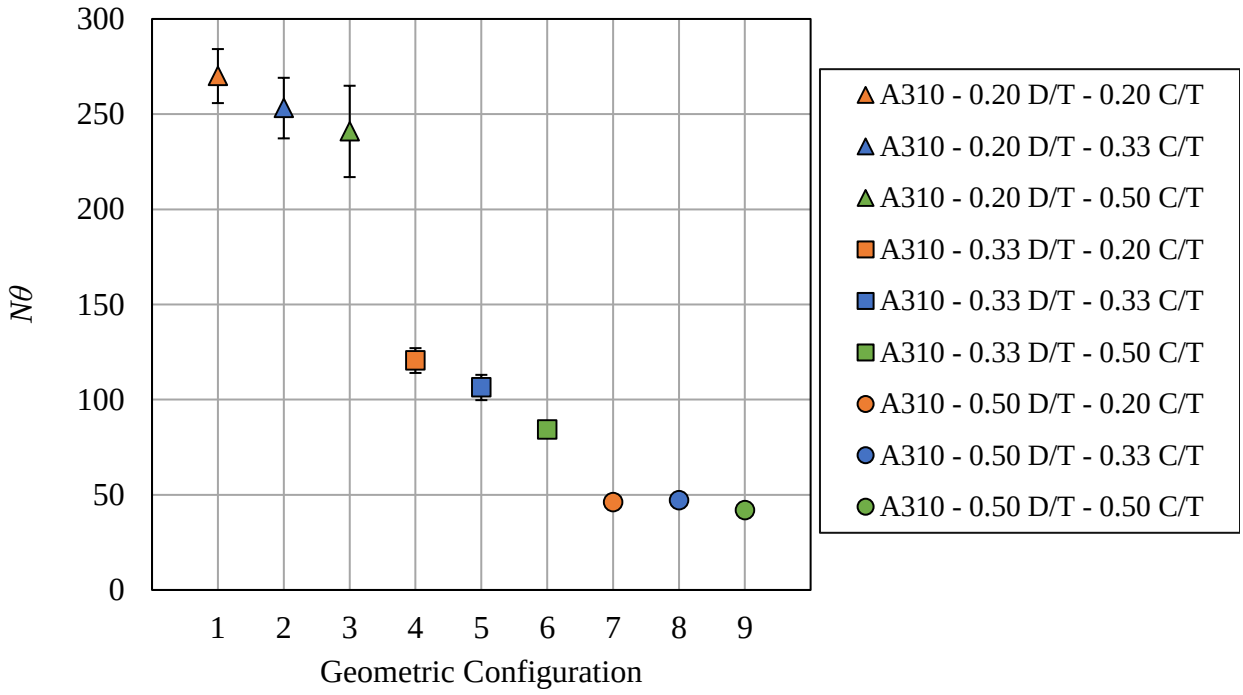

Figure 7.3.1. Average *Nθ* with *95%* confidence intervals, obtained from *24* measurements, for *9* A310 geometric configurations.

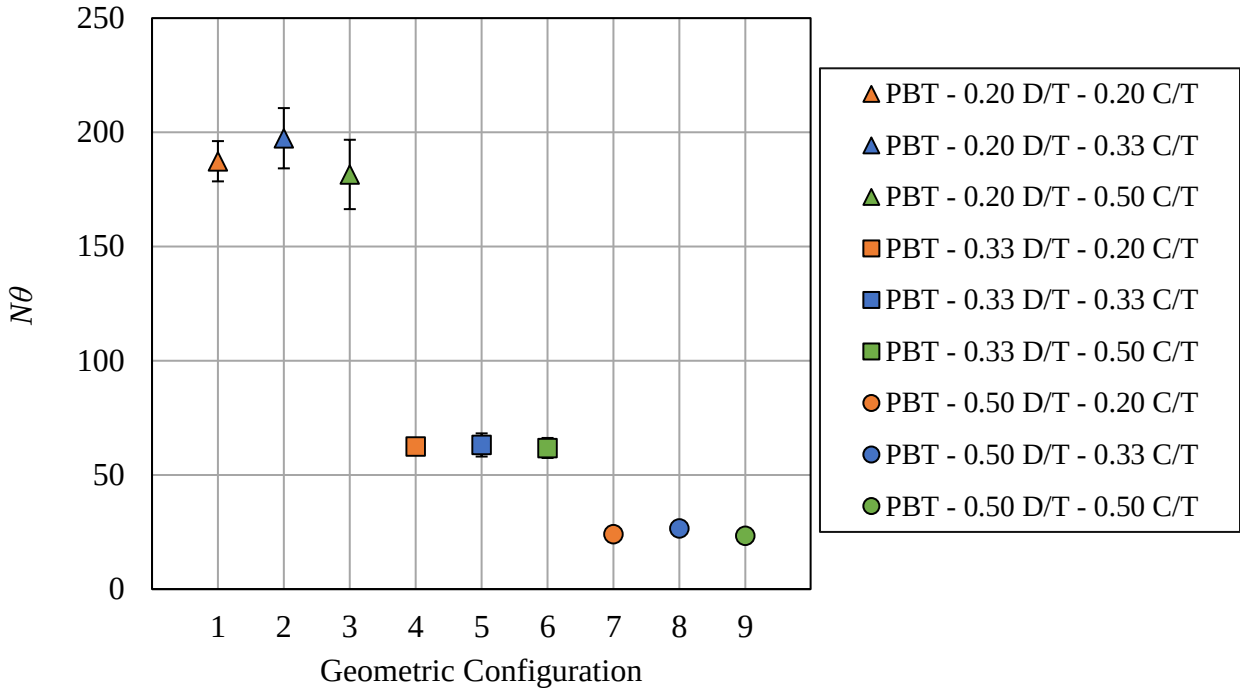

Figure 7.3.2. Average *Nθ* with *95%* confidence intervals, obtained from *24* measurements, for *9* PBT geometric configurations.

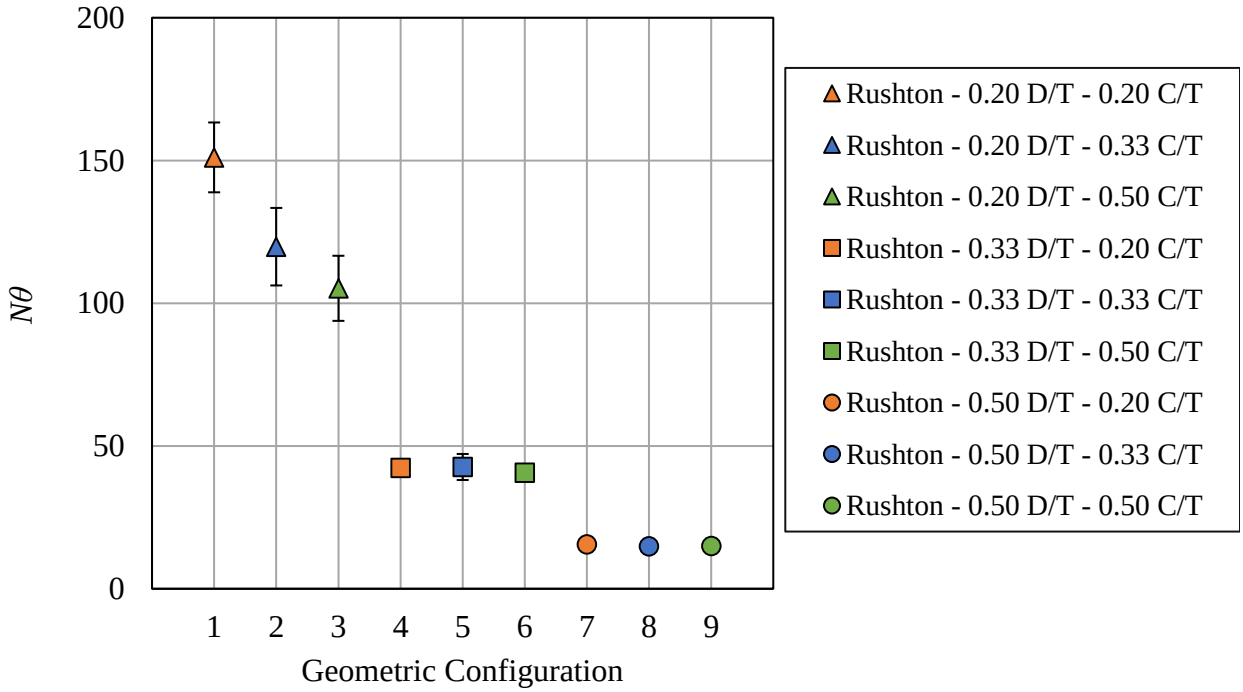

Figure 7.3.3. Average *Nθ* with *95%* confidence intervals, obtained from *24* measurements, for *9* Rushton geometric configurations.

Nθ values for combinations of the three *D/T* levels and A310, PBT, and Rushton impellers were calculated by averaging all *72* values for each combination. The standard deviation, coefficient of variance, and *95%* confidence interval were also calculated from each set of *72* values. *Nθ* for the A310, PBT, and Rushton impellers at the three *D/T* levels and corresponding statistical analysis is presented in Table 7.3.1.

Table 7.3.1. *Nθ* values with statistical analysis for combinations of impeller type and *D/T* levels.

Impeller	A310	A310	A310	PBT	PBT	PBT	Rushton	Rushton	Rushton
D/T	0.20	0.33	0.50	0.20	0.33	0.50	0.20	0.33	0.50
Nθ	255	104	45	189	62	25	125	42	15
StDev	45	20	7	30	10	4	35	8	2
CoeffVar	17.6%	19.5%	16.0%	16.1%	15.7%	15.1%	27.8%	18.0%	13.8%
95% CI	10.5	4.8	1.7	7.1	2.3	0.9	8.2	1.8	0.5

7.4 Turbulent Blend Time Correlation Suitability

The measured *95%* homogeneity blend times, θ_{95}, were compared to predicted blend times calculated from Grenville's turbulent blend time correlation (Equation 1.5) by plotting one against the other in Figure 7.4.1. If measured θ_{95} was predicted by the correlation, the data points would lie on a line with a slope of one. The equivalence line as well as *10%* and *20%* deviation lines were included. The correlation utilized the stated P_o values of *0.3*, *1.27*, and *5.1* for the A310, PBT, and Rushton impellers.

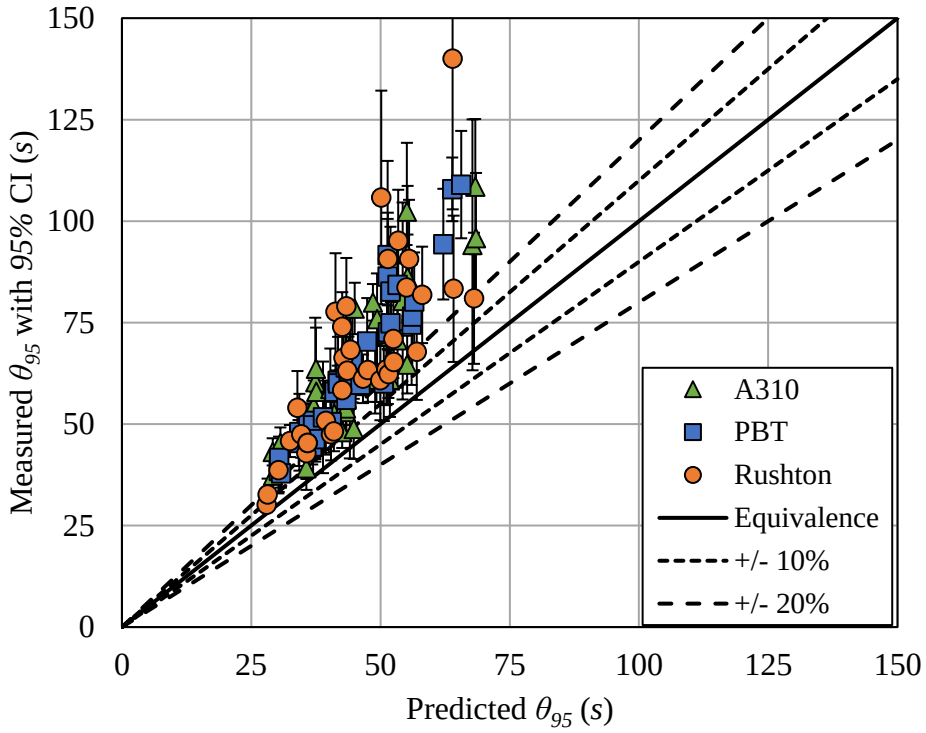

Figure 7.4.1. Measured values of θ_{95} compared to predicted values from Grenville's turbulent blend time correlation utilizing single stated values of P_o (*0.30*, *1.27*, and *5.10*).

To determine if the turbulent blend time correlation was a suitable, Equation 7.4.1 coefficients were fit to the measured values of θ_{95} using MatLab's *nonlinfit* function and compared to the stated values in Equation 3.2.6.

$$\theta_{95} = k\left(\frac{T}{D}\right)^{c} N^{-d} P_o^{-e} \tag{7.4.1}$$

The coefficients were fit four times using the single stated, single measured, geometric configuration, and individual setup values of P_o with known values of *D/T* and *N*. The coefficients with *95%* confidence intervals were reported in Table 7.4.1 for all four sets of P_o.

Table 7.4.1. Four coefficient fit of turbulent blend time correlation across four sets of P_o.

P_o Set	Single Stated		Single Measured		Geometric Configuration		Individual Setup	
Coefficient	Value	*95% CI*	Value	*95% CI*	Value	*95% CI*	Value	*95% CI*
k	5.65	3.86 - 7.44	5.87	4.04 - 7.70	5.27	3.69 - 6.85	5.44	3.85 - 7.02
c	2.24	1.95 - 2.52	2.24	1.96 - 2.52	2.34	2.07 - 2.61	2.31	2.04 - 2.57
d	1.05	0.89 - 1.21	1.05	0.89 - 1.21	1.10	0.94 - 1.25	1.09	0.94 - 1.24
e	0.34	0.28 - 0.40	0.35	0.29 - 0.41	0.37	0.31 - 0.42	0.36	0.30 - 0.41

Provided the turbulent blend time correlation was a suitable predictor of blend time, the leading coefficient in Equation 7.4.2 was fit to the measured values of θ_{95} using MatLab's *nonlinfit* function.

$$\theta_{95} = k\left(\frac{T}{D}\right)^{2} N^{-1} {P_o}^{-1/3} \tag{7.4.2}$$

The coefficient was fit four times using the single stated, single measured, geometric configuration, and individual setup values of P_o with known values of *D/T* and *N*. The coefficient with *95%* confidence interval was reported in Table 7.4.2 for all four sets of P_o.

Table 7.4.2. Leading coefficient fit of turbulent blend time correlation across four sets of P_o.

P_o Set	Single Stated		Single Measured		Geometric Configuration		Individual Setup	
Coefficient	Value	*95% CI*	Value	*95% CI*	Value	*95% CI*	Value	*95% CI*
k	7.51	7.29 - 7.72	7.80	7.57 - 8.03	7.80	7.58 - 8.02	7.79	7.57 - 8.01

The coefficient of determination, R^2, was calculated using the measured and predicted blend times for each of the eight fits (four *4* coefficient and four leading coefficient only) to compare their capability at predicting θ_{95}. The R^2 values are summarized in Table 7.4.3.

Table 7.4.3. Coefficient of determination, R^2, calculated for eight unique turbulent blend time correlation fits to compare their capability of predicting θ_{95}

P_o Set	Single Stated	Single Measured	Geometric Configuration	Individual Setup
4 Coefficient R^2	0.76	0.76	0.78	0.79
Leading Coefficient R^2	0.72	0.72	0.74	0.74

An example fit is shown in Figure 7.4.2 in which the measured *95%* homogeneity blend times, θ_{95}, were compared to predicted blend times calculated from the turbulent theory correlation (Equation 7.4.2) utilizing the leading coefficient fit from the single, stated values of P_o (*0.3*, *1.27*, and *5.1* for the A310, PBT, and Rushton). If measured θ_{95} was predicted by the correlation, the data points would lie on a line with a slope of one. The equivalence line as well as *10%* and *20%* deviation lines were included.

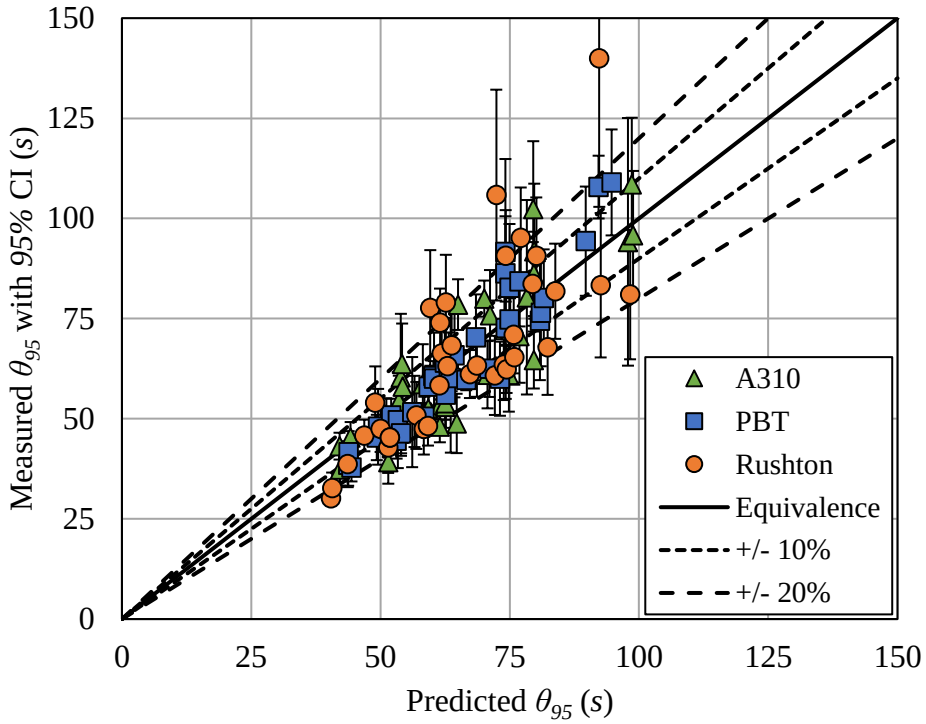

Figure 7.4.2. Measured values of θ_{95} compared to predicted values from turbulent blend time correlation utilizing single stated values of P_o (*0.30, 1.27,* and *5.10*) and leading coefficient of 7.5.

Setups with measured blend times whose *95%* confidence intervals did not fall within or overlap the *±10%* bounds were deemed outliers of the prediction. The outliers for the turbulent blend time correlation utilizing the single stated values of P_o (*0.3*, *1.27*, and *5.1* for the A310, PBT, and Rushton) and leading coefficient of 7.5 were compiled in Table 7.4.4.

Table 7.4.4. List of outlier setups whose measured blend times with *95%* confidence intervals did not fall within or overlap *+/- 10%* bounds of turbulent blend time correlation utilizing single stated values of P_o and leading coefficient of 7.5.

Measured θ_{95} Behavior	*T* (*m*)	Impeller	*D/T*	*C/T*	*C/D*
Longer than Predicted	1.22	A310	0.33	0.20	0.60
Longer than Predicted	1.22	Rushton	0.20	0.20	1.00
Quicker than Predicted	1.22	A310	0.33	0.50	1.50
Quicker than Predicted	1.22	Rushton	0.50	0.50	1.00
Quicker than Predicted	0.80	A310	0.33	0.50	1.50
Quicker than Predicted	0.80	A310	0.33	0.50	1.50
Quicker than Predicted	0.80	Rushton	0.50	0.33	0.67
Quicker than Predicted	0.80	Rushton	0.50	0.50	1.00
Quicker than Predicted	0.80	A310	0.20	0.50	2.50

7.5 Impeller Off-Bottom Distance Correction Factor

An initial impeller off-bottom location to tank diameter, *C/T*, correction factor was added to the modified turbulent blend time correlation according to Equation 7.5.1 to determine if blend time prediction would improve if *C/T* was accounted for.

$$\theta_{95} = 7.5\left(\frac{T}{D}\right)^{2} N^{-1} {P_o}^{-1/3} \left(\frac{1/3}{C/T}\right)^{f} = 7.5\left(\frac{T}{D}\right)^{2} N^{-1} {P_o}^{-1/3} \left(\frac{T}{3C}\right)^{f} \quad (7.5.1)$$

The initial *C/T* correction factor assumed an exponential form and was normalized to a *C/T* of *1/3*. The exponential coefficient, *f*, was fit using MatLab's *nonlinfit* function which returned a value of *0.16* with a *95%* confidence interval from *0.09* to *0.23*. The coefficient of determination between the measured and predicted values of θ_{95} was *0.77*. The outliers for the modified turbulent blend time correlation with exponential *C/T* correction factor utilizing the single stated values of P_o (*0.3*, *1.27*, and *5.1* for the A310, PBT, and Rushton) were compiled in Table 7.5.1.

Table 7.5.1. List of outlier setups whose measured blend times with *95%* confidence intervals did not fall within or overlap +/- *10%* bounds of the modified turbulent blend time correlation with exponential *C/T* correction factor utilizing single stated values of P_o.

Measured θ_{95} Behavior	*T (m)*	Impeller	*D/T*	*C/T*	*C/D*
Quicker than Predicted	0.80	PBT	0.33	0.20	0.60
Quicker than Predicted	0.80	PBT	0.33	0.20	0.60
Quicker than Predicted	0.80	PBT	0.50	0.20	0.40
Quicker than Predicted	0.80	PBT	0.50	0.20	0.40
Quicker than Predicted	0.80	Rushton	0.50	0.33	0.67
Quicker than Predicted	0.80	Rushton	0.50	0.20	0.40
Quicker than Predicted	0.80	A310	0.20	0.20	1.00

A polynomial *C/T* correction factor was then proposed according to Equation 7.5.2 for reasons explained in Section 8.5.

$$\theta_{95} = 7.5\left(\frac{T}{D}\right)^{2} N^{-1} {P_o}^{-1/3} \left[h\left(\frac{C}{T} - \frac{1}{2}\right)^{2} + j\right] \quad (7.5.2)$$

The vertex of the polynomial *C/T* correction factor was set to a *C/T* of *1/2*. The coefficients, *h* and *j*, were fit using MatLab's *nonlinfit* function which returned values of *1.60* and *0.94* with *95%* confidence intervals from *0.88* to *2.31* and *0.90* and *0.98*. The coefficient of determination between the measured and predicted values of θ_{95} was *0.76*. The outliers for the modified turbulent blend time correlation with polynomial *C/T* correction factor utilizing the single stated values of P_o (*0.3*, *1.27*, and *5.1* for the A310, PBT, and Rushton) were compiled in Table 7.5.2.

Table 7.5.2. List of outlier setups whose measured blend times with *95%* confidence intervals did not fall within or overlap *+/- 10%* bounds of the modified turbulent blend time correlation with polynomial *C/T* correction factor utilizing single stated values of P_o.

Measured θ_{95} Behavior	*T (m)*	Impeller	*D/T*	*C/T*	*C/D*
Longer than Predicted	1.22	PBT	0.20	0.33	1.67
Quicker than Predicted	0.80	PBT	0.33	0.20	0.60
Quicker than Predicted	0.80	PBT	0.33	0.20	0.60
Quicker than Predicted	0.80	PBT	0.50	0.20	0.40
Quicker than Predicted	0.80	PBT	0.50	0.20	0.40
Quicker than Predicted	0.80	Rushton	0.50	0.33	0.67
Quicker than Predicted	0.80	Rushton	0.50	0.20	0.40
Quicker than Predicted	0.80	A310	0.20	0.20	1.00
Quicker than Predicted	0.80	A310	0.20	0.50	2.50

The polynomial *C/T* correction factor coefficients, *h* and *j*, were also manually tuned to values of *1.00* and *0.96* as shown in Equation 7.5.3.

$$\theta_{95} = 7.5\left(\frac{T}{D}\right)^2 N^{-1} P_o^{\,-1/3}\left[\left(\frac{C}{T}-\frac{1}{2}\right)^2 + 0.96\right] \tag{7.5.3}$$

The coefficient of determination between the measured and predicted values of θ_{95} was *0.76*. The outliers for the modified turbulent blend time correlation with tuned polynomial *C/T* correction factor utilizing the single stated values of P_o (*0.3*, *1.27*, and *5.1* for the A310, PBT, and Rushton) were compiled in Table 7.5.3.

Table 7.5.3. List of outlier setups whose measured blend times with *95%* confidence intervals did not fall within or overlap *+/- 10%* bounds of the modified turbulent blend time correlation with tuned polynomial *C/T* correction factor utilizing single stated values of P_o.

Measured θ_{95} Behavior	*T (m)*	Impeller	*D/T*	*C/T*	*C/D*
Quicker than Predicted	0.80	PBT	0.33	0.20	0.60
Quicker than Predicted	0.80	PBT	0.50	0.20	0.40
Quicker than Predicted	0.80	Rushton	0.50	0.33	0.67
Quicker than Predicted	0.80	A310	0.20	0.50	2.50

All three *C/T* correction factors were compared in Figure 7.5.1 by plotting the blend time correction as a function of *C/T*. The correction factor applied at the three experimental *C/T* levels was called out for the three equations.

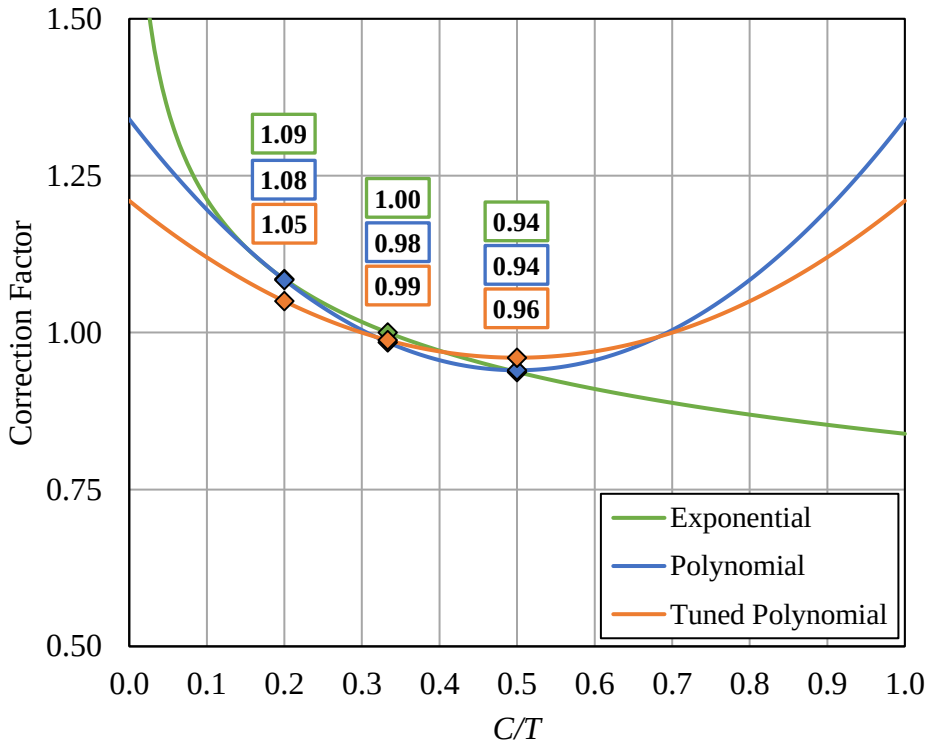

Figure 7.5.1. Comparison of the exponential, polynomial, and tuned polynomial *C/T* correction factor equations.

In Figure 7.5.2, the measured *95%* homogeneity blend times, θ_{95}, were compared to predicted blend times calculated from the modified turbulent theory correlation with tuned polynomial *C/T* correction factor utilizing single, stated values of P_o (*0.3*, *1.27*, and *5.1* for the A310, PBT, and Rushton). If measured θ_{95} was predicted by the correlation, the data points would lie on a line with a slope of one. The equivalence line as well as *10%* and *20%* deviation lines were included.

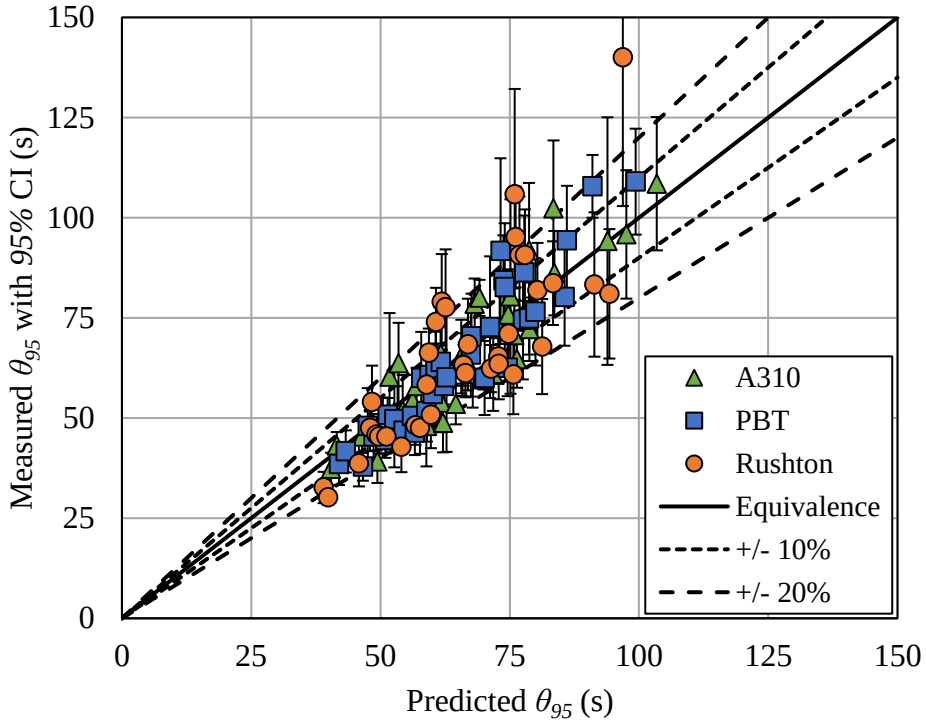

Figure 7.5.2. Measured values of θ_{95} compared to predicted values from the modified turbulent blend time correlation with tuned polynomial *C/T* correction factor utilizing single stated values of P_o (*0.30*, *1.27*, and *5.10*).

7.6 Investigation of Impeller Type Dependence

The comparison between measured and predicted blend time was separated by impeller type (A310, PBT, and Rushton) in Figures 7.6.1-3. The predicted blend times were calculated from the modified turbulent correlation with tuned polynomial *C/T* correction factor utilizing single stated values of P_o. If measured θ_{95} was predicted by the correlation, the data points would lie on a line with a slope of one. The equivalence line as well as *10%* and *20%* deviation lines were included.

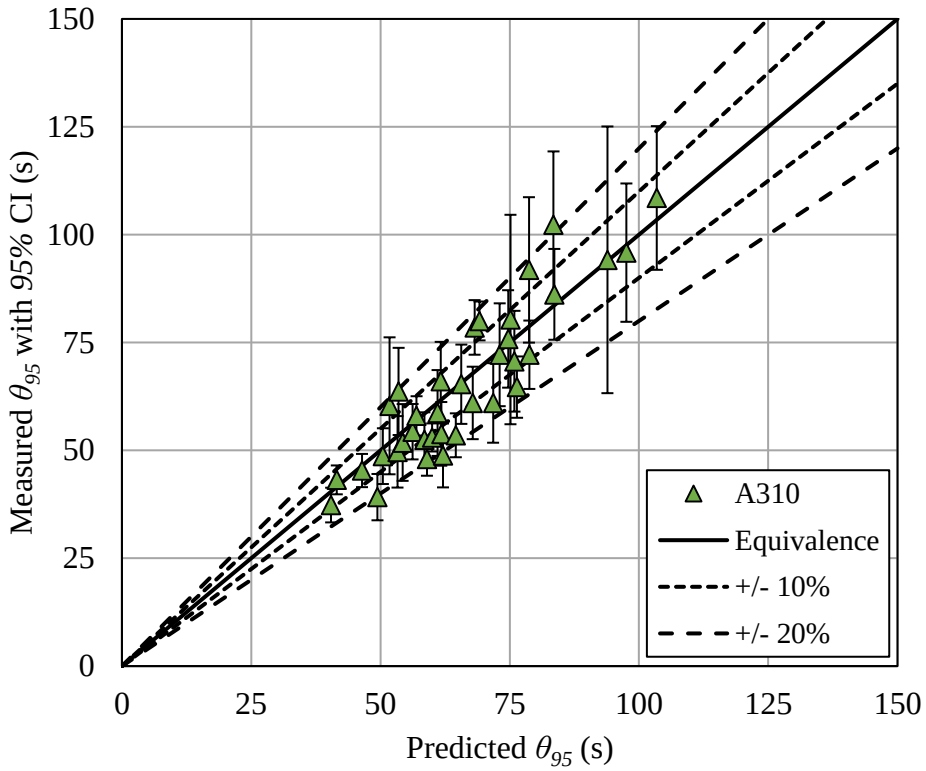

Figure 7.6.1. Measured values of θ_{95} compared to predicted values for the A310 impeller.

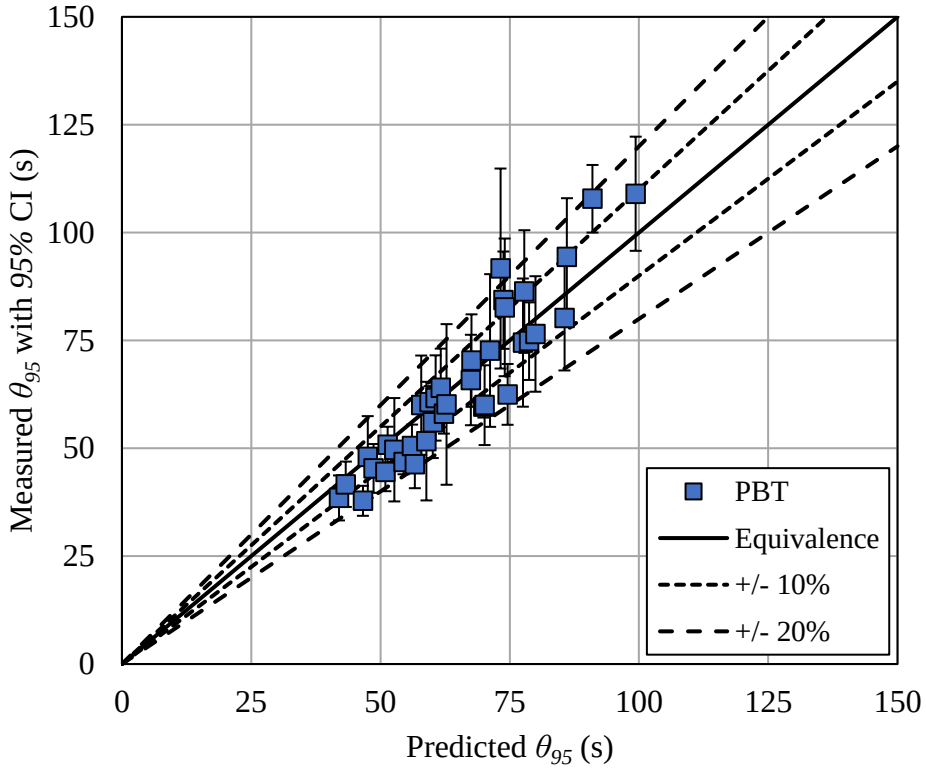

Figure 7.6.2. Measured values of θ_{95} compared to predicted values for the PBT impeller.

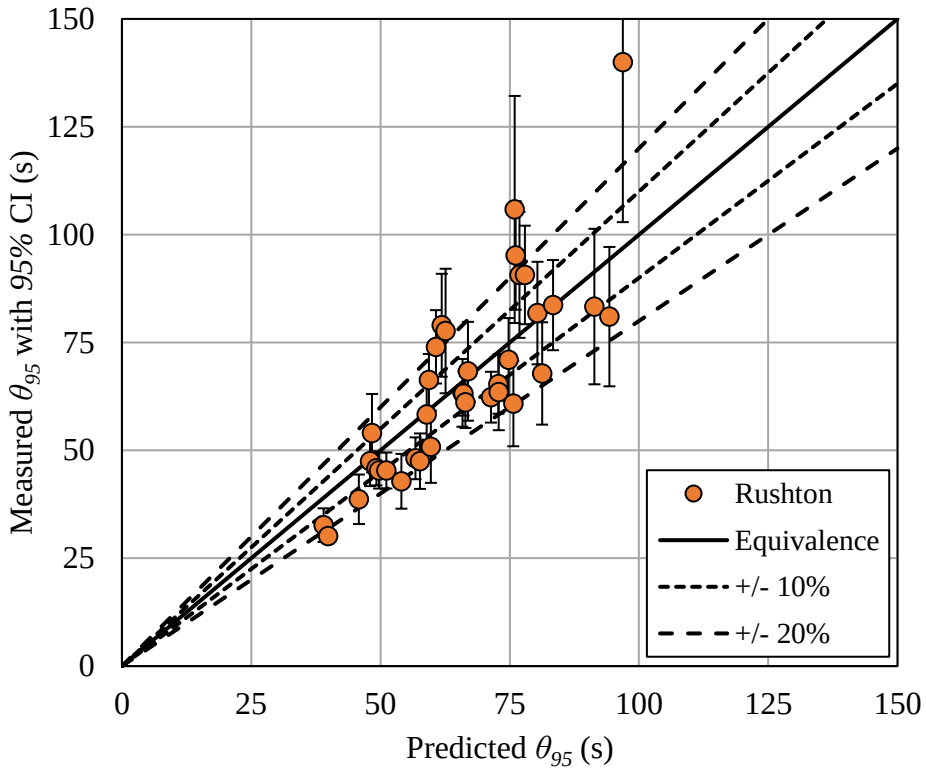

Figure 7.6.3. Measured values of θ_{95} compared to predicted values for the Rushton impeller.

The average coefficient of variance and coefficient of determination for θ_{95} were listed in Table 7.6.1 by impeller type.

Table 7.6.1. Average coefficient of variance and determination for θ_{95} by impeller type.

Impeller Type	A310	PBT	Rushton	All
θ_{95} *CoeffVar*	13.6%	14.1%	13.3%	13.7%
θ_{95} R^2	0.82	0.84	0.66	0.76

8.0 Discussion

8.1 Probe Location and Blend Time Determination

More than half of the time, the last probe to enter the *95%* homogeneity range was Probe 1. Probe 1 was located at the surface injection point. The two surface probes, Probes 1 and 2, determined the blend time almost *85%* of the time. There are at least three possible explanations for the observed behavior. The first is that the fluid surface near the walls is the furthest distance from the impeller so it requires the most time to blend. The second is that the last region to blend coincides with the injection and would relocate accordingly. The third is that a denser tracer injected at the surface sinks and must be transported back to the surface.

The first potential explanation is rooted in turbulent theory and could be tested by placing impellers in the upper half of the tank to determine if the last-to-blend location switches to the bottom of the tank. The second possible explanation has been previously disproved as relocating the injection near the impeller does not also relocate the last-to-blend location. The third possible explanation contradicts turbulent theory as blend time is not derived to be a function of physical properties in the fully turbulent regime, and could be tested with a tracer that is less dense than the bulk fluid.

8.2 Mean specific energy dissipation, ε, and power number, P_o

Reynolds numbers for the *108* setups ranged from *35,000* to *350,000*. All setups were operated in the fully turbulent regime as all exceeded the critical Reynolds number of *10,000*. However, Reynolds number only spanned one order of magnitude. Spanning two or three orders of magnitude would have been preferable, but mean specific energy dissipation was set to low levels to produce blend times in excess of *30 s*. Future testing in larger diameter tanks would increase experimental Reynolds numbers and span multiple orders of magnitude while maintaining blend times in excess of *30 s*.

Out of *108* total setups shown in Figure 7.2.1, *106* had average mean specific energy dissipation, ε, values within *20%* of the target values, *0.005* and *0.010 W/kg*. The two setups that exceeded the *20%* threshold both belonged to *0.2 D/T* A310 trials in the smaller, *0.80 m* diameter tank. The *0.2 D/T* A310 in the *0.80 m* diameter tank drew the least amount of torque, *0.0862* and *0.156 Nm*, so its power measurement was most prone to error. Variances in mean specific energy dissipation were inherently accounted for in all subsequent results. Due to measurements within acceptable tolerances, it was determined that experimental trials were conducted at acceptable levels of ε that coincided with target values.

As observed in Figure 7.2.2, the power number, P_o, of the A310 decreased as *D/T* increased except for the seventh geometric configuration. Additionally, P_o was statistically the same for a given *D/T* as *C/T* varied except for the seventh configuration. Axial impellers were previously reported to experience proximity effects that increased P_o at relatively close off-bottom locations, and the seventh configuration was the only case where *C/D* fell below *0.5* [1]. The seventh configuration outlier was explained by this phenomena, and indicated that the critical *C/D* for A310 proximity effects was between *0.4* and *0.6*. Across all A310 geometric configurations, the measured values of P_o exceeded the stated value of 0.3 and was unexpected [1].

For the A310 impeller, uncertainty in power number, P_o, decreased as *D/T* increased. This trend was expected as larger impellers had greater torque requirements which reduced the impact of variability originating from the torque cell. The A310 also had the lowest power number of the three impeller geometries which made it the most susceptible to torque cell noise because P_o is directly proportional to torque requirement.

As observed in Figure 7.2.3, the P_o of the PBT did not trend with *D/T*, but the range of reported values increased with *D/T*. For *0.20 D/T* configurations, P_o was statistically the same regardless of *C/T*. However, for *0.33 D/T* and *0.50 D/T* configurations, P_o was dependent on *C/T*. Proximity effects were observed and suggested that the critical *C/D* for PBT proximity effects was between *0.60* and *0.66*. The ninth geometric configuration had a reported P_o that suggested a proximity effect, but its *C/D* was *1* so it was an outlier to the trend and also possessed uncharacteristically high uncertainty. Seven of the PBT geometric configurations had measured values of P_o that exceeded the stated value of *1.27* [1].

For the PBT impeller, P_o uncertainty decreased significantly between *0.20 D/T* and *0.33 D/T* before remaining relatively constant between *0.33 D/T* and *0.50 D/T* except for the ninth geometric configuration. The reduction in uncertainty due to larger impeller diameters was expected but appeared to plateau; indicative of some base level of uncertainty. When reviewing the data for the ninth geometric configuration, possible scale dependence was discovered. The *0.80 m* vessel consistently measured P_o around *1.40* while the *1.22 m* vessel consistently measured P_o around *1.65*. Scale dependence introduced a second source of possible uncertainty besides torque cell variability.

As observed in Figure 7.2.4, Rushton P_o was statistically constant across *D/T* at a given *C/T*. Although not always statistically significant, P_o increased as *C/T* increased which was evidence of a fairly universal proximity effect. Radial impellers were previously reported to experience proximity effects that decreased P_o as the impeller was moved closer to the tank bottom [1]. Unlike the axial impellers, the Rushton proximity effect appeared to be a function of *C/T* instead of *C/D*. Reported values of Rushton P_o typically range between *5* and *6*, so there is no single stated value for comparison [1].

Across all geometric configurations, the Rushton impeller experienced relatively high levels of uncertainty which were previously only observed for *0.2 D/T* configurations with the exception of one outlier. Review of data from geometric configurations revealed there was significantly more uncertainty at *0.2 D/T* than at *0.33* and *0.5 D/T* for a given scale and operating condition as observed for the A310 and PBT, but there was also significant scale dependence that impacted *0.33* and *0.5 D/T* configurations more than *0.2 D/T*. Rushton P_o scale dependence has been previously reported and is a contributing factor as to why there is no single stated value [1].

The single P_o values for the A310 and PBT were statistically different than their stated values. A 10% reduction in P_o aligned the average measured value of both impellers with their stated values and signaled a discrepancy between measured P_o and actual P_o. Unconventional calibration of the strain-gauge torque cell signal was likely the source of the measurement discrepancy. Due to a significant zero shift from previous and unrelated testing, it was not possible to calibrate the signal using a minimum/maximum switch. Instead, a *0.4 m* calibration A310 impeller was utilized through an iterative process to set the zero and slope of the signal. The target value of the calibration A310's P_o was *0.33*: 10% higher than the stated value. At the time, this was done to ensure conservative power measurement. In hindsight, a calibration value of *0.30* should have been used to avoid a correction afterwards. If P_o was over measured by 10% then power draw and ε were also overstated by 10%. Fortunately, subsequent blend time correlation analysis could account and was performed for numerous values of P_o to gauge the effect.

For correlation analysis where a single P_o was used for a given impeller geometry, the measured P_o was *0.35*, *1.39*, and *5.64* for the A310, PBT, and Rushton while the stated P_o was *0.30*, *1.27*, and *5.1*. The stated Rushton P_o of *5.1* was selected to be consistent with the 10% over measurement that appeared to occur for the A310 and PBT.

Single P_o values, specifically the stated values, would be used by industrialists as they typically do not account for proximity effects or conduct live P_o measurements. As such, single stated P_o values were primarily utilized for correlation analysis due to their widespread adoption and simplicity. Agitator vendors with knowledge of proximity effects would adjust P_o accordingly, so correlation analysis was also performed with the average P_o for a given geometric configuration (values shown in Figures 7.2.2-4). Lastly, correlation analysis was performed with the measured P_o values for each of the *108* setups for the least common case in which live P_o measurements are made on a specific setup. By considering three levels of P_o specificity, it was possible to determine and quantify its impact on the accuracy of blend time prediction via turbulent theory correlations in Sections 7.4 and 8.4.

8.3 *Nθ*

Across Figures 7.3.1-3, *Nθ* decreased as *D/T* increased. This was expected as proportionally larger impellers achieve equal power input at lower rotational frequencies, and the trend is widely reported in previous studies [3]. *Nθ* also decreased for a given *D/T* as P_o increased (i.e. from the A310 to PBT to Rushton). This was also expected as impellers with greater power numbers achieve equal power input at lower rotational frequencies, and once again the trend is widely reported in previous studies [3]. Turbulent theory blend time correlations state *Nθ* is proportional to approximately the squared inverse of *D/T* and the cubic root of P_o. Meanwhile, Circulation theory blend time correlations predict *Nθ* is proportional to approximately the cubed inverse of *D/T*. Subsequent correlation analysis in Section 8.4 quantified the relationship between *Nθ*, *D/T*, and P_o.

A qualitative relationship between *Nθ* and *C/T* was also investigated with Figures 7.3.1-3. Seven out of the nine impeller and *D/T* combinations exhibited *C/T* independence while two (A310 at *0.33 D/T* and Rushton at *0.20 D/T*) exhibited dependence. For the two cases exhibiting *C/T* dependence, *Nθ* decreased as *C/T* increased. The effect of *C/T* on *Nθ* was preliminarily determined to be nonexistent or marginal and additional quantitative analysis is described in Section 8.5.

Experimental *Nθ* values were listed for impeller and *D/T* combinations in Table 7.3.1 and may be used to predict blend time for cases with geometric similarity. Kramers *et al.* reported that the relative standard deviation, otherwise known as coefficient of variance, for *Nθ* was *10%* [3, 14]. The average coefficient of variance of *Nθ* for the *108* setups, composed of *6* trials each, was *13.6%*. As setups were consolidated, the coefficient of variance rose and the values in Table 7.3.1 averaged to *17.7%*. The variance for a given setup was considered representative of inherent blend time variance and experimental error within a setup whereas the consolidated variance was considered to be the combined variance from blend time, any *C/T* effects, and experimental errors both within and across setups.

In general, the coefficient of variance for *Nθ* decreased as *D/T* increased for a given impeller. This made sense as proportionally larger impellers disperse energy more evenly and consistently within a vessel: theoretically reducing blend time fluctuations. The effect was marginal for the A310 and PBT, but quite significant for the Rushton as its variance more than halved when transitioning from *0.20 D/T* to *0.50 D/T*. A possible explanation for the discrepancy is that the Rushton is a flow-inefficient, shear-dominant impeller while the PBT is a mixed flow and shear impeller and the A310 is a flow-efficient, low-shear impeller. Because of the different characteristics, *0.20 D/T* Rushton impellers may not generate bulk tank circulation as consistently as proportionally larger Rushton impellers or other impeller geometries such as the A310 or PBT to disperse energy and blend the tank. Conversely, *0.50 D/T* Rushtons exhibited the lowest *Nθ* variance and produced the most consistent blend times which implied that they generated the most consistent bulk tank circulation and energy dissipation. The difference was

experimentally observed as *0.20 D/T* Rushtons exhibited significant transient flow behavior with haphazard surface plumes whereas *0.50 D/T* Rushtons exhibited consistent and stable surface flow. Meanwhile other impeller and *D/T* combinations behavior was between the two extremes.

8.4 Turbulent Blend Time Correlation Suitability

Grenville's turbulent blend time correlation was not a suitable predictor of blend time, θ_{95}, in this experiment. Measured values of θ_{95} were consistently longer than those predicted by the existing correlation which was easily observed in Figure 7.4.1 as all data points lied above the equivalence line. This was expected for two reasons. The first was a difference in probe location. The furthest probes from the impeller were positioned behind baffles at the liquid surface while FMP, from which Grenville's correlation is derived, positioned the probe furthest from the impeller a distance *T/3* from the surface [3]. Increased distance would result in increased blend time which was accounted for by the increased constant. The second was the definition of *95%* homogeneity differed from Grenville's original work. Grenville and his predecessors defined *95%* homogeneity as the point at which the root mean square conductivity fluctuation was *5%* of the total conductivity change [3]. However in this study, *95%* homogeneity was simply defined as the point at which *5%* of the magnitude of the total conductivity change was remaining in targeted last-to-blend locations. If the turbulent blend time correlation was suitable, then the differing probe location and *95%* homogeneity definition would only require a modification to the leading coefficient proposed by Grenville.

After Equation 7.4.1 was fit to the measured values of θ_{95}, the four coefficients, presented in Table 7.4.1, were compared to those in Equation 1.5. The leading coefficients of all four P_o sets ranged from *5.27* to *5.87* and were statistically the same as Grenville's leading coefficient of *5.2* due to large *95%* confidence intervals. The exponential coefficient for operating frequency, *d*, ranged from *1.05* to *1.10* and was statistically the same as the turbulent blend time correlation value of *1*. The exponential coefficient for impeller power number, *e*, ranged from *0.34* to *0.37* and was statistically the same as the turbulent blend time correlation value of *0.33*.

The exponential coefficient for *T/D*, *c*, ranged from *2.24* to *2.34* and was only statistically similar to Grenville's value of *2* when single values of P_o were utilized. The exponent on the *D/T* component of the turbulent blend time correlation contained a correction factor, so a deviation did not necessarily mean that the turbulent blend time correlation was unsuitable. If θ_{95} was strictly a function of power input, the *T/D* exponential coefficient would be *5/3* as stated in Equation 3.2.10. However, previous studies observed a *D/T* dependence so an exponential correction factor, *a*, was added to *5/3* as seen in Equation 3.2.11 [3,11,14-20]. The *D/T* exponential correction factor has been reported as *1/2* as well as *1/3* [3]. A value of *1/2* yielded a total *T/D* exponent of *2.17* while a value of *1/3* yielded a total exponent of *2*. An exponent of

2.17 was statistically similar to the fitted coefficient values across all four P_o sets while an exponent of *2* was only statistically similar for sets containing single values of P_o. Even though some uncertainty remained regarding the exponential correction factor for *D/T*, all four coefficients from Equation 7.4.1 were statistically similar to the turbulent blend time correlation coefficients when using single values of P_o for a given impeller geometry. Therefore, only the leading coefficient had to be modified from Grenville's turbulent blend time correlation.

After fitting Equation 7.4.2 to the measured values of θ_{95}, it was determined that the leading coefficient, *k*, ranged from *7.51* to *7.80* with a *95%* confidence interval of *7.29* to *8.03* across all four sets of P_o as observed in Table 7.4.2. The leading coefficients were greater for the single versus four coefficient fits because the leading coefficient compensated for the decreased contributions from *T/D*; the *N* and P_o changes were off-setting. Interestingly, the Single Measured, Geometric Configuration, and Individual Setup sets of P_o all returned leading coefficient values of *7.8* which indicated that more comprehensive P_o information did not impact the fit. The Single Stated leading coefficient was expected to be lower than the other three as a decrease in the leading coefficient offset the *10%* reduction correction in P_o. In fact, the *10%* reduction in P_o was exactly offset by the leading coefficient (*7.5* is *96%* of *7.8* and *0.9* raised to a third is *0.96*). The same phenomena was observed between the two single P_o sets in the four coefficient fit presented in Table 7.4.1 while the exponential coefficients remained unchanged.

The coefficients of determination, R^2, calculated from measured and predicted values of θ_{95} for the eight fits, shown in Table 7.4.3, ranged between *0.72* and *0.79*. The four coefficient fits ranged between *0.76* and *0.79* and provided better predictability than leading coefficient fits which ranged between *0.72* and *0.74*. More comprehensive information regarding P_o resulted in a better prediction. This was expected as the turbulent blend time theory is based on power input which is directly proportional to P_o. There was no difference in predictability between the single measured and stated sets of P_o as the *10%* difference was offset by the leading coefficients. Unfortunately, the lowest coefficient of determination, *0.72*, belonged to the most commonly utilized method of predicting θ_{95}, single stated values of P_o plugged into the standard turbulent blend time correlation with modified leading coefficient in this case.

A visual comparison of measured and predicted θ_{95} for the turbulent blend time correlation with modified leading coefficient utilizing single stated values of P_o in Figure 7.4.2 showed that simply changing the leading coefficient from *5.2* to *7.5* greatly improved the accuracy of the turbulent blend time correlation in this study. Of the *108* total setups, only *9* were outliers: meaning that the *95%* confidence interval for a measured blend time did not fall within or overlap the *+/- 10%* bounds of the prediction. The turbulent blend time correlation with modified leading coefficient utilizing single stated values of P_o was capable of predicting θ_{95} for more than *90%* of setups when considering intrinsic variance in $N\theta$ and measurement uncertainty.

Since the turbulent blend time correlation was suitable and only required a modified leading coefficient from Grenville's value of *5.2* to the modified value of *7.5*, the sources of discrepancy

were differing probe location and definition of *95%* homogeneity. Kresta *et al.* proposed a leading coefficient of *5.8*, and the third reference point enabled comparisons to determine approximate contributions of the two sources on discrepancy [7]. Kresta *et al*. positioned two probes at the liquid surface behind baffles (similar to this study's experimental setup) and a third probe was placed *0.1 m* below the surface in the *0.14* and *0.24 m* tanks [7]. However, Kresta *et al*. determined *95%* homogeneity from the average of the three probes' coefficients of variance which shared more similarity with Grenville's definition than this study's [3,7]. Therefore, the contribution of probe location may be approximated as the difference between Kresta *et al*.'s and Grenville's leading coefficients compared to the difference between this study's and Grenville's leading coefficients: *0.6/2.3* or approximately *25%*. The remaining *75%* may be attributed to differing definitions of *95%* homogeneity. An important distinction between the definitions was whether spatial averaging was utilized (as was the case for Grenville and Kresta *et al.*) or if a single "last-to-blend" probe location determined the threshold for *95%* homogeneity (as was the case for this study) [3,7]. Spatial averaging is less conservative and reduces the measured blend time as probes (i.e. local regions) above *95%* counterweight probes below *95%*. Meanwhile, determining measured blend time with a single "last-to-blend" probe location (i.e. local region) is more conservative, increases the measured value, and ensures a minimum homogeneity is achieved throughout the vessel, but comes with the caveat that the bulk homogeneity is actually above *95%*. Additional analysis would be required to separate the spatial averaging versus local determination discrepancy contribution from that of the three separate calculation methods (i.e. root mean square conductivity fluctuation, coefficient of variance, and normalized magnitude), but was not pursued in this study. The increase in the leading coefficient from *5.2* to *7.5* may be attributed to approximately *25%* differing probe location and *75%* differing definition of *95%* homogeneity.

8.5 Impeller Off-Bottom Distance Correction Factor

The nine outliers listed in Table 7.4.4 were categorized by the relationship between the measured and predicted blend times. In two of the setups, the turbulent blend time correlation with modified leading coefficient utilizing single stated values of P_o underestimated the measured blend time. This result was not desirable as the correlation should be conservative to ensure blending occurs within the predicted time. Both setups possessed a *C/T* of *1/5* while *D/T* and *C/D* varied. The measured blend times for the other seven setups were overestimated by the modified turbulent blend time correlation. While this outcome was also undesirable, overestimation was preferable to underestimation. Six of the seven overestimation setups possessed a *C/T* of *1/2* while *D/T* and *C/D* varied. The nine outliers suggested that a *C/T* correction factor, similar to the *D/T* correction factor, may be warranted as impellers in close proximity to the tank bottom took longer than expected to blend while centrally located impellers took shorter than expected to blend.

An exponential *C/T* correction factor was added in Equation 7.5.1 to test if accounting for *C/T* improved blend time prediction. It was normalized to a *C/T* of *1/3* as that impeller location was predominantly utilized in previous studies [3]. Accounting for C/T improved predictability as the coefficient of determination increased from *0.72* to *0.77*. However, the number of outliers was only reduced from nine to seven. The correlation became exclusively conservative as all seven outliers overestimated blend time with the measured value occurring more quickly, but the correlation appeared to overcorrect for close proximity as six of the seven outliers possessed a *C/T* of *1/5*.

A more significant issue than overcorrection was that an exponential *C/T* correction factor was not theoretically sound. For a square batch with *H/T = 1*, *C/T* could range between *0* and *1*. Plotting the exponential correction term along the possible *C/T* range in Figure 7.5.1 revealed the theoretical dilemma. According to the exponential correction term, an impeller moved towards the tank bottom would take an increasingly steep blend time penalty while an impeller moved towards the liquid surface would blend the fluid more quickly. While a low *C/T* penalty was observed, it was not expected to approach infinity if an impeller was placed at the tank bottom. Conversely, an impeller located at the liquid surface was not expected to produce the quickest blend time as it would be splashing: struggling to both dissipate energy and establish bulk flow in the fluid. In general, an impeller located in the upper half of the tank was not expected to blend the fluid quicker than an impeller located in the lower half of the tank. As an impeller approached the liquid surface, blend time was expected to increase similarly to an impeller approaching the tank bottom as the maximum distance for energy dissipation from impeller to furthest wall location increased in both cases. While the exponential *C/T* correction factor improved blend time prediction, erroneous extrapolation based on a theoretical analysis necessitated a change in the mathematical form.

A polynomial *C/T* correction factor was introduced in Equation 7.5.2 to replace the exponential version as it coincided with theoretical expectations. The vertex of the polynomial was set to a *C/T* of *1/2* which was the optimum theoretical location as it minimized the maximum distance for energy dissipation by placing the impeller such that the liquid level was split in two. As the impeller approached the tank bottom or liquid surface, the correction factor increased the predicted blend time. The penalty for an impeller at a given distance above or below a half *C/T* was assumed equal because density and gravitational effects have no impact on fully turbulent blend time according to the turbulent theory and correlation.

Similar to the exponential form, accounting for C/T with the polynomial correction factor improved predictability as the coefficient of determination increased from *0.72* to *0.76*. However, the number of outliers returned to nine. One blend time was underestimated while the other eight were overestimated. Once again the *C/T* factor appeared to overcorrect for close proximity setups as six of the eight overestimated outliers possessed a *C/T* of *1/5*. Manually tuning the polynomial fit coefficients from *1.60* and *0.94* to *1.00* and *0.96* reduced the magnitude of the correction factor as observed in Figure 7.5.1, maintained an R^2 of *0.76*, and decreased the number of outliers from nine to four. The improved blend time prediction was shown in Figure 7.5.2.

The four outliers, listed in Table 7.5.3, were all overestimated, so the prediction was conservative. The four outliers all occurred in the smaller *0.8 m* vessel, but were otherwise a random assortment containing all three impeller types, *D/T*, and *C/T*. Further inspection revealed that only one outlier exceeded *+/- 13%* bounds with the final outlier requiring *+/- 21%* bounds to be considered statistically similar. The modified turbulent blend time correlation with tuned polynomial *C/T* correction factor utilizing single stated values of P_o was capable of predicting statistically similar θ_{95} for more than *95%* of setups given *+/- 10%* bounds and *99%* of setups given *+/- 13%* bounds.

8.6 Investigation of Impeller Type Dependence and Comments on Turbulent Blend Time Theory

If impeller type was a contributing factor, the blend time data for a better performing impeller would fall below the equivalence line while a worse performing impeller's data would fall above the equivalence line. Inspection of Figures 7.5.2 and 7.6.1-3 revealed that no impeller type was blending the fluid consistently quicker than any other type of impeller. Based on this observation, turbulent blend time theory was supported while circulation blend time theory was refuted.

The average coefficient of variation for θ_{95} across all 108 setups was *13.7%* and the averages for each impeller type varied by less than a percent. This meant that on average, each impeller type experienced a similar variance in blend time. This further supported turbulent blend time theory as a given impeller type did not produce more consistent blend times than another.

The average coefficient of variance for $N\theta$ (*13.6%*) was synonymous with that of θ_{95} (*13.7%*) because *N* was easily measured accurately. Kramers *et al.* reported a coefficient of variance of *10%* for $N\theta$ which was supported by Grenville as well as others and attributed to the inherently transient nature of stirred tanks [3]. The additional variance in this study was likely caused by the observed variance in P_o across varying *D/T* and *C/T* as P_o was previously reported to be constant [1]. The observed *10.7%* variance in P_o would contribute an additional variance of *3.3%* to *3.8%* to $N\theta$ according to the proportionality in Equation 7.5.3 which is in line with the observed excess.

Grenville's leading coefficient was *5.2 +/- 10%* relative variation, and he concluded that the relative variation in the leading coefficient originated solely from the variation in $N\theta$. Grenville's conclusion was supported as the variation required to predict statistically similar blend time for *99%* of setups was *+/- 13%* which was within a percent of the observed variance for $N\theta$. Once again, turbulent blend time theory was supported.

Interestingly though, the A310 and PBT had coefficients of determination of *0.82* and *0.84* while the Rushton's coefficient of determination was significantly lower at *0.66*. This meant that the A310 and PBT experienced less blend time variability between setups than the Rushton. The modified turbulent blend time correlation with tuned polynomial *C/T* correction factor utilizing single stated values of P_o predicted θ_{95} more accurately and consistently for the A310 and PBT versus the Rushton.

9.0 Conclusions and Recommendations

9.1 Conclusions

1. Turbulence based blend time theory was well supported for predicting blend time of a turbulent, Newtonian fluid as the exponential coefficients for *D/T*, *N*, and P_o were statistically similar to theoretical values when fit to experimental results. The turbulent blend time correlation with modified leading coefficient, Equation 9.1.1, predicted statistically similar θ_{95} for *93.5%* of experimental setups given *+/- 10%* bounds when utilizing single stated values of P_o (*0.3*, *1.27*, and *5.1* for the A310, PBT, and Rushton).

$$\theta_{95} = 7.5\left(\frac{T}{D}\right)^2 N^{-1} {P_o}^{-1/3} \tag{9.1.1}$$

   Modification of the leading coefficient from *5.2* to *7.5* was required as probe location and the definition of 95% homogeneity differed from Grenville's previous work.

2. θ_{95} exhibited *D/T* dependence which was expressed as an additive component on the *T/D* exponent. If blend time was independent of impeller to tank diameter ratio, the *T/D* exponent would have been *5/3*. Previous studies reported additive components of *1/3* and *1/2* to account for *D/T* dependence and resulted in total exponents of *2* and *13/6*. When fit to experimental results, an exponent of *5/3* was excluded while exponents of *2* and *13/6* were statistically acceptable when using single stated values of P_o. To maintain consistency with Grenville's well-accepted turbulent blend time correlation, a *T/D* exponent of *2* was selected.

3. θ_{95} exhibited *C/T* dependence which was expressed as a polynomial correction factor multiplied through Equation 9.1.1 as shown in Equation 9.1.2.

$$\theta_{95} = 7.5\left(\frac{T}{D}\right)^2 N^{-1} {P_o}^{-1/3}\left[\left(\frac{C}{T} - \frac{1}{2}\right)^2 + 0.96\right] \tag{9.1.2}$$

   The modified turbulent blend time correlation with *C/T* correction factor predicted statistically similar θ_{95} for *96%* of experimental setups given *+/- 10%* bounds and *99%* of setups given *+/- 13%* bounds when utilizing single stated values of P_o (*0.3*, *1.27*, and *5.1* for the A310, PBT, and Rushton).

4. θ_{95} was independent of impeller type as none of the three impellers were consistently blending the vessel quicker than the other two. Impeller type independence strongly supported power input based turbulence theory and refuted circulation theory. Different impeller types blended fluid in the turbulent regime at the same rate as long as power input, *D/T*, and *C/T* were equivalent for a given scale.

5. The *+/- 13%* bounds on the leading coefficient in Equation 9.1.2 were consistent with the relative variance observed for $N\theta$ (*13.7%*) which originated from the inherently transient nature of stirred tanks (*≈10%* contribution) and P_o variance (*3.3-3.8%* contribution).

6. P_o had an average relative variance of *10.7%* across scales, energy dissipation rates, and geometric configurations for a given impeller geometry and was not constant.

7. Conductivity probes positioned behind baffles at the liquid surface determined the blend time for almost *85%* of setups when using a denser tracer added at the liquid surface.

9.2 Recommendations

1. The turbulent blend time correlation with modified leading coefficient and tuned polynomial *C/T* correction factor presented in Equation 9.1.2 should be utilized to predict θ_{95} using single stated values of P_o for turbulent, Newtonian fluids blended by vertical, on-center mounted agitators in baffled tanks that possess an *H/T* of *1*. The correlation interpolates and is verified between *1/5* and *1/2* for *D/T* and *C/T*, but extrapolates beyond those bounds. The most power efficient configuration within experimental bounds was a *1/2 D/T* impeller located at *1/2 C/T*. Per the recommended correlation, such a configuration will blend a vessel *33%* quicker than a *1/5 D/T* impeller at *1/5 C/T* at equal power input.

   The recommended correlation can likely be used for turbulent, pseudo-plastic fluids as well per Grenville's previous findings, but pseudo-plastic fluids were not within the experimental scope [3].

2. Evidence of an optimum *D/T* was not observed within the experimental range of *1/5* to *1/2* as blend time continued to decrease as *D/T* increased. Therefore, θ_{95} may be reduced by selecting larger *D/T* impellers versus smaller *D/T* impellers at equal power input. For example, selecting *1/2 D/T* over *1/5 D/T* would provide a *25%* blend time reduction at equal power per the recommended correlation. However, exceeding a *D/T* of *1/2* is not suggested without additional experimentation. Future work should test *2/3* and *4/5 D/T* impellers in addition to *1/5*, *1/3*, and *1/2* to determine if an optimum *D/T* exists. If an optimum does exist, the turbulent blend time correlation should be modified to inherently direct users towards the optimum.

3. Evidence of an optimum *C/T* was not observed within the experimental range of *1/5* to *1/2* as blend time continued to decrease as *C/T* increased. For example, selecting *1/2 C/T* over *1/5 C/T* would provide a *10%* blend time reduction at equal power per the

recommended correlation. An optimum was theorized to exist at a *C/T* of *1/2* and was implemented with the tuned polynomial correction factor. Future work should test *2/3* and *4/5 C/T* locations in addition to *1/5*, *1/3*, and *1/2* to verify or refute the theorized optimum.

Since *H/T* was constrained to *1*, *C/T* and *C/H* were equivalent. However, for cases in which *H/T* is not *1*, *C/T* and *C/H* would not be equivalent. Since the theoretical basis for the *C/T* correction factor relied on splitting the liquid level with impeller placement, *C/H* should likely replace *C/T*. As *H/T* varies above and below *1*, the magnitude of the *C/H* correction factor at a given setting should likely vary as well: decreasing in severity below an *H/T* of *1* due to decreased maximum distance for energy dissipation and increasing in severity above an *H/T* of *1* due to increased maximum distance for energy dissipation. A possible form of a *C/H* correction factor was multiplied through Grenville's turbulent blend time correlation for varying *H/T*, Equation 1.5, and was presented in Equation 9.2.1

$$\theta_{95} = 5.2\frac{T^{3/2}H^{1/2}}{D^2}N^{-1}{P_o}^{-1/3}\left[\left(\frac{H}{T}\right)^p\left(\frac{C}{H}-\frac{1}{2}\right)^2 + 0.96\left(\frac{H}{T}\right)^q\right] \qquad (9.2.1)$$

The proposed form would account for varying *H/T* and *C/H*. Future work would be required to determine if the off-bottom distance correction factor is dependent on *C/T* or *C/H* and if the proposed form accurately accounts for varying *H/T* and *C/T* or *C/H* when predicting θ_{95}. Future work should test *H/T* from *0.5* to *2.0* in half *H/T* intervals with *C/H* values of *0.20*, *0.35*, *0.50*, and *0.65*.

4. All impeller types should be considered equally power efficient at blending turbulent, Newtonian fluids in baffled vessels with a single impeller mounted vertical on-center. However, the correlation predicted θ_{95} more accurately for the A310 and PBT compared to the Rushton so their use would be preferable. Further work on blending with single impellers should utilize a single impeller geometry, such as an A310 or PBT, to minimize variables and required trials.

   It is important to note that impeller type independence for blending of turbulent, Newtonian fluids is only valid for single impeller agitators and does not hold for multiple impeller agitators.

5. Stirred tanks are inherently transient, so any application that is strongly dependent on blend time should be treated conservatively. This means applying an additional *13%* to the recommended leading coefficient of *7.5* to produce a conservative prediction of θ_{95} that the agitator will consistently meet.

6. While P_o is widely considered constant in the turbulent regime and a constant P_o accurately predicts blend time, it is worth noting that P_o was observed to have a relative variance of *10.7%* on average across scales, energy dissipation rates, and geometric configurations. A more accurate blend time θ_{95} prediction was achieved if geometric configuration or direct P_o measurements were considered.

7. If limited in quantity, conductivity probes determining θ_{95} should be placed behind baffles at the liquid surface when injecting a denser tracer at the liquid surface. This is likely true for any system in which the impeller is placed in the lower half of the vessel, but was not confirmed.

10.0 Acknowledgements

I would like to offer a general thank you to the numerous individuals that have supported my educational pursuit and contributed knowledge throughout the years including my parents, siblings, extended family, friends, teachers, professors, colleagues, and employers. This thesis is the culmination of their invested time and effort. Additionally, several individuals or organizations were directly involved with the project, and I would like to recognize their specific contributions.

First, I would like to thank SPX Flow Lightnin and their customers for inspiring the thesis topic as well as supplying the required resources and funding for the investigation.

Second, I would like to thank Dr. Edward Hensel for his unrelenting support throughout the project, his valuable input on the investigation's content and communication, and his editing of both the proposal and thesis.

Third, I would like to thank my thesis committee, Dr. Edward Hensel, Dr. Risa Robinson, and Dr. Steven Day, for reviewing the proposal and thesis, asking questions, and providing feedback.

Fourth, I would like to thank Richard Kehn and Kevin Logsdon for their support and feedback as the thesis progressed from concept to completion.

Fifth, I would like to thank Jeffery Flint for preparing the physical experimental apparatus so I could perform efficient and consistent trials.

Sixth, I would like to thank Jeffery Flint, Richard Howk, and Kevin Logsdon for assisting with troubleshooting of probe and meter signals. Without their help, it would have taken me significantly longer to commence trials.

Seventh, I would like to thank Dr. Steven Day and Mark Spirko for proofreading the thesis.

Last and not least, I would like to thank my fiancé, Tracey Dickinson, for her patience, handling of additional responsibilities, and acceptance of reduced togetherness as the thesis consumed the majority of my free time in 2017.

Finally, I would like to dedicate this work to Joseph Radell (July 7, 1986 – October 22, 2017). He was a dear friend that I lost far too soon.

11.0 References

[1] Paul, E. L., Atiemo-Obeng, V. A., and Kresta, S. M., 2004, Handbook of Industrial Mixing : Science and Practice, Wiley-Interscience, Hoboken, N.J.
[2] 2015, "Mixing Xxv Final Program," Proc. Mixing XXV Final Program, Quebec City, CAN.
[3] Grenville, R. K., 1992, "Blending of Viscous Newtonian and Pseudo-Plastic Fluids," Doctor of Philosophy Cranfield Institute of Technology.
[4] Liu, M., 2014, "Efficiencies of Impeller Performance for Turbulent Blending," North American Mixing Forum, Lake George, NY USA.
[5] Myers, K. J., Jones, J. K., Janz, E. E., and Fasano, J. B., 2014, "Effect of Liquid Level and Agitator Pumping Direction on Turbulent Blend Times," Canadian Journal of Chemical Engineering, 92(4), pp. 643-647.
[6] Strand, A., and Kehn, R., 2016, "Flow Efficiency of an Axial Impeller with Varying Diameter and Off Bottom Location," North American Mixing Forum, Quebec City, CAN.
[7] Kresta, S. M., Mao, D. M., and Roussinova, V., 2006, "Batch Blend Time in Square Stirred Tanks," Chemical Engineering Science, 61(9), pp. 2823-2825.
[8] Vickroy, B., 2015, "Correlation of Non-Baffled, Angled & Off Center Agitated Process Vessel Blend Times."
[9] Nienow, A. W., 2014, "Stirring and Stirred-Tank Reactors," Chemie Ingenieur Technik, 86(12), pp. 2063-2074.
[10] Thomson, J., 1855, "Report Made to the President and Council of the Royal Society, of Experiments on the Friction of Discs Revolving in Water," Proceedings of the Royal Society of London, 7, pp. 509-511.
[11] White, A. M., and Brenner, E., 1934, Trans. AIChE, 30, pp. 585-592.
[12] Rushton, J. H., Costich, E. W., and Everett, J. H., 1950, "Power Characteristics of Mixing Impellers," Chem. Eng. Progress, 46, pp. 395-404, 467-476.
[13] Nienow, A. W., 1997, "On Impeller Circulation and Mixing Effectiveness in the Turbulent Flow Regime," Chemical Engineering Science, 52(15), pp. 2557-2565.
[14] Kramers, H., Baars, G. M., and Knoll, W. H., 1953, "A Comparative Study on the Rate of Mixing in Stirred Tanks," Chemical Engineering Science, 2(1), pp. 35-42.
[15] Van De Vusse, J. G., 1955, "Mixing by Agitation of Miscible Liquids: Parts I and Ii," Chemical Engineering Science, 4, pp. 178-200, 209-220.
[16] Prochazka, J., and Landau, J., 1961, "Studies on Mixing Xii: Homogenisation of Liquids in the Turbulent Regime," Coll. Czech. Chem. Commun., 26, pp. 2961-2973.
[17] Hiraoka, S., and Ito, R., 1977, "Simple Relationship between Power Input and Mixing Time in Turbulent Agitated Vessel," Chem. Eng. Japan, 10(1), pp. 75-77.
[18] Havas, G., Sawinsky, J., Deak, A., and Fekete, A., 1978, "Investigation of the Homogenisation Efficiency of Various Propeller Agitators Types," Period. Polytech., 22, pp. 331-343.
[19] Sano, and Usui, 1985.
[20] Mackinnon, C. P., April 1987, "Research Review: Comparative Mixing Times," FMP Report 029.
[21] Raghav Rao, K. S. M. S., and Joshi, J. B., 1988, "Liquid Phase Mixing in Mechanically Agitated Vessels," Chem. Eng. Commun., 74, pp. 1-25.
[22] Corrsin, S., 1964, "The Isotropic Turbulent Mixer: Part Ii, Arbitrary Schmidt Number," A.I.Ch.E. J., 9, pp. 870-877.
[23] Evangelista, J. J., Katz, S., and Shinnar, R., 1969, "Scale-up Criteria for Stirred Tank Reactors," A.I.Ch.E. J., 15, pp. 843-853.
[24] Brodkey, R. S., 1975, Mixing in Turbulent Fields, Academic Press, New York.
[25] Voncken, R. M., Holmes, D. B., and Den Hartog, H. W., 1964, "Fluid Flow in Turbine Stirred Baffled Tanks, Part 2, Circulation Time," Chem. Eng. Sci., 19, pp. 209-213.

[26] Cooke, M., Middleton, J. C., and Bush, J. R., 1988, "Mixing and Mass Transfer in Filamentous Fermentations," BHR Group, Cranfield, U.K.
[27] Ruszkowski, S., 1994, "A Rational Method for Measuring Blending Performance and Comparison of Different Impeller Types," Inst. Chem. Engrs., Rugby, U.K.
[28] Jaworski, Z., Nienow, A. W., Koutsakos, E., Dyster, K. N., and Bujalski, W., 1991, "An Lda Study of Turbulent Flow in a Baffled Vessel Agitated by a Pitched Blade Turbine," Chem. Engng. Res. Des., 69, pp. 313-320.

Appendix A – Experimental Setup

Table A.1. *108* experimental setups produced by progressing through the five variables (tank diameter, *T*, impeller type, *R*, impeller to tank diameter ratio, *D/T*, impeller off-bottom distance to tank diameter ratio, *C/T*, and the mean energy dissipation rate, *ε*) and their levels.

Setup	*T* (*m*)	Impeller Type	*D (m)*	*D/T*	*C (m)*	*C/T*	*ε (W/kg)*
1	1.22	A310	0.41	0.33	0.41	0.33	0.010
2	1.22	A310	0.41	0.33	0.41	0.33	0.005
3	1.22	A310	0.41	0.33	0.24	0.20	0.010
4	1.22	A310	0.41	0.33	0.24	0.20	0.005
5	1.22	A310	0.41	0.33	0.61	0.50	0.010
6	1.22	A310	0.41	0.33	0.61	0.50	0.005
7	1.22	PBT	0.41	0.33	0.41	0.33	0.010
8	1.22	PBT	0.41	0.33	0.41	0.33	0.005
9	1.22	PBT	0.41	0.33	0.24	0.20	0.010
10	1.22	PBT	0.41	0.33	0.24	0.20	0.005
11	1.22	PBT	0.41	0.33	0.61	0.50	0.010
12	1.22	PBT	0.41	0.33	0.61	0.50	0.005
13	1.22	Rushton	0.41	0.33	0.41	0.33	0.010
14	1.22	Rushton	0.41	0.33	0.41	0.33	0.005
15	1.22	Rushton	0.41	0.33	0.24	0.20	0.010
16	1.22	Rushton	0.41	0.33	0.24	0.20	0.005
17	1.22	Rushton	0.41	0.33	0.61	0.50	0.010
18	1.22	Rushton	0.41	0.33	0.61	0.50	0.005
19	1.22	A310	0.61	0.50	0.41	0.33	0.010
20	1.22	A310	0.61	0.50	0.41	0.33	0.005
21	1.22	A310	0.61	0.50	0.24	0.20	0.010
22	1.22	A310	0.61	0.50	0.24	0.20	0.005
23	1.22	A310	0.61	0.50	0.61	0.50	0.010
24	1.22	A310	0.61	0.50	0.61	0.50	0.005
25	1.22	PBT	0.61	0.50	0.41	0.33	0.010
26	1.22	PBT	0.61	0.50	0.41	0.33	0.005
27	1.22	PBT	0.61	0.50	0.24	0.20	0.010
28	1.22	PBT	0.61	0.50	0.24	0.20	0.005
29	1.22	PBT	0.61	0.50	0.61	0.50	0.010
30	1.22	PBT	0.61	0.50	0.61	0.50	0.005
31	1.22	Rushton	0.58	0.48	0.41	0.33	0.010
32	1.22	Rushton	0.58	0.48	0.41	0.33	0.005
33	1.22	Rushton	0.58	0.48	0.24	0.20	0.010
34	1.22	Rushton	0.58	0.48	0.24	0.20	0.005
35	1.22	Rushton	0.58	0.48	0.61	0.50	0.010
36	1.22	Rushton	0.58	0.48	0.61	0.50	0.005
37	1.22	A310	0.25	0.21	0.41	0.33	0.010
38	1.22	A310	0.25	0.21	0.41	0.33	0.005
39	1.22	A310	0.25	0.21	0.24	0.20	0.010
40	1.22	A310	0.25	0.21	0.24	0.20	0.005
41	1.22	A310	0.25	0.21	0.61	0.50	0.010
42	1.22	A310	0.25	0.21	0.61	0.50	0.005

43	1.22	PBT	0.25	0.21	0.41	0.33	0.010
44	1.22	PBT	0.25	0.21	0.41	0.33	0.005
45	1.22	PBT	0.25	0.21	0.24	0.20	0.010
46	1.22	PBT	0.25	0.21	0.24	0.20	0.005
47	1.22	PBT	0.25	0.21	0.61	0.50	0.010
48	1.22	PBT	0.25	0.21	0.61	0.50	0.005
49	1.22	Rushton	0.25	0.21	0.41	0.33	0.010
50	1.22	Rushton	0.25	0.21	0.41	0.33	0.005
51	1.22	Rushton	0.25	0.21	0.24	0.20	0.010
52	1.22	Rushton	0.25	0.21	0.24	0.20	0.005
53	1.22	Rushton	0.25	0.21	0.61	0.50	0.010
54	1.22	Rushton	0.25	0.21	0.61	0.50	0.005
55	0.80	A310	0.25	0.32	0.27	0.33	0.010
56	0.80	A310	0.25	0.32	0.27	0.33	0.005
57	0.80	A310	0.25	0.32	0.16	0.20	0.010
58	0.80	A310	0.25	0.32	0.16	0.20	0.005
59	0.80	A310	0.25	0.32	0.40	0.50	0.010
60	0.80	A310	0.25	0.32	0.40	0.50	0.005
61	0.80	PBT	0.25	0.32	0.27	0.33	0.010
62	0.80	PBT	0.25	0.32	0.27	0.33	0.005
63	0.80	PBT	0.25	0.32	0.16	0.20	0.010
64	0.80	PBT	0.25	0.32	0.16	0.20	0.005
65	0.80	PBT	0.25	0.32	0.40	0.50	0.010
66	0.80	PBT	0.25	0.32	0.40	0.50	0.005
67	0.80	Rushton	0.25	0.32	0.27	0.33	0.010
68	0.80	Rushton	0.25	0.32	0.27	0.33	0.005
69	0.80	Rushton	0.25	0.32	0.16	0.20	0.010
70	0.80	Rushton	0.25	0.32	0.16	0.20	0.005
71	0.80	Rushton	0.25	0.32	0.40	0.50	0.010
72	0.80	Rushton	0.25	0.32	0.40	0.50	0.005
73	0.80	A310	0.41	0.51	0.27	0.33	0.010
74	0.80	A310	0.41	0.51	0.27	0.33	0.005
75	0.80	A310	0.41	0.51	0.16	0.20	0.010
76	0.80	A310	0.41	0.51	0.16	0.20	0.005
77	0.80	A310	0.41	0.51	0.40	0.50	0.010
78	0.80	A310	0.41	0.51	0.40	0.50	0.005
79	0.80	PBT	0.41	0.51	0.27	0.33	0.010
80	0.80	PBT	0.41	0.51	0.27	0.33	0.005
81	0.80	PBT	0.41	0.51	0.16	0.20	0.010
82	0.80	PBT	0.41	0.51	0.16	0.20	0.005
83	0.80	PBT	0.41	0.51	0.40	0.50	0.010
84	0.80	PBT	0.41	0.51	0.40	0.50	0.005
85	0.80	Rushton	0.41	0.51	0.27	0.33	0.010
86	0.80	Rushton	0.41	0.51	0.27	0.33	0.005
87	0.80	Rushton	0.41	0.51	0.16	0.20	0.010
88	0.80	Rushton	0.41	0.51	0.16	0.20	0.005
89	0.80	Rushton	0.41	0.51	0.40	0.50	0.010
90	0.80	Rushton	0.41	0.51	0.40	0.50	0.005
91	0.80	A310	0.16	0.20	0.27	0.33	0.010

92	0.80	A310	0.16	0.20	0.27	0.33	0.005
93	0.80	A310	0.16	0.20	0.16	0.20	0.010
94	0.80	A310	0.16	0.20	0.16	0.20	0.005
95	0.80	A310	0.16	0.20	0.40	0.50	0.010
96	0.80	A310	0.16	0.20	0.40	0.50	0.005
97	0.80	PBT	0.15	0.19	0.27	0.33	0.010
98	0.80	PBT	0.15	0.19	0.27	0.33	0.005
99	0.80	PBT	0.15	0.19	0.16	0.20	0.010
100	0.80	PBT	0.15	0.19	0.16	0.20	0.005
101	0.80	PBT	0.15	0.19	0.40	0.50	0.010
102	0.80	PBT	0.15	0.19	0.40	0.50	0.005
103	0.80	Rushton	0.15	0.19	0.27	0.33	0.010
104	0.80	Rushton	0.15	0.19	0.27	0.33	0.005
105	0.80	Rushton	0.15	0.19	0.16	0.20	0.010
106	0.80	Rushton	0.15	0.19	0.16	0.20	0.005
107	0.80	Rushton	0.15	0.19	0.40	0.50	0.010
108	0.80	Rushton	0.15	0.19	0.40	0.50	0.005

Table A.2. Predicted operating parameters (rotational frequency, *N*, torque, τ, power, *P*, Reynolds number, *Re*) and predicted *95%* homogeneity blend time, θ_{95}, according to Grenville's correlation for all *108* experimental setups. Table A.1 may be referenced for setup parameters.

Setup	*N* (*Hz*)	τ (*Nm*)	*P* (*W*)	*Re*	*Predicted* θ_{95} *(s)* [3]
1	1.62	1.38	14.05	267,032	43.3
2	1.28	0.87	7.02	211,944	54.6
3	1.62	1.38	14.05	267,032	43.3
4	1.28	0.87	7.02	211,944	54.6
5	1.62	1.38	14.05	267,032	43.3
6	1.28	0.87	7.02	211,944	54.6
7	1.01	2.21	14.05	166,841	43.3
8	0.80	1.39	7.02	132,422	54.6
9	1.01	2.21	14.05	166,841	43.3
10	0.80	1.39	7.02	132,422	54.6
11	1.01	2.21	14.05	166,841	43.3
12	0.80	1.39	7.02	132,422	54.6
13	0.60	3.70	14.05	99,781	43.3
14	0.48	2.33	7.02	79,196	54.6
15	0.60	3.70	14.05	99,781	43.3
16	0.48	2.33	7.02	79,196	54.6
17	0.60	3.70	14.05	99,781	43.3
18	0.48	2.33	7.02	79,196	54.6
19	0.82	2.72	14.05	305,675	37.8
20	0.65	1.71	7.02	242,615	47.7
21	0.82	2.72	14.05	305,675	37.8
22	0.65	1.71	7.02	242,615	47.7
23	0.82	2.72	14.05	305,675	37.8
24	0.65	1.71	7.02	242,615	47.7
25	0.51	4.35	14.05	190,985	37.8
26	0.41	2.74	7.02	151,585	47.7
27	0.51	4.35	14.05	190,985	37.8
28	0.41	2.74	7.02	151,585	47.7
29	0.51	4.35	14.05	190,985	37.8
30	0.41	2.74	7.02	151,585	47.7
31	0.33	6.73	14.05	112,448	38.4
32	0.26	4.24	7.02	89,250	48.4
33	0.33	6.73	14.05	112,448	38.4
34	0.26	4.24	7.02	89,250	48.4
35	0.33	6.73	14.05	112,448	38.4
36	0.26	4.24	7.02	89,250	48.4
37	3.54	0.63	14.05	228,309	50.6
38	2.81	0.40	7.02	181,209	63.8
39	3.54	0.63	14.05	228,309	50.6

40	2.81	0.40	7.02	181,209	63.8
41	3.54	0.63	14.05	228,309	50.6
42	2.81	0.40	7.02	181,209	63.8
43	2.21	1.01	14.05	142,647	50.6
44	1.75	0.64	7.02	113,219	63.8
45	2.21	1.01	14.05	142,647	50.6
46	1.75	0.64	7.02	113,219	63.8
47	2.21	1.01	14.05	142,647	50.6
48	1.75	0.64	7.02	113,219	63.8
49	1.32	1.69	14.05	85,312	50.6
50	1.05	1.07	7.02	67,712	63.8
51	1.32	1.69	14.05	85,312	50.6
52	1.05	1.07	7.02	67,712	63.8
53	1.32	1.69	14.05	85,312	50.6
54	1.05	1.07	7.02	67,712	63.8
55	2.32	0.27	3.96	149,711	33.2
56	1.84	0.17	1.98	118,826	41.8
57	2.32	0.27	3.96	149,711	33.2
58	1.84	0.17	1.98	118,826	41.8
59	2.32	0.27	3.96	149,711	33.2
60	1.84	0.17	1.98	118,826	41.8
61	1.45	0.43	3.96	93,539	33.2
62	1.15	0.27	1.98	74,242	41.8
63	1.45	0.43	3.96	93,539	33.2
64	1.15	0.27	1.98	74,242	41.8
65	1.45	0.43	3.96	93,539	33.2
66	1.15	0.27	1.98	74,242	41.8
67	0.87	0.73	3.96	55,942	33.2
68	0.69	0.46	1.98	44,401	41.8
69	0.87	0.73	3.96	55,942	33.2
70	0.69	0.46	1.98	44,401	41.8
71	0.87	0.73	3.96	55,942	33.2
72	0.69	0.46	1.98	44,401	41.8
73	1.06	0.59	3.96	175,103	28.4
74	0.84	0.37	1.98	138,979	35.8
75	1.06	0.59	3.96	175,103	28.4
76	0.84	0.37	1.98	138,979	35.8
77	1.06	0.59	3.96	175,103	28.4
78	0.84	0.37	1.98	138,979	35.8
79	0.66	0.95	3.96	109,404	28.4
80	0.53	0.60	1.98	86,834	35.8
81	0.66	0.95	3.96	109,404	28.4
82	0.53	0.60	1.98	86,834	35.8

83	0.66	0.95	3.96	109,404	28.4
84	0.53	0.60	1.98	86,834	35.8
85	0.40	1.59	3.96	65,430	28.4
86	0.31	1.00	1.98	51,932	35.8
87	0.40	1.59	3.96	65,430	28.4
88	0.31	1.00	1.98	51,932	35.8
89	0.40	1.59	3.96	65,430	28.4
90	0.31	1.00	1.98	51,932	35.8
91	5.01	0.13	3.96	128,342	38.7
92	3.98	0.08	1.98	101,865	48.8
93	5.01	0.13	3.96	128,342	38.7
94	3.98	0.08	1.98	101,865	48.8
95	5.01	0.13	3.96	128,342	38.7
96	3.98	0.08	1.98	101,865	48.8
97	3.40	0.19	3.96	78,894	39.4
98	2.70	0.12	1.98	62,618	49.6
99	3.40	0.19	3.96	78,894	39.4
100	2.70	0.12	1.98	62,618	49.6
101	3.40	0.19	3.96	78,894	39.4
102	2.70	0.12	1.98	62,618	49.6
103	2.03	0.31	3.96	47,183	39.4
104	1.61	0.20	1.98	37,449	49.6
105	2.03	0.31	3.96	47,183	39.4
106	1.61	0.20	1.98	37,449	49.6
107	2.03	0.31	3.96	47,183	39.4
108	1.61	0.20	1.98	37,449	49.6

Appendix B – Experimental Results

Table B.1. Measured parameters and experimental results for *648* trials spanning *108* setups. Table A.1 may be referenced for additional setup information.

Setup	Trial	Impeller	*D/T*	*C/T*	*N (Hz)*	*τ (Nm)*	ε *(W/kg)*	P_o	θ_{95} *(s)*	$N\theta$	Probe
1	1	A310	0.33	0.33	1.617	1.376	0.0098	0.339	71	114.8	1
1	2	A310	0.33	0.33	1.615	1.371	0.0098	0.338	77	124.4	1
1	3	A310	0.33	0.33	1.615	1.371	0.0098	0.338	65	105.0	1
1	4	A310	0.33	0.33	1.615	1.378	0.0098	0.340	64	103.4	1
1	5	A310	0.33	0.33	1.617	1.410	0.0100	0.347	51	82.5	1
1	6	A310	0.33	0.33	1.615	1.384	0.0098	0.341	68	109.8	1
2	1	A310	0.33	0.33	1.265	0.889	0.0049	0.357	90	113.9	1
2	2	A310	0.33	0.33	1.265	0.903	0.0051	0.363	107	135.4	1
2	3	A310	0.33	0.33	1.265	0.878	0.0049	0.353	69	87.3	2
2	4	A310	0.33	0.33	1.265	0.891	0.0049	0.358	113	142.9	1
2	5	A310	0.33	0.33	1.265	0.895	0.0049	0.360	83	105.0	2
2	6	A310	0.33	0.33	1.267	0.870	0.0049	0.349	89	112.7	2
3	1	A310	0.33	0.20	1.553	1.387	0.0095	0.326	80	124.3	1
3	2	A310	0.33	0.20	1.552	1.389	0.0095	0.327	79	122.6	1
3	3	A310	0.33	0.20	1.553	1.377	0.0095	0.324	85	132.0	1
3	4	A310	0.33	0.20	1.552	1.400	0.0097	0.330	67	104.0	1
3	5	A310	0.33	0.20	1.552	1.400	0.0097	0.329	80	124.1	2
3	6	A310	0.33	0.20	1.552	1.392	0.0095	0.327	80	124.1	4
4	1	A310	0.33	0.20	1.268	0.924	0.0051	0.326	91	115.4	2
4	2	A310	0.33	0.20	1.268	0.921	0.0051	0.325	96	121.8	1
4	3	A310	0.33	0.20	1.268	0.926	0.0051	0.326	102	129.4	1
4	4	A310	0.33	0.20	1.268	0.937	0.0053	0.330	91	115.4	3
4	5	A310	0.33	0.20	1.268	0.924	0.0051	0.326	100	126.8	2
4	6	A310	0.33	0.20	1.268	0.926	0.0051	0.327	134	170.0	1
5	1	A310	0.33	0.50	1.613	1.413	0.0100	0.308	49	79.1	4
5	2	A310	0.33	0.50	1.613	1.403	0.0100	0.306	54	87.1	1
5	3	A310	0.33	0.50	1.613	1.412	0.0100	0.308	51	82.3	2
5	4	A310	0.33	0.50	1.613	1.410	0.0100	0.307	52	83.9	2
5	5	A310	0.33	0.50	1.613	1.427	0.0102	0.311	58	93.6	1
5	6	A310	0.33	0.50	1.613	1.387	0.0098	0.302	54	87.1	1
6	1	A310	0.33	0.50	1.267	0.885	0.0049	0.313	59	74.7	2
6	2	A310	0.33	0.50	1.267	0.878	0.0049	0.310	67	84.9	1
6	3	A310	0.33	0.50	1.267	0.890	0.0049	0.314	76	96.3	1
6	4	A310	0.33	0.50	1.267	0.875	0.0049	0.309	66	83.6	1
6	5	A310	0.33	0.50	1.267	0.889	0.0049	0.314	63	79.8	2
6	6	A310	0.33	0.50	1.267	0.887	0.0049	0.313	57	72.2	2
7	1	PBT	0.33	0.33	0.980	2.222	0.0097	1.312	57	55.9	1
7	2	PBT	0.33	0.33	0.980	2.201	0.0095	1.298	45	44.1	1
7	3	PBT	0.33	0.33	0.980	2.215	0.0097	1.305	59	57.8	1

7	4	PBT	0.33	0.33	0.980	2.213	0.0097	1.308	95	93.1	1
7	5	PBT	0.33	0.33	0.983	2.175	0.0095	1.276	52	51.1	1
7	6	PBT	0.33	0.33	0.980	2.230	0.0097	1.317	53	51.9	3
8	1	PBT	0.33	0.33	0.770	1.351	0.0045	1.290	74	57.0	2
8	2	PBT	0.33	0.33	0.770	1.384	0.0047	1.324	93	71.6	1
8	3	PBT	0.33	0.33	0.770	1.381	0.0047	1.321	66	50.8	1
8	4	PBT	0.33	0.33	0.770	1.364	0.0047	1.303	75	57.8	1
8	5	PBT	0.33	0.33	0.770	1.366	0.0047	1.304	90	69.3	1
8	6	PBT	0.33	0.33	0.770	1.384	0.0047	1.324	61	47.0	1
9	1	PBT	0.33	0.20	0.970	2.431	0.0104	1.462	58	56.3	1
9	2	PBT	0.33	0.20	0.968	2.456	0.0104	1.483	78	75.5	3
9	3	PBT	0.33	0.20	0.970	2.452	0.0104	1.476	79	76.6	1
9	4	PBT	0.33	0.20	0.970	2.461	0.0104	1.482	57	55.3	2
9	5	PBT	0.33	0.20	0.970	2.445	0.0104	1.472	62	60.1	4
9	6	PBT	0.33	0.20	0.970	2.461	0.0104	1.483	61	59.2	2
10	1	PBT	0.33	0.20	0.763	1.539	0.0051	1.495	101	77.1	1
10	2	PBT	0.33	0.20	0.765	1.517	0.0051	1.469	72	55.1	3
10	3	PBT	0.33	0.20	0.765	1.519	0.0051	1.469	81	62.0	1
10	4	PBT	0.33	0.20	0.765	1.550	0.0053	1.501	84	64.3	1
10	5	PBT	0.33	0.20	0.765	1.554	0.0053	1.504	71	54.3	1
10	6	PBT	0.33	0.20	0.765	1.537	0.0051	1.486	72	55.1	1/3
11	1	PBT	0.33	0.50	0.987	2.158	0.0095	1.257	58	57.2	2
11	2	PBT	0.33	0.50	0.988	2.128	0.0093	1.236	50	49.4	3
11	3	PBT	0.33	0.50	0.985	2.167	0.0095	1.265	72	70.9	2
11	4	PBT	0.33	0.50	0.987	2.118	0.0093	1.233	74	73.0	2
11	5	PBT	0.33	0.50	0.987	2.124	0.0093	1.236	60	59.2	1
11	6	PBT	0.33	0.50	0.985	2.147	0.0093	1.253	56	55.2	1
12	1	PBT	0.33	0.50	0.772	1.331	0.0045	1.265	55	42.4	1
12	2	PBT	0.33	0.50	0.772	1.321	0.0045	1.257	74	57.1	1
12	3	PBT	0.33	0.50	0.772	1.339	0.0045	1.272	75	57.9	2
12	4	PBT	0.33	0.50	0.773	1.300	0.0045	1.234	95	73.5	2
12	5	PBT	0.33	0.50	0.770	1.342	0.0045	1.284	84	64.7	1
12	6	PBT	0.33	0.50	0.772	1.310	0.0045	1.244	64	49.4	2
13	1	Rushton	0.33	0.33	0.585	3.803	0.0098	6.313	56	32.8	4
13	2	Rushton	0.33	0.33	0.587	3.770	0.0098	6.221	67	39.3	2
13	3	Rushton	0.33	0.33	0.583	3.766	0.0097	6.275	55	32.1	1
13	4	Rushton	0.33	0.33	0.582	3.764	0.0097	6.317	66	38.4	3
13	5	Rushton	0.33	0.33	0.582	3.760	0.0097	6.285	66	38.4	1
13	6	Rushton	0.33	0.33	0.580	3.765	0.0097	6.333	57	33.1	3
14	1	Rushton	0.33	0.33	0.477	2.503	0.0053	6.259	54	25.7	3/4
14	2	Rushton	0.33	0.33	0.475	2.534	0.0053	6.387	80	38.0	2
14	3	Rushton	0.33	0.33	0.477	2.511	0.0053	6.262	71	33.8	2
14	4	Rushton	0.33	0.33	0.478	2.517	0.0053	6.239	68	32.5	1
14	5	Rushton	0.33	0.33	0.477	2.531	0.0053	6.299	55	26.2	1
14	6	Rushton	0.33	0.33	0.477	2.533	0.0053	6.319	79	37.7	2

15	1	Rushton	0.33	0.20	0.615	3.570	0.0097	5.365	78	48.0	2
15	2	Rushton	0.33	0.20	0.615	3.574	0.0097	5.368	58	35.7	1
15	3	Rushton	0.33	0.20	0.615	3.578	0.0097	5.366	55	33.8	1
15	4	Rushton	0.33	0.20	0.617	3.587	0.0098	5.333	79	48.7	2
15	5	Rushton	0.33	0.20	0.615	3.613	0.0098	5.427	77	47.4	2
15	6	Rushton	0.33	0.20	0.615	3.595	0.0098	5.387	63	38.7	4
16	1	Rushton	0.33	0.20	0.493	2.350	0.0051	5.484	87	42.9	1
16	2	Rushton	0.33	0.20	0.495	2.358	0.0051	5.469	65	32.2	2
16	3	Rushton	0.33	0.20	0.495	2.352	0.0051	5.457	89	44.1	2
16	4	Rushton	0.33	0.20	0.493	2.343	0.0051	5.454	90	44.4	2
16	5	Rushton	0.33	0.20	0.492	2.344	0.0051	5.490	80	39.3	2
16	6	Rushton	0.33	0.20	0.495	2.361	0.0051	5.465	91	45.0	2
17	1	Rushton	0.33	0.50	0.570	3.835	0.0097	6.704	68	38.8	4
17	2	Rushton	0.33	0.50	0.573	3.816	0.0097	6.569	64	36.7	3
17	3	Rushton	0.33	0.50	0.573	3.812	0.0097	6.569	63	36.1	2
17	4	Rushton	0.33	0.50	0.572	3.814	0.0097	6.616	66	37.7	1
17	5	Rushton	0.33	0.50	0.570	3.805	0.0097	6.626	49	27.9	4
17	6	Rushton	0.33	0.50	0.572	3.800	0.0097	6.597	70	40.0	2
18	1	Rushton	0.33	0.50	0.467	2.563	0.0053	6.651	71	33.1	4
18	2	Rushton	0.33	0.50	0.468	2.552	0.0053	6.598	84	39.3	1
18	3	Rushton	0.33	0.50	0.470	2.555	0.0053	6.556	75	35.3	3
18	4	Rushton	0.33	0.50	0.468	2.578	0.0053	6.648	101	47.3	1
18	5	Rushton	0.33	0.50	0.468	2.575	0.0053	6.656	87	40.7	1
18	6	Rushton	0.33	0.50	0.468	2.548	0.0053	6.598	73	34.2	2
19	1	A310	0.50	0.33	0.832	2.866	0.0104	0.310	45	37.4	2
19	2	A310	0.50	0.33	0.832	2.860	0.0104	0.309	58	48.2	2
19	3	A310	0.50	0.33	0.830	2.838	0.0104	0.308	40	33.2	1
19	4	A310	0.50	0.33	0.832	2.835	0.0104	0.306	43	35.8	2
19	5	A310	0.50	0.33	0.828	2.821	0.0102	0.306	57	47.2	1
19	6	A310	0.50	0.33	0.830	2.817	0.0102	0.306	55	45.7	1
20	1	A310	0.50	0.33	0.642	1.682	0.0047	0.306	81	52.0	1
20	2	A310	0.50	0.33	0.640	1.699	0.0047	0.310	79	50.6	1
20	3	A310	0.50	0.33	0.640	1.680	0.0047	0.306	72	46.1	1
20	4	A310	0.50	0.33	0.640	1.695	0.0047	0.309	83	53.1	1
20	5	A310	0.50	0.33	0.638	1.697	0.0047	0.310	81	51.7	1
20	6	A310	0.50	0.33	0.640	1.689	0.0047	0.308	84	53.8	1/2
21	1	A310	0.50	0.20	0.773	2.665	0.0091	0.333	45	34.8	2
21	2	A310	0.50	0.20	0.775	2.651	0.0091	0.329	60	46.5	1
21	3	A310	0.50	0.20	0.770	2.657	0.0091	0.334	61	47.0	1/3
21	4	A310	0.50	0.20	0.768	2.656	0.0091	0.336	73	56.1	1
21	5	A310	0.50	0.20	0.768	2.648	0.0091	0.335	61	46.9	4
21	6	A310	0.50	0.20	0.770	2.650	0.0091	0.334	52	40.0	4
22	1	A310	0.50	0.20	0.630	1.763	0.0049	0.332	76	47.9	1
22	2	A310	0.50	0.20	0.630	1.784	0.0049	0.336	84	52.9	1
22	3	A310	0.50	0.20	0.630	1.768	0.0049	0.332	68	42.8	1

22	4	A310	0.50	0.20	0.630	1.785	0.0049	0.335	67	42.2	1
22	5	A310	0.50	0.20	0.632	1.773	0.0049	0.332	67	42.3	1
22	6	A310	0.50	0.20	0.628	1.798	0.0049	0.339	93	58.4	2
23	1	A310	0.50	0.50	0.792	2.616	0.0091	0.312	37	29.3	3
23	2	A310	0.50	0.50	0.793	2.612	0.0091	0.310	55	43.6	2
23	3	A310	0.50	0.50	0.793	2.655	0.0093	0.315	50	39.7	2
23	4	A310	0.50	0.50	0.793	2.627	0.0093	0.311	58	46.0	1
23	5	A310	0.50	0.50	0.792	2.627	0.0093	0.313	50	39.6	2
23	6	A310	0.50	0.50	0.792	2.613	0.0091	0.312	61	48.3	1
24	1	A310	0.50	0.50	0.633	1.699	0.0047	0.315	69	43.7	1
24	2	A310	0.50	0.50	0.633	1.705	0.0047	0.317	52	32.9	2
24	3	A310	0.50	0.50	0.633	1.722	0.0047	0.320	67	42.4	2
24	4	A310	0.50	0.50	0.635	1.705	0.0047	0.315	52	33.0	4
24	5	A310	0.50	0.50	0.635	1.719	0.0047	0.318	58	36.8	1
24	6	A310	0.50	0.50	0.635	1.699	0.0047	0.315	68	43.2	2
25	1	PBT	0.50	0.33	0.528	4.619	0.0108	1.236	53	28.0	2
25	2	PBT	0.50	0.33	0.532	4.587	0.0108	1.216	57	30.3	1
25	3	PBT	0.50	0.33	0.533	4.611	0.0108	1.213	52	27.7	3
25	4	PBT	0.50	0.33	0.535	4.629	0.0108	1.212	46	24.6	2
25	5	PBT	0.50	0.33	0.533	4.615	0.0108	1.213	48	25.6	4
25	6	PBT	0.50	0.33	0.533	4.613	0.0108	1.210	49	26.1	2
26	1	PBT	0.50	0.33	0.428	2.968	0.0055	1.211	64	27.4	1
26	2	PBT	0.50	0.33	0.398	2.581	0.0045	1.216	84	33.5	2
26	3	PBT	0.50	0.33	0.402	2.618	0.0047	1.217	74	29.7	2
26	4	PBT	0.50	0.33	0.402	2.602	0.0045	1.205	79	31.7	2
26	5	PBT	0.50	0.33	0.398	2.610	0.0045	1.231	58	23.1	2
26	6	PBT	0.50	0.33	0.400	2.591	0.0045	1.209	63	25.2	1
27	1	PBT	0.50	0.20	0.493	4.918	0.0106	1.505	46	22.7	2
27	2	PBT	0.50	0.20	0.495	4.932	0.0108	1.503	61	30.2	1
27	3	PBT	0.50	0.20	0.495	4.959	0.0108	1.507	42	20.8	4
27	4	PBT	0.50	0.20	0.495	4.926	0.0108	1.502	74	36.6	1
27	5	PBT	0.50	0.20	0.492	4.907	0.0106	1.517	41	20.2	2
27	6	PBT	0.50	0.20	0.493	4.867	0.0106	1.490	46	22.7	1/2
28	1	PBT	0.50	0.20	0.388	3.125	0.0053	1.544	62	24.1	2
28	2	PBT	0.50	0.20	0.387	3.118	0.0053	1.556	61	23.6	2
28	3	PBT	0.50	0.20	0.392	3.196	0.0055	1.559	61	23.9	1
28	4	PBT	0.50	0.20	0.393	3.202	0.0055	1.546	67	26.4	2
28	5	PBT	0.50	0.20	0.390	3.193	0.0055	1.566	52	20.3	1
28	6	PBT	0.50	0.20	0.390	3.231	0.0055	1.583	72	28.1	1
29	1	PBT	0.50	0.50	0.475	4.967	0.0104	1.650	42	20.0	4
29	2	PBT	0.50	0.50	0.473	4.965	0.0104	1.656	53	25.1	2
29	3	PBT	0.50	0.50	0.475	4.974	0.0104	1.652	48	22.8	1
29	4	PBT	0.50	0.50	0.475	4.941	0.0104	1.640	53	25.2	3
29	5	PBT	0.50	0.50	0.472	4.927	0.0102	1.653	55	25.9	2
29	6	PBT	0.50	0.50	0.473	4.934	0.0102	1.650	52	24.6	4

30	1	PBT	0.50	0.50	0.378	3.184	0.0053	1.665	51	19.3	4
30	2	PBT	0.50	0.50	0.383	3.236	0.0055	1.644	60	23.0	1
30	3	PBT	0.50	0.50	0.377	3.195	0.0053	1.676	71	26.7	4
30	4	PBT	0.50	0.50	0.380	3.196	0.0053	1.655	61	23.2	2
30	5	PBT	0.50	0.50	0.377	3.190	0.0053	1.675	49	18.5	4
30	6	PBT	0.50	0.50	0.380	3.167	0.0053	1.643	68	25.8	1
31	1	Rushton	0.48	0.33	0.328	6.960	0.0100	6.120	39	12.8	1/3
31	2	Rushton	0.48	0.33	0.328	6.941	0.0100	6.084	51	16.7	3
31	3	Rushton	0.48	0.33	0.330	6.909	0.0100	6.021	48	15.8	4
31	4	Rushton	0.48	0.33	0.327	6.894	0.0100	6.088	41	13.4	1
31	5	Rushton	0.48	0.33	0.328	6.920	0.0100	6.045	53	17.4	3
31	6	Rushton	0.48	0.33	0.327	6.888	0.0098	6.124	53	17.3	4
32	1	Rushton	0.48	0.33	0.260	4.344	0.0049	6.078	70	18.2	2
32	2	Rushton	0.48	0.33	0.258	4.357	0.0049	6.135	51	13.2	3
32	3	Rushton	0.48	0.33	0.260	4.377	0.0051	6.111	59	15.3	1
32	4	Rushton	0.48	0.33	0.260	4.361	0.0049	6.069	60	15.6	2
32	5	Rushton	0.48	0.33	0.258	4.363	0.0049	6.144	67	17.3	3
32	6	Rushton	0.48	0.33	0.260	4.366	0.0049	6.103	74	19.2	2
33	1	Rushton	0.48	0.20	0.337	6.981	0.0104	5.829	61	20.5	1
33	2	Rushton	0.48	0.20	0.338	6.982	0.0104	5.787	53	17.9	2
33	3	Rushton	0.48	0.20	0.335	6.986	0.0104	5.854	53	17.8	1
33	4	Rushton	0.48	0.20	0.335	6.926	0.0102	5.803	39	13.1	1/3
33	5	Rushton	0.48	0.20	0.335	6.931	0.0102	5.831	55	18.4	1
33	6	Rushton	0.48	0.20	0.338	6.969	0.0104	5.768	44	14.9	3
34	1	Rushton	0.48	0.20	0.265	4.342	0.0051	5.870	67	17.8	1
34	2	Rushton	0.48	0.20	0.265	4.345	0.0051	5.878	56	14.8	2/4
34	3	Rushton	0.48	0.20	0.265	4.358	0.0051	5.833	55	14.6	1
34	4	Rushton	0.48	0.20	0.267	4.353	0.0051	5.805	77	20.5	1
34	5	Rushton	0.48	0.20	0.265	4.362	0.0051	5.859	52	13.8	3
34	6	Rushton	0.48	0.20	0.267	4.401	0.0051	5.849	58	15.5	1
35	1	Rushton	0.48	0.50	0.325	6.933	0.0100	6.194	55	17.9	1
35	2	Rushton	0.48	0.50	0.322	7.014	0.0100	6.379	47	15.1	4
35	3	Rushton	0.48	0.50	0.323	7.023	0.0100	6.331	48	15.5	3
35	4	Rushton	0.48	0.50	0.320	7.012	0.0098	6.449	52	16.6	1
35	5	Rushton	0.48	0.50	0.328	7.007	0.0100	6.171	43	14.1	3
35	6	Rushton	0.48	0.50	0.323	6.953	0.0098	6.313	44	14.2	1
36	1	Rushton	0.48	0.50	0.258	4.315	0.0049	6.148	53	13.7	3
36	2	Rushton	0.48	0.50	0.255	4.343	0.0049	6.349	65	16.6	2
36	3	Rushton	0.48	0.50	0.257	4.347	0.0049	6.260	59	15.1	1
36	4	Rushton	0.48	0.50	0.258	4.361	0.0049	6.166	65	16.8	2
36	5	Rushton	0.48	0.50	0.258	4.374	0.0049	6.178	63	16.3	2
36	6	Rushton	0.48	0.50	0.258	4.370	0.0049	6.226	69	17.8	2
37	1	A310	0.21	0.33	3.400	0.705	0.0106	0.362	66	224.4	2
37	2	A310	0.21	0.33	3.398	0.711	0.0106	0.365	65	220.9	1
37	3	A310	0.21	0.33	3.338	0.686	0.0100	0.366	58	193.6	3

37	4	A310	0.21	0.33	3.337	0.672	0.0098	0.359	84	280.3	1
37	5	A310	0.21	0.33	3.338	0.689	0.0102	0.368	85	283.8	1
37	6	A310	0.21	0.33	3.338	0.696	0.0102	0.371	66	220.3	1
38	1	A310	0.21	0.33	2.613	0.419	0.0049	0.365	75	196.0	1
38	2	A310	0.21	0.33	2.613	0.421	0.0049	0.367	98	256.1	1
38	3	A310	0.21	0.33	2.613	0.426	0.0049	0.371	121	316.2	1
38	4	A310	0.21	0.33	2.613	0.428	0.0049	0.372	90	235.2	1
38	5	A310	0.21	0.33	2.613	0.434	0.0049	0.377	90	235.2	1
38	6	A310	0.21	0.33	2.613	0.442	0.0051	0.384	101	263.9	1
39	1	A310	0.21	0.20	3.242	0.678	0.0097	0.384	67	217.2	3
39	2	A310	0.21	0.20	3.240	0.680	0.0097	0.385	94	304.6	1
39	3	A310	0.21	0.20	3.240	0.690	0.0098	0.391	89	288.4	1
39	4	A310	0.21	0.20	3.240	0.690	0.0098	0.390	85	275.4	1
39	5	A310	0.21	0.20	3.242	0.686	0.0098	0.388	94	304.7	1
39	6	A310	0.21	0.20	3.242	0.687	0.0098	0.389	88	285.3	1
40	1	A310	0.21	0.20	2.620	0.438	0.0051	0.380	92	241.0	1/2
40	2	A310	0.21	0.20	2.618	0.442	0.0051	0.383	123	322.1	1
40	3	A310	0.21	0.20	2.620	0.433	0.0049	0.374	112	293.4	1
40	4	A310	0.21	0.20	2.620	0.438	0.0051	0.380	109	285.6	1
40	5	A310	0.21	0.20	2.620	0.437	0.0051	0.378	127	332.7	1
40	6	A310	0.21	0.20	2.620	0.435	0.0051	0.377	88	230.6	1
41	1	A310	0.21	0.50	3.297	0.694	0.0100	0.379	104	342.9	1
41	2	A310	0.21	0.50	3.298	0.705	0.0102	0.385	62	204.5	1
41	3	A310	0.21	0.50	3.297	0.681	0.0098	0.372	93	306.6	1
41	4	A310	0.21	0.50	3.298	0.678	0.0098	0.370	57	188.0	1
41	5	A310	0.21	0.50	3.298	0.682	0.0098	0.372	60	197.9	3
41	6	A310	0.21	0.50	3.298	0.679	0.0098	0.371	106	349.6	1
42	1	A310	0.21	0.50	2.617	0.418	0.0049	0.363	86	225.0	1
42	2	A310	0.21	0.50	2.615	0.415	0.0047	0.360	80	209.2	3
42	3	A310	0.21	0.50	2.617	0.406	0.0047	0.352	99	259.1	1
42	4	A310	0.21	0.50	2.663	0.418	0.0049	0.351	151	402.2	1
42	5	A310	0.21	0.50	2.662	0.428	0.0051	0.359	79	210.3	3
42	6	A310	0.21	0.50	2.662	0.432	0.0051	0.362	70	186.3	1
43	1	PBT	0.21	0.33	2.152	1.026	0.0097	1.316	80	172.1	1
43	2	PBT	0.21	0.33	2.152	1.036	0.0098	1.330	80	172.1	1
43	3	PBT	0.21	0.33	2.153	1.028	0.0098	1.317	83	178.7	1
43	4	PBT	0.21	0.33	2.153	1.041	0.0098	1.333	133	286.4	1
43	5	PBT	0.21	0.33	2.153	1.041	0.0098	1.334	74	159.3	1
43	6	PBT	0.21	0.33	2.153	1.053	0.0100	1.351	100	215.3	1
44	1	PBT	0.21	0.33	1.733	0.665	0.0051	1.317	100	173.3	1
44	2	PBT	0.21	0.33	1.732	0.671	0.0051	1.330	104	180.1	1
44	3	PBT	0.21	0.33	1.732	0.668	0.0051	1.324	109	188.8	1
44	4	PBT	0.21	0.33	1.732	0.679	0.0051	1.344	103	178.4	1
44	5	PBT	0.21	0.33	1.732	0.670	0.0051	1.327	110	190.5	1
44	6	PBT	0.21	0.33	1.732	0.689	0.0053	1.366	121	209.5	2

45	1	PBT	0.21	0.20	2.153	1.089	0.0104	1.396	93	200.3	1
45	2	PBT	0.21	0.20	2.153	1.082	0.0102	1.388	99	213.2	2
45	3	PBT	0.21	0.20	2.153	1.095	0.0104	1.404	76	163.7	2
45	4	PBT	0.21	0.20	2.152	1.082	0.0102	1.388	84	180.7	1
45	5	PBT	0.21	0.20	2.152	1.096	0.0104	1.406	66	142.0	3
45	6	PBT	0.21	0.20	2.152	1.086	0.0102	1.392	100	215.2	1
46	1	PBT	0.21	0.20	1.687	0.663	0.0049	1.385	93	156.9	1
46	2	PBT	0.21	0.20	1.685	0.668	0.0049	1.397	105	176.9	1
46	3	PBT	0.21	0.20	1.687	0.667	0.0049	1.393	118	199.0	1
46	4	PBT	0.21	0.20	1.687	0.660	0.0049	1.378	105	177.1	1
46	5	PBT	0.21	0.20	1.687	0.655	0.0049	1.368	129	217.6	1
46	6	PBT	0.21	0.20	1.685	0.676	0.0051	1.413	104	175.2	1
47	1	PBT	0.21	0.50	2.150	0.972	0.0093	1.249	55	118.3	1
47	2	PBT	0.21	0.50	2.152	0.976	0.0093	1.254	83	178.6	1
47	3	PBT	0.21	0.50	2.150	0.967	0.0093	1.242	66	141.9	2
47	4	PBT	0.21	0.50	2.152	0.982	0.0093	1.261	55	118.3	2
47	5	PBT	0.21	0.50	2.152	0.952	0.0091	1.222	97	208.7	1
47	6	PBT	0.21	0.50	2.152	0.963	0.0091	1.235	80	172.1	2
48	1	PBT	0.21	0.50	1.728	0.606	0.0045	1.204	90	155.6	1
48	2	PBT	0.21	0.50	1.790	0.651	0.0051	1.205	104	186.2	1
48	3	PBT	0.21	0.50	1.792	0.637	0.0051	1.180	94	168.4	1
48	4	PBT	0.21	0.50	1.790	0.643	0.0051	1.192	92	164.7	1
48	5	PBT	0.21	0.50	1.788	0.656	0.0051	1.219	74	132.3	1
48	6	PBT	0.21	0.50	1.790	0.636	0.0051	1.179	112	200.5	1
49	1	Rushton	0.21	0.33	1.325	1.603	0.0095	5.419	74	98.1	1
49	2	Rushton	0.21	0.33	1.327	1.600	0.0095	5.407	69	91.5	3
49	3	Rushton	0.21	0.33	1.325	1.608	0.0095	5.434	88	116.6	1
49	4	Rushton	0.21	0.33	1.327	1.600	0.0095	5.404	64	84.9	1
49	5	Rushton	0.21	0.33	1.325	1.599	0.0093	5.405	68	90.1	3
49	6	Rushton	0.21	0.33	1.327	1.613	0.0095	5.455	63	83.6	2
50	1	Rushton	0.21	0.33	1.085	1.086	0.0051	5.485	67	72.7	2/3
50	2	Rushton	0.21	0.33	1.085	1.087	0.0051	5.489	75	81.4	3
50	3	Rushton	0.21	0.33	1.085	1.086	0.0051	5.483	96	104.2	2
50	4	Rushton	0.21	0.33	1.085	1.080	0.0051	5.447	95	103.1	1
50	5	Rushton	0.21	0.33	1.085	1.082	0.0051	5.462	63	68.4	3
50	6	Rushton	0.21	0.33	1.085	1.087	0.0051	5.487	104	112.8	4
51	1	Rushton	0.21	0.20	1.387	1.610	0.0098	4.977	89	123.4	2
51	2	Rushton	0.21	0.20	1.387	1.608	0.0098	4.968	132	183.0	2
51	3	Rushton	0.21	0.20	1.388	1.599	0.0098	4.935	89	123.6	2
51	4	Rushton	0.21	0.20	1.388	1.609	0.0098	4.963	126	174.9	2
51	5	Rushton	0.21	0.20	1.387	1.613	0.0098	4.989	126	174.7	2
51	6	Rushton	0.21	0.20	1.388	1.617	0.0098	4.991	73	101.3	3
52	1	Rushton	0.21	0.20	1.087	1.010	0.0049	5.076	195	211.9	2
52	2	Rushton	0.21	0.20	1.088	1.009	0.0049	5.065	92	100.1	1/4
52	3	Rushton	0.21	0.20	1.088	1.015	0.0049	5.093	147	160.0	2

52	4	Rushton	0.21	0.20	1.088	1.013	0.0049	5.088	156	169.8	2
52	5	Rushton	0.21	0.20	1.088	1.011	0.0049	5.076	116	126.2	2
52	6	Rushton	0.21	0.20	1.088	1.011	0.0049	5.079	134	145.8	2
53	1	Rushton	0.21	0.50	1.325	1.690	0.0098	5.727	64	84.8	4
53	2	Rushton	0.21	0.50	1.323	1.690	0.0098	5.727	75	99.3	2
53	3	Rushton	0.21	0.50	1.323	1.690	0.0098	5.728	63	83.4	2
53	4	Rushton	0.21	0.50	1.323	1.699	0.0098	5.760	70	92.6	1/4
53	5	Rushton	0.21	0.50	1.323	1.698	0.0098	5.753	64	84.7	1
53	6	Rushton	0.21	0.50	1.323	1.698	0.0098	5.755	56	74.1	1
54	1	Rushton	0.21	0.50	1.022	1.037	0.0047	5.895	75	76.6	1
54	2	Rushton	0.21	0.50	1.022	1.035	0.0047	5.883	66	67.4	1
54	3	Rushton	0.21	0.50	1.022	1.038	0.0047	5.907	88	89.9	1/3
54	4	Rushton	0.21	0.50	1.023	1.030	0.0047	5.854	108	110.5	3
54	5	Rushton	0.21	0.50	1.023	1.028	0.0047	5.838	69	70.6	4
54	6	Rushton	0.21	0.50	1.022	1.033	0.0047	5.870	80	81.7	3
55	1	A310	0.32	0.33	2.262	0.296	0.0110	0.344	40	90.5	3
55	2	A310	0.32	0.33	2.263	0.304	0.0114	0.352	45	101.9	1
55	3	A310	0.32	0.33	2.155	0.271	0.0097	0.347	53	114.2	2
55	4	A310	0.32	0.33	2.153	0.275	0.0098	0.352	57	122.7	2
55	5	A310	0.32	0.33	2.155	0.279	0.0098	0.357	46	99.1	1
55	6	A310	0.32	0.33	2.153	0.280	0.0100	0.359	51	109.8	1
56	1	A310	0.32	0.33	1.792	0.164	0.0049	0.303	55	98.5	1
56	2	A310	0.32	0.33	1.792	0.165	0.0049	0.306	43	77.0	4
56	3	A310	0.32	0.33	1.788	0.163	0.0047	0.301	48	85.8	1/2
56	4	A310	0.32	0.33	1.790	0.166	0.0049	0.308	62	111.0	2
56	5	A310	0.32	0.33	1.788	0.171	0.0051	0.317	57	101.9	1
56	6	A310	0.32	0.33	1.788	0.173	0.0051	0.320	58	103.7	2
57	1	A310	0.32	0.20	2.090	0.290	0.0100	0.395	55	115.0	2
57	2	A310	0.32	0.20	2.090	0.289	0.0100	0.394	55	115.0	1
57	3	A310	0.32	0.20	2.092	0.282	0.0098	0.384	44	92.0	1
57	4	A310	0.32	0.20	2.090	0.275	0.0095	0.373	53	110.8	2
57	5	A310	0.32	0.20	2.092	0.280	0.0097	0.380	63	131.8	1
57	6	A310	0.32	0.20	2.090	0.269	0.0093	0.365	56	117.0	2
58	1	A310	0.32	0.20	1.790	0.177	0.0053	0.328	69	123.5	1
58	2	A310	0.32	0.20	1.790	0.174	0.0051	0.323	66	118.1	1
58	3	A310	0.32	0.20	1.790	0.176	0.0051	0.326	51	91.3	3
58	4	A310	0.32	0.20	1.790	0.174	0.0051	0.322	78	139.6	1
58	5	A310	0.32	0.20	1.790	0.176	0.0053	0.328	64	114.6	1
58	6	A310	0.32	0.20	1.790	0.174	0.0051	0.324	64	114.6	1
59	1	A310	0.32	0.50	2.263	0.285	0.0106	0.330	36	81.5	1
59	2	A310	0.32	0.50	2.155	0.266	0.0095	0.340	43	92.7	1
59	3	A310	0.32	0.50	2.155	0.267	0.0095	0.341	32	69.0	2
59	4	A310	0.32	0.50	2.155	0.270	0.0097	0.345	37	79.7	2
59	5	A310	0.32	0.50	2.155	0.272	0.0097	0.348	46	99.1	2
59	6	A310	0.32	0.50	2.155	0.277	0.0098	0.354	41	88.4	3

60	1	A310	0.32	0.50	1.728	0.173	0.0049	0.345	55	95.1	1
60	2	A310	0.32	0.50	1.730	0.179	0.0051	0.355	38	65.7	3
60	3	A310	0.32	0.50	1.728	0.182	0.0051	0.362	54	93.3	1
60	4	A310	0.32	0.50	1.730	0.182	0.0051	0.360	52	90.0	1
60	5	A310	0.32	0.50	1.730	0.185	0.0053	0.369	42	72.7	1
60	6	A310	0.32	0.50	1.730	0.190	0.0053	0.376	52	90.0	1
61	1	PBT	0.32	0.33	1.402	0.429	0.0100	1.298	54	75.7	2
61	2	PBT	0.32	0.33	1.405	0.437	0.0102	1.318	42	59.0	1/2
61	3	PBT	0.32	0.33	1.405	0.426	0.0098	1.283	43	60.4	1
61	4	PBT	0.32	0.33	1.403	0.436	0.0100	1.319	39	54.7	2/3
61	5	PBT	0.32	0.33	1.403	0.430	0.0100	1.297	49	68.8	1/2/3
61	6	PBT	0.32	0.33	1.405	0.421	0.0098	1.268	45	63.2	1
62	1	PBT	0.32	0.33	1.108	0.271	0.0049	1.313	62	68.7	2
62	2	PBT	0.32	0.33	1.108	0.277	0.0051	1.339	75	83.1	1
62	3	PBT	0.32	0.33	1.108	0.276	0.0051	1.331	65	72.0	1
62	4	PBT	0.32	0.33	1.108	0.276	0.0051	1.337	69	76.5	1
62	5	PBT	0.32	0.33	1.108	0.268	0.0049	1.293	64	70.9	1
62	6	PBT	0.32	0.33	1.108	0.267	0.0049	1.290	49	54.3	1
63	1	PBT	0.32	0.20	1.335	0.443	0.0098	1.476	50	66.8	1
63	2	PBT	0.32	0.20	1.335	0.442	0.0098	1.472	47	62.7	1
63	3	PBT	0.32	0.20	1.332	0.445	0.0098	1.491	50	66.6	1/2
63	4	PBT	0.32	0.20	1.335	0.437	0.0097	1.456	44	58.7	3
63	5	PBT	0.32	0.20	1.335	0.446	0.0098	1.489	46	61.4	2
63	6	PBT	0.32	0.20	1.332	0.449	0.0098	1.504	44	58.6	1/3
64	1	PBT	0.32	0.20	1.040	0.281	0.0049	1.544	61	63.4	1
64	2	PBT	0.32	0.20	1.038	0.279	0.0047	1.536	61	63.3	3
64	3	PBT	0.32	0.20	1.040	0.282	0.0049	1.550	55	57.2	1
64	4	PBT	0.32	0.20	1.040	0.280	0.0049	1.544	61	63.4	2
64	5	PBT	0.32	0.20	1.038	0.288	0.0049	1.585	59	61.3	3
64	6	PBT	0.32	0.20	1.038	0.287	0.0049	1.579	61	63.3	1
65	1	PBT	0.32	0.50	1.397	0.426	0.0098	1.298	48	67.0	2
65	2	PBT	0.32	0.50	1.395	0.430	0.0098	1.312	48	67.0	1
65	3	PBT	0.32	0.50	1.398	0.421	0.0097	1.279	59	82.5	1
65	4	PBT	0.32	0.50	1.397	0.420	0.0097	1.281	34	47.5	1
65	5	PBT	0.32	0.50	1.397	0.428	0.0098	1.302	43	60.1	2
65	6	PBT	0.32	0.50	1.397	0.434	0.0100	1.323	56	78.2	1
66	1	PBT	0.32	0.50	1.105	0.276	0.0051	1.343	44	48.6	1
66	2	PBT	0.32	0.50	1.103	0.264	0.0047	1.289	66	72.8	1
66	3	PBT	0.32	0.50	1.103	0.262	0.0047	1.280	61	67.3	2
66	4	PBT	0.32	0.50	1.103	0.268	0.0049	1.303	52	57.4	2
66	5	PBT	0.32	0.50	1.105	0.266	0.0049	1.293	60	66.3	2
66	6	PBT	0.32	0.50	1.105	0.264	0.0049	1.284	53	58.6	2
67	1	Rushton	0.32	0.33	0.858	0.629	0.0089	5.081	59	50.6	1
67	2	Rushton	0.32	0.33	0.918	0.715	0.0108	5.038	45	41.3	1
67	3	Rushton	0.32	0.33	0.920	0.716	0.0108	5.038	45	41.4	2

67	4	Rushton	0.32	0.33	0.918	0.724	0.0110	5.103	49	45.0	1
67	5	Rushton	0.32	0.33	0.858	0.629	0.0089	5.074	63	54.1	1
67	6	Rushton	0.32	0.33	0.858	0.632	0.0091	5.090	63	54.1	1
68	1	Rushton	0.32	0.33	0.695	0.416	0.0047	5.112	87	60.5	1
68	2	Rushton	0.32	0.33	0.695	0.418	0.0047	5.146	82	57.0	1
68	3	Rushton	0.32	0.33	0.695	0.417	0.0047	5.129	57	39.6	1
68	4	Rushton	0.32	0.33	0.695	0.416	0.0047	5.119	85	59.1	2
68	5	Rushton	0.32	0.33	0.695	0.423	0.0049	5.209	77	53.5	1
68	6	Rushton	0.32	0.33	0.695	0.418	0.0047	5.145	86	59.8	1
69	1	Rushton	0.32	0.20	0.928	0.711	0.0108	4.895	42	39.0	1
69	2	Rushton	0.32	0.20	0.928	0.706	0.0108	4.875	41	38.1	1/2/4
69	3	Rushton	0.32	0.20	0.928	0.716	0.0110	4.939	49	45.5	2
69	4	Rushton	0.32	0.20	0.928	0.714	0.0110	4.915	45	41.8	1
69	5	Rushton	0.32	0.20	0.928	0.704	0.0108	4.859	48	44.6	3
69	6	Rushton	0.32	0.20	0.928	0.703	0.0108	4.843	50	46.4	2
70	1	Rushton	0.32	0.20	0.692	0.400	0.0045	4.972	64	44.3	1
70	2	Rushton	0.32	0.20	0.692	0.406	0.0047	5.038	59	40.8	1
70	3	Rushton	0.32	0.20	0.692	0.403	0.0045	5.006	67	46.3	2
70	4	Rushton	0.32	0.20	0.692	0.399	0.0045	4.965	70	48.4	2
70	5	Rushton	0.32	0.20	0.692	0.402	0.0045	4.995	57	39.4	1
70	6	Rushton	0.32	0.20	0.692	0.401	0.0045	4.990	62	42.9	1
71	1	Rushton	0.32	0.50	0.870	0.677	0.0097	5.308	49	42.6	1
71	2	Rushton	0.32	0.50	0.870	0.678	0.0098	5.318	45	39.2	1
71	3	Rushton	0.32	0.50	0.872	0.670	0.0097	5.247	57	49.7	1
71	4	Rushton	0.32	0.50	0.870	0.667	0.0097	5.222	42	36.5	4
71	5	Rushton	0.32	0.50	0.870	0.680	0.0098	5.336	49	42.6	2/4
71	6	Rushton	0.32	0.50	0.870	0.665	0.0097	5.228	43	37.4	1
72	1	Rushton	0.32	0.50	0.703	0.437	0.0051	5.245	69	48.5	1
72	2	Rushton	0.32	0.50	0.703	0.437	0.0051	5.254	64	45.0	1
72	3	Rushton	0.32	0.50	0.703	0.429	0.0049	5.144	75	52.8	2
72	4	Rushton	0.32	0.50	0.703	0.430	0.0049	5.168	69	48.5	1
72	5	Rushton	0.32	0.50	0.705	0.428	0.0049	5.123	60	42.3	2
72	6	Rushton	0.32	0.50	0.703	0.428	0.0049	5.135	61	42.9	2
73	1	A310	0.51	0.33	1.038	0.555	0.0095	0.291	43	44.6	1/2
73	2	A310	0.51	0.33	1.040	0.555	0.0095	0.291	44	45.8	2
73	3	A310	0.51	0.33	1.038	0.552	0.0095	0.290	47	48.8	2
73	4	A310	0.51	0.33	1.040	0.554	0.0095	0.290	39	40.6	1/2
73	5	A310	0.51	0.33	1.038	0.557	0.0097	0.292	40	41.5	1
73	6	A310	0.51	0.33	1.040	0.563	0.0097	0.295	46	47.8	1
74	1	A310	0.51	0.33	0.808	0.362	0.0049	0.314	63	50.9	2
74	2	A310	0.51	0.33	0.807	0.365	0.0049	0.318	62	50.0	2
74	3	A310	0.51	0.33	0.807	0.360	0.0047	0.315	71	57.3	1
74	4	A310	0.51	0.33	0.807	0.369	0.0049	0.323	64	51.6	2
74	5	A310	0.51	0.33	0.807	0.363	0.0049	0.315	47	37.9	1
74	6	A310	0.51	0.33	0.807	0.364	0.0049	0.317	75	60.5	2

75	1	A310	0.51	0.20	0.988	0.598	0.0098	0.347	43	42.5	1
75	2	A310	0.51	0.20	0.988	0.590	0.0097	0.342	44	43.5	2
75	3	A310	0.51	0.20	0.990	0.598	0.0098	0.346	44	43.6	1
75	4	A310	0.51	0.20	0.988	0.594	0.0097	0.345	47	46.5	2
75	5	A310	0.51	0.20	0.988	0.593	0.0097	0.345	42	41.5	1
75	6	A310	0.51	0.20	0.988	0.594	0.0097	0.345	52	51.4	1
76	1	A310	0.51	0.20	0.805	0.395	0.0053	0.346	61	49.1	1
76	2	A310	0.51	0.20	0.807	0.399	0.0053	0.348	53	42.8	2
76	3	A310	0.51	0.20	0.805	0.401	0.0053	0.350	63	50.7	1
76	4	A310	0.51	0.20	0.807	0.402	0.0053	0.351	57	46.0	1
76	5	A310	0.51	0.20	0.807	0.404	0.0053	0.353	61	49.2	1
76	6	A310	0.51	0.20	0.803	0.401	0.0053	0.352	53	42.6	4
77	1	A310	0.51	0.50	1.038	0.554	0.0095	0.291	39	40.5	1
77	2	A310	0.51	0.50	1.037	0.555	0.0095	0.292	36	37.3	2
77	3	A310	0.51	0.50	1.038	0.558	0.0097	0.293	37	38.4	1
77	4	A310	0.51	0.50	1.037	0.560	0.0097	0.295	35	36.3	1
77	5	A310	0.51	0.50	1.037	0.549	0.0095	0.289	44	45.6	4
77	6	A310	0.51	0.50	1.035	0.558	0.0097	0.295	33	34.2	1
78	1	A310	0.51	0.50	0.810	0.349	0.0047	0.302	49	39.7	2
78	2	A310	0.51	0.50	0.810	0.347	0.0047	0.299	81	65.6	1
78	3	A310	0.51	0.50	0.812	0.348	0.0047	0.300	56	45.5	2
78	4	A310	0.51	0.50	0.810	0.349	0.0047	0.302	49	39.7	1
78	5	A310	0.51	0.50	0.810	0.350	0.0047	0.302	49	39.7	1
78	6	A310	0.51	0.50	0.812	0.349	0.0047	0.301	78	63.3	1
79	1	PBT	0.51	0.33	0.617	0.861	0.0089	1.283	46	28.4	2
79	2	PBT	0.51	0.33	0.617	0.853	0.0087	1.269	34	21.0	1
79	3	PBT	0.51	0.33	0.617	0.859	0.0087	1.282	46	28.4	2
79	4	PBT	0.51	0.33	0.615	0.868	0.0089	1.300	37	22.8	1
79	5	PBT	0.51	0.33	0.617	0.855	0.0087	1.275	44	27.1	2/4
79	6	PBT	0.51	0.33	0.617	0.856	0.0087	1.279	43	26.5	2
80	1	PBT	0.51	0.33	0.507	0.582	0.0049	1.289	48	24.3	1
80	2	PBT	0.51	0.33	0.507	0.588	0.0049	1.301	52	26.3	1
80	3	PBT	0.51	0.33	0.507	0.580	0.0049	1.279	40	20.3	4
80	4	PBT	0.51	0.33	0.507	0.586	0.0049	1.297	38	19.3	2
80	5	PBT	0.51	0.33	0.507	0.583	0.0049	1.286	50	25.3	2
80	6	PBT	0.51	0.33	0.507	0.582	0.0049	1.284	70	35.5	2
81	1	PBT	0.51	0.20	0.607	1.024	0.0102	1.572	33	20.0	1/2
81	2	PBT	0.51	0.20	0.608	1.028	0.0104	1.573	42	25.6	1
81	3	PBT	0.51	0.20	0.607	1.033	0.0104	1.591	37	22.4	1
81	4	PBT	0.51	0.20	0.610	1.036	0.0104	1.577	38	23.2	1
81	5	PBT	0.51	0.20	0.610	1.041	0.0104	1.587	41	25.0	1
81	6	PBT	0.51	0.20	0.612	1.020	0.0102	1.549	36	22.0	2
82	1	PBT	0.51	0.20	0.502	0.713	0.0059	1.608	49	24.6	1
82	2	PBT	0.51	0.20	0.502	0.705	0.0059	1.592	40	20.1	2
82	3	PBT	0.51	0.20	0.502	0.712	0.0059	1.603	50	25.1	1

82	4	PBT	0.51	0.20	0.500	0.705	0.0059	1.598	50	25.0	1
82	5	PBT	0.51	0.20	0.498	0.707	0.0059	1.609	50	24.9	2
82	6	PBT	0.51	0.20	0.502	0.701	0.0057	1.580	39	19.6	1
83	1	PBT	0.51	0.50	0.618	0.932	0.0095	1.382	30	18.6	2
83	2	PBT	0.51	0.50	0.617	0.952	0.0097	1.417	42	25.9	2
83	3	PBT	0.51	0.50	0.618	0.950	0.0097	1.410	40	24.7	2
83	4	PBT	0.51	0.50	0.618	0.938	0.0097	1.390	44	27.2	2
83	5	PBT	0.51	0.50	0.618	0.929	0.0095	1.377	39	24.1	1
83	6	PBT	0.51	0.50	0.617	0.937	0.0097	1.394	36	22.2	1
84	1	PBT	0.51	0.50	0.508	0.652	0.0055	1.433	40	20.3	4
84	2	PBT	0.51	0.50	0.510	0.614	0.0051	1.334	44	22.4	1
84	3	PBT	0.51	0.50	0.510	0.637	0.0053	1.394	39	19.9	3
84	4	PBT	0.51	0.50	0.508	0.646	0.0055	1.415	47	23.9	2
84	5	PBT	0.51	0.50	0.508	0.639	0.0053	1.402	48	24.4	2
84	6	PBT	0.51	0.50	0.508	0.644	0.0053	1.411	49	24.9	2
85	1	Rushton	0.51	0.33	0.422	1.638	0.0114	5.246	30	12.7	1
85	2	Rushton	0.51	0.33	0.422	1.657	0.0116	5.312	28	11.8	1
85	3	Rushton	0.51	0.33	0.422	1.655	0.0116	5.290	32	13.5	4
85	4	Rushton	0.51	0.33	0.420	1.644	0.0114	5.283	29	12.2	1
85	5	Rushton	0.51	0.33	0.420	1.648	0.0114	5.285	31	13.0	1/4
85	6	Rushton	0.51	0.33	0.420	1.651	0.0114	5.303	31	13.0	3
86	1	Rushton	0.51	0.33	0.327	1.001	0.0055	5.306	45	14.7	2
86	2	Rushton	0.51	0.33	0.328	0.999	0.0055	5.256	44	14.4	1
86	3	Rushton	0.51	0.33	0.328	1.009	0.0055	5.334	47	15.4	2
86	4	Rushton	0.51	0.33	0.328	1.006	0.0055	5.287	40	13.1	1
86	5	Rushton	0.51	0.33	0.328	1.017	0.0055	5.375	52	17.1	2
86	6	Rushton	0.51	0.33	0.330	1.001	0.0055	5.225	44	14.5	1
87	1	Rushton	0.51	0.20	0.390	1.334	0.0087	4.962	44	17.2	1
87	2	Rushton	0.51	0.20	0.390	1.337	0.0087	4.996	34	13.3	1
87	3	Rushton	0.51	0.20	0.388	1.333	0.0087	4.996	46	17.9	1
87	4	Rushton	0.51	0.20	0.390	1.338	0.0087	4.991	34	13.3	2
87	5	Rushton	0.51	0.20	0.388	1.343	0.0087	5.030	34	13.2	1
87	6	Rushton	0.51	0.20	0.390	1.346	0.0087	5.036	40	15.6	1
88	1	Rushton	0.51	0.20	0.330	0.983	0.0053	5.106	37	12.2	1
88	2	Rushton	0.51	0.20	0.330	0.983	0.0053	5.106	36	11.9	2
88	3	Rushton	0.51	0.20	0.330	0.986	0.0053	5.129	52	17.2	2
88	4	Rushton	0.51	0.20	0.332	0.983	0.0053	5.090	41	13.6	4
88	5	Rushton	0.51	0.20	0.330	0.982	0.0053	5.105	45	14.9	1
88	6	Rushton	0.51	0.20	0.330	0.986	0.0053	5.122	46	15.2	1
89	1	Rushton	0.51	0.50	0.415	1.611	0.0110	5.293	33	13.7	1/2
89	2	Rushton	0.51	0.50	0.418	1.661	0.0114	5.395	36	15.1	2
89	3	Rushton	0.51	0.50	0.418	1.655	0.0114	5.369	29	12.1	1
89	4	Rushton	0.51	0.50	0.420	1.661	0.0116	5.367	38	16.0	4
89	5	Rushton	0.51	0.50	0.418	1.667	0.0116	5.404	29	12.1	3
89	6	Rushton	0.51	0.50	0.420	1.670	0.0116	5.381	31	13.0	1

90	1	Rushton	0.51	0.50	0.328	1.026	0.0055	5.415	42	13.8	2
90	2	Rushton	0.51	0.50	0.328	1.021	0.0055	5.355	43	14.1	2
90	3	Rushton	0.51	0.50	0.328	1.023	0.0055	5.371	52	17.1	2
90	4	Rushton	0.51	0.50	0.328	1.026	0.0055	5.393	42	13.8	2
90	5	Rushton	0.51	0.50	0.328	1.028	0.0055	5.431	48	15.8	2
90	6	Rushton	0.51	0.50	0.327	1.028	0.0055	5.438	45	14.7	2
91	1	A310	0.20	0.33	4.762	0.130	0.0102	0.344	56	266.7	1
91	2	A310	0.20	0.33	4.760	0.132	0.0104	0.350	43	204.7	1
91	3	A310	0.20	0.33	4.760	0.143	0.0112	0.378	53	252.3	1
91	4	A310	0.20	0.33	4.762	0.157	0.0124	0.414	61	290.5	1
91	5	A310	0.20	0.33	4.762	0.173	0.0136	0.455	50	238.1	1
91	6	A310	0.20	0.33	4.760	0.192	0.0152	0.507	52	247.5	2
92	1	A310	0.20	0.33	3.812	0.072	0.0045	0.297	83	316.4	1
92	2	A310	0.20	0.33	3.813	0.075	0.0047	0.308	81	308.9	1
92	3	A310	0.20	0.33	3.812	0.086	0.0053	0.353	52	198.2	3
92	4	A310	0.20	0.33	3.813	0.096	0.0061	0.397	75	286.0	2
92	5	A310	0.20	0.33	3.812	0.104	0.0065	0.430	67	255.4	2
92	6	A310	0.20	0.33	3.812	0.114	0.0073	0.472	75	285.9	2
93	1	A310	0.20	0.20	4.585	0.181	0.0138	0.515	56	256.8	3
93	2	A310	0.20	0.20	4.587	0.168	0.0128	0.480	49	224.7	3
93	3	A310	0.20	0.20	4.585	0.154	0.0116	0.439	60	275.1	1
93	4	A310	0.20	0.20	4.585	0.129	0.0097	0.365	57	261.3	1
93	5	A310	0.20	0.20	4.583	0.127	0.0097	0.362	51	233.8	3
93	6	A310	0.20	0.20	4.583	0.134	0.0102	0.382	48	220.0	2/4
94	1	A310	0.20	0.20	3.707	0.081	0.0049	0.354	68	252.1	1
94	2	A310	0.20	0.20	3.768	0.075	0.0045	0.312	87	327.8	1
94	3	A310	0.20	0.20	3.768	0.075	0.0045	0.310	70	263.8	1
94	4	A310	0.20	0.20	3.768	0.072	0.0045	0.305	70	263.8	1
94	5	A310	0.20	0.20	3.767	0.078	0.0049	0.328	72	271.2	2
94	6	A310	0.20	0.20	3.767	0.080	0.0049	0.339	66	248.6	1
95	1	A310	0.20	0.50	4.587	0.175	0.0132	0.497	51	233.9	1
95	2	A310	0.20	0.50	4.587	0.185	0.0142	0.528	50	229.3	1
95	3	A310	0.20	0.50	4.587	0.179	0.0136	0.507	49	224.7	3
95	4	A310	0.20	0.50	4.588	0.164	0.0124	0.466	51	234.0	2
95	5	A310	0.20	0.50	4.587	0.150	0.0114	0.427	42	192.6	3
95	6	A310	0.20	0.50	4.587	0.129	0.0098	0.366	45	206.4	3
96	1	A310	0.20	0.50	3.770	0.071	0.0043	0.299	57	214.9	2
96	2	A310	0.20	0.50	3.768	0.078	0.0049	0.326	67	252.5	2
96	3	A310	0.20	0.50	3.772	0.086	0.0053	0.363	57	215.0	1
96	4	A310	0.20	0.50	3.768	0.095	0.0059	0.398	75	282.6	1
96	5	A310	0.20	0.50	3.768	0.103	0.0065	0.434	60	226.1	2
96	6	A310	0.20	0.50	3.770	0.112	0.0071	0.473	50	188.5	1
97	1	PBT	0.19	0.33	3.190	0.208	0.0110	1.561	63	201.0	1
97	2	PBT	0.19	0.33	3.190	0.217	0.0114	1.626	64	204.2	1
97	3	PBT	0.19	0.33	3.188	0.214	0.0112	1.607	54	172.2	1

97	4	PBT	0.19	0.33	3.190	0.216	0.0114	1.624	62	197.8	1
97	5	PBT	0.19	0.33	3.192	0.210	0.0110	1.577	61	194.7	1
97	6	PBT	0.19	0.33	3.188	0.206	0.0108	1.542	60	191.3	1
98	1	PBT	0.19	0.33	2.565	0.121	0.0051	1.403	82	210.3	1
98	2	PBT	0.19	0.33	2.565	0.119	0.0051	1.383	72	184.7	1
98	3	PBT	0.19	0.33	2.565	0.116	0.0049	1.358	83	212.9	1
98	4	PBT	0.19	0.33	2.565	0.111	0.0047	1.284	112	287.3	1
98	5	PBT	0.19	0.33	2.563	0.107	0.0045	1.242	71	182.0	3
98	6	PBT	0.19	0.33	2.565	0.102	0.0043	1.180	76	194.9	2
99	1	PBT	0.19	0.20	3.253	0.180	0.0097	1.300	51	165.9	1
99	2	PBT	0.19	0.20	3.252	0.188	0.0100	1.354	55	178.8	1
99	3	PBT	0.19	0.20	3.250	0.193	0.0104	1.400	58	188.5	1
99	4	PBT	0.19	0.20	3.250	0.206	0.0110	1.490	61	198.3	1
99	5	PBT	0.19	0.20	3.250	0.215	0.0116	1.557	60	195.0	1
99	6	PBT	0.19	0.20	3.188	0.212	0.0112	1.594	63	200.9	1
100	1	PBT	0.19	0.20	2.565	0.110	0.0047	1.272	65	166.7	2
100	2	PBT	0.19	0.20	2.563	0.108	0.0045	1.260	70	179.4	1
100	3	PBT	0.19	0.20	2.563	0.105	0.0045	1.224	84	215.3	1
100	4	PBT	0.19	0.20	2.562	0.101	0.0043	1.169	79	202.4	2
100	5	PBT	0.19	0.20	2.563	0.098	0.0041	1.136	84	215.3	1
100	6	PBT	0.19	0.20	2.563	0.097	0.0041	1.135	67	171.7	1
101	1	PBT	0.19	0.50	3.185	0.166	0.0087	1.248	48	152.9	2
101	2	PBT	0.19	0.50	3.185	0.168	0.0089	1.264	49	156.1	1
101	3	PBT	0.19	0.50	3.188	0.173	0.0091	1.297	55	175.4	1
101	4	PBT	0.19	0.50	3.187	0.191	0.0100	1.438	67	213.5	2
101	5	PBT	0.19	0.50	3.187	0.191	0.0100	1.441	66	210.3	1
101	6	PBT	0.19	0.50	3.185	0.197	0.0104	1.478	75	238.9	1
102	1	PBT	0.19	0.50	2.500	0.124	0.0051	1.521	92	230.0	1
102	2	PBT	0.19	0.50	2.500	0.130	0.0053	1.591	81	202.5	1
102	3	PBT	0.19	0.50	2.500	0.133	0.0055	1.626	88	220.0	2
102	4	PBT	0.19	0.50	2.500	0.129	0.0053	1.578	64	160.0	3
102	5	PBT	0.19	0.50	2.498	0.131	0.0053	1.602	92	229.8	1
102	6	PBT	0.19	0.50	2.498	0.128	0.0053	1.568	89	222.4	1
103	1	Rushton	0.19	0.33	1.967	0.316	0.0102	6.244	72	141.6	1
103	2	Rushton	0.19	0.33	1.967	0.316	0.0102	6.245	86	169.1	1
103	3	Rushton	0.19	0.33	1.967	0.310	0.0100	6.123	70	137.7	1
103	4	Rushton	0.19	0.33	1.965	0.313	0.0102	6.191	82	161.1	1
103	5	Rushton	0.19	0.33	1.967	0.312	0.0102	6.164	66	129.8	1
103	6	Rushton	0.19	0.33	1.965	0.306	0.0100	6.059	68	133.6	1
104	1	Rushton	0.19	0.33	1.568	0.197	0.0051	6.107	81	127.0	1
104	2	Rushton	0.19	0.33	1.567	0.189	0.0049	5.879	102	159.8	1
104	3	Rushton	0.19	0.33	1.568	0.184	0.0047	5.714	95	149.0	1
104	4	Rushton	0.19	0.33	1.567	0.181	0.0047	5.622	113	177.0	1
104	5	Rushton	0.19	0.33	1.568	0.177	0.0045	5.520	97	152.1	1
104	6	Rushton	0.19	0.33	1.570	0.177	0.0045	5.511	83	130.3	1

105	1	Rushton	0.19	0.20	2.028	0.282	0.0095	5.241	56	113.6	3
105	2	Rushton	0.19	0.20	2.028	0.281	0.0095	5.230	80	162.3	1
105	3	Rushton	0.19	0.20	2.028	0.284	0.0095	5.264	85	172.4	2
105	4	Rushton	0.19	0.20	2.027	0.280	0.0095	5.207	80	162.1	1
105	5	Rushton	0.19	0.20	2.028	0.284	0.0095	5.260	69	140.0	1
105	6	Rushton	0.19	0.20	2.027	0.289	0.0097	5.387	96	194.6	1
106	1	Rushton	0.19	0.20	1.628	0.192	0.0051	5.529	86	140.0	2
106	2	Rushton	0.19	0.20	1.628	0.198	0.0053	5.700	77	125.4	1
106	3	Rushton	0.19	0.20	1.630	0.205	0.0055	5.900	95	154.9	2
106	4	Rushton	0.19	0.20	1.630	0.207	0.0055	5.956	106	172.8	1
106	5	Rushton	0.19	0.20	1.630	0.210	0.0057	6.041	82	133.7	2
106	6	Rushton	0.19	0.20	1.630	0.216	0.0057	6.200	98	159.7	2
107	1	Rushton	0.19	0.50	1.970	0.323	0.0104	6.356	58	114.3	1
107	2	Rushton	0.19	0.50	1.970	0.331	0.0108	6.516	73	143.8	1
107	3	Rushton	0.19	0.50	1.968	0.325	0.0106	6.418	50	98.4	1
107	4	Rushton	0.19	0.50	1.968	0.328	0.0106	6.459	60	118.1	2
107	5	Rushton	0.19	0.50	1.967	0.325	0.0106	6.426	57	112.1	1
107	6	Rushton	0.19	0.50	1.967	0.325	0.0106	6.435	52	102.3	1
108	1	Rushton	0.19	0.50	1.508	0.197	0.0049	6.619	81	122.2	2
108	2	Rushton	0.19	0.50	1.508	0.192	0.0047	6.434	80	120.7	2
108	3	Rushton	0.19	0.50	1.510	0.182	0.0045	6.090	94	141.9	2
108	4	Rushton	0.19	0.50	1.510	0.169	0.0041	5.670	79	119.3	2
108	5	Rushton	0.19	0.50	1.508	0.172	0.0043	5.768	115	173.5	2
108	6	Rushton	0.19	0.50	1.510	0.175	0.0043	5.885	95	143.5	1

Table B.2. Measured parameters and experimental results for *108* setups as a mean of the *6* trials per setup. Table A.1 may be referenced for additional setup information.

Setup	Impeller	*D/T*	*C/T*	*N (Hz)*	*τ (Nm)*	ε *(W/kg)*	P_o	θ_{95} *(s)*	$N\theta$
1	A310	0.33	0.33	1.616	1.382	0.0099	0.341	66.0	106.6
2	A310	0.33	0.33	1.265	0.888	0.0050	0.357	91.8	116.2
3	A310	0.33	0.20	1.552	1.391	0.0095	0.327	78.5	121.9
4	A310	0.33	0.20	1.268	0.926	0.0052	0.327	102.3	129.8
5	A310	0.33	0.50	1.613	1.409	0.0100	0.307	53.0	85.5
6	A310	0.33	0.50	1.267	0.884	0.0049	0.312	64.7	81.9
7	PBT	0.33	0.33	0.981	2.209	0.0096	1.303	60.2	59.0
8	PBT	0.33	0.33	0.770	1.372	0.0047	1.311	76.5	58.9
9	PBT	0.33	0.20	0.970	2.451	0.0104	1.476	65.8	63.8
10	PBT	0.33	0.20	0.765	1.536	0.0052	1.487	80.2	61.3
11	PBT	0.33	0.50	0.986	2.140	0.0093	1.247	61.7	60.8
12	PBT	0.33	0.50	0.772	1.324	0.0045	1.259	74.5	57.5
13	Rushton	0.33	0.33	0.583	3.771	0.0097	6.291	61.2	35.7
14	Rushton	0.33	0.33	0.477	2.521	0.0053	6.294	67.8	32.3
15	Rushton	0.33	0.20	0.615	3.586	0.0098	5.374	68.3	42.0
16	Rushton	0.33	0.20	0.494	2.352	0.0051	5.470	83.7	41.3
17	Rushton	0.33	0.50	0.572	3.814	0.0097	6.614	63.3	36.2
18	Rushton	0.33	0.50	0.468	2.562	0.0053	6.618	81.8	38.3
19	A310	0.50	0.33	0.831	2.840	0.0104	0.308	49.7	41.2
20	A310	0.50	0.33	0.640	1.690	0.0047	0.308	80.0	51.2
21	A310	0.50	0.20	0.771	2.655	0.0091	0.334	58.7	45.2
22	A310	0.50	0.20	0.630	1.778	0.0049	0.334	75.8	47.8
23	A310	0.50	0.50	0.793	2.625	0.0092	0.312	51.8	41.1
24	A310	0.50	0.50	0.634	1.708	0.0047	0.317	61.0	38.7
25	PBT	0.50	0.33	0.533	4.612	0.0108	1.217	50.8	27.1
26	PBT	0.50	0.33	0.405	2.662	0.0047	1.215	70.3	28.4
27	PBT	0.50	0.20	0.494	4.918	0.0107	1.504	51.7	25.5
28	PBT	0.50	0.20	0.390	3.178	0.0055	1.559	62.5	24.4
29	PBT	0.50	0.50	0.474	4.951	0.0104	1.650	50.5	23.9
30	PBT	0.50	0.50	0.379	3.195	0.0054	1.660	60.0	22.8
31	Rushton	0.48	0.33	0.328	6.919	0.0100	6.080	47.5	15.6
32	Rushton	0.48	0.33	0.259	4.361	0.0050	6.107	63.5	16.5
33	Rushton	0.48	0.20	0.336	6.963	0.0104	5.812	50.8	17.1
34	Rushton	0.48	0.20	0.266	4.360	0.0051	5.849	60.8	16.2
35	Rushton	0.48	0.50	0.324	6.990	0.0100	6.306	48.2	15.6
36	Rushton	0.48	0.50	0.258	4.352	0.0049	6.221	62.3	16.1
37	A310	0.21	0.33	3.358	0.693	0.0103	0.365	70.7	237.2
38	A310	0.21	0.33	2.613	0.428	0.0050	0.373	95.8	250.4
39	A310	0.21	0.20	3.241	0.685	0.0098	0.388	86.2	279.2
40	A310	0.21	0.20	2.620	0.437	0.0051	0.379	108.5	284.2
41	A310	0.21	0.50	3.298	0.687	0.0099	0.375	80.3	264.9
42	A310	0.21	0.50	2.639	0.419	0.0049	0.358	94.2	248.7
43	PBT	0.21	0.33	2.153	1.037	0.0098	1.330	91.7	197.3
44	PBT	0.21	0.33	1.732	0.674	0.0052	1.335	107.8	186.8
45	PBT	0.21	0.20	2.153	1.088	0.0103	1.396	86.3	185.8

46	PBT	0.21	0.20	1.686	0.665	0.0050	1.389	109.0	183.8
47	PBT	0.21	0.50	2.151	0.969	0.0092	1.244	72.7	156.3
48	PBT	0.21	0.50	1.780	0.638	0.0050	1.197	94.3	167.9
49	Rushton	0.21	0.33	1.326	1.604	0.0094	5.421	71.0	94.1
50	Rushton	0.21	0.33	1.085	1.085	0.0051	5.476	83.3	90.4
51	Rushton	0.21	0.20	1.388	1.609	0.0098	4.971	105.8	146.8
52	Rushton	0.21	0.20	1.088	1.012	0.0049	5.080	140.0	152.3
53	Rushton	0.21	0.50	1.324	1.694	0.0098	5.742	65.3	86.5
54	Rushton	0.21	0.50	1.022	1.034	0.0047	5.875	81.0	82.8
55	A310	0.32	0.33	2.190	0.284	0.0103	0.352	48.7	106.4
56	A310	0.32	0.33	1.790	0.167	0.0050	0.309	53.8	96.3
57	A310	0.32	0.20	2.091	0.281	0.0097	0.382	54.3	113.6
58	A310	0.32	0.20	1.790	0.175	0.0052	0.325	65.3	116.9
59	A310	0.32	0.50	2.173	0.273	0.0098	0.343	39.2	85.1
60	A310	0.32	0.50	1.729	0.182	0.0052	0.361	48.8	84.5
61	PBT	0.32	0.33	1.404	0.430	0.0100	1.297	45.3	63.6
62	PBT	0.32	0.33	1.108	0.272	0.0050	1.317	64.0	70.9
63	PBT	0.32	0.20	1.334	0.444	0.0098	1.481	46.8	62.5
64	PBT	0.32	0.20	1.039	0.283	0.0049	1.556	59.7	62.0
65	PBT	0.32	0.50	1.397	0.427	0.0098	1.299	48.0	67.0
66	PBT	0.32	0.50	1.104	0.267	0.0049	1.299	56.0	61.8
67	Rushton	0.32	0.33	0.889	0.674	0.0099	5.071	54.0	47.8
68	Rushton	0.32	0.33	0.695	0.418	0.0048	5.143	79.0	54.9
69	Rushton	0.32	0.20	0.928	0.709	0.0109	4.888	45.8	42.5
70	Rushton	0.32	0.20	0.692	0.402	0.0046	4.994	63.2	43.7
71	Rushton	0.32	0.50	0.870	0.673	0.0097	5.277	47.5	41.3
72	Rushton	0.32	0.50	0.704	0.432	0.0050	5.178	66.3	46.7
73	A310	0.51	0.33	1.039	0.556	0.0095	0.292	43.2	44.9
74	A310	0.51	0.33	0.807	0.364	0.0049	0.317	63.7	51.4
75	A310	0.51	0.20	0.989	0.594	0.0097	0.345	45.3	44.8
76	A310	0.51	0.20	0.806	0.401	0.0053	0.350	58.0	46.7
77	A310	0.51	0.50	1.037	0.556	0.0096	0.293	37.3	38.7
78	A310	0.51	0.50	0.811	0.349	0.0047	0.301	60.3	48.9
79	PBT	0.51	0.33	0.616	0.859	0.0087	1.281	41.7	25.7
80	PBT	0.51	0.33	0.507	0.583	0.0049	1.289	49.7	25.2
81	PBT	0.51	0.20	0.609	1.030	0.0104	1.575	37.8	23.0
82	PBT	0.51	0.20	0.501	0.707	0.0059	1.598	46.3	23.2
83	PBT	0.51	0.50	0.618	0.940	0.0096	1.395	38.5	23.8
84	PBT	0.51	0.50	0.509	0.639	0.0054	1.398	44.5	22.6
85	Rushton	0.51	0.33	0.421	1.649	0.0115	5.287	30.2	12.7
86	Rushton	0.51	0.33	0.328	1.005	0.0055	5.297	45.3	14.9
87	Rushton	0.51	0.20	0.389	1.339	0.0087	5.002	38.7	15.1
88	Rushton	0.51	0.20	0.330	0.984	0.0053	5.110	42.8	14.1
89	Rushton	0.51	0.50	0.418	1.654	0.0115	5.368	32.7	13.7
90	Rushton	0.51	0.50	0.328	1.025	0.0055	5.401	45.3	14.9
91	A310	0.20	0.33	4.761	0.155	0.0122	0.408	52.5	249.9
92	A310	0.20	0.33	3.812	0.091	0.0057	0.376	72.2	275.1
93	A310	0.20	0.20	4.585	0.149	0.0113	0.424	53.5	245.3
94	A310	0.20	0.20	3.758	0.077	0.0047	0.325	72.2	271.2

95	A310	0.20	0.50	4.587	0.164	0.0124	0.465	48.0	220.2
96	A310	0.20	0.50	3.769	0.091	0.0057	0.382	61.0	229.9
97	PBT	0.19	0.33	3.190	0.212	0.0112	1.590	60.7	193.5
98	PBT	0.19	0.33	2.565	0.113	0.0048	1.308	82.7	212.0
99	PBT	0.19	0.20	3.241	0.199	0.0107	1.449	58.0	187.9
100	PBT	0.19	0.20	2.563	0.103	0.0044	1.199	74.8	191.8
101	PBT	0.19	0.50	3.186	0.181	0.0095	1.361	60.0	191.2
102	PBT	0.19	0.50	2.499	0.129	0.0053	1.581	84.3	210.8
103	Rushton	0.19	0.33	1.966	0.312	0.0102	6.171	74.0	145.5
104	Rushton	0.19	0.33	1.568	0.184	0.0048	5.726	95.2	149.2
105	Rushton	0.19	0.20	2.028	0.283	0.0095	5.265	77.7	157.5
106	Rushton	0.19	0.20	1.629	0.205	0.0055	5.888	90.7	147.7
107	Rushton	0.19	0.50	1.968	0.326	0.0106	6.435	58.3	114.8
108	Rushton	0.19	0.50	1.509	0.181	0.0045	6.078	90.7	136.8